SULFUR DIOXIDE REACTIONS WITH AQUEOUS SOLUTIONS OF MANGANESE AT HIGH TEMPERATURE AND WITH AMMONIA IN THE GAS PHASE

A Thesis

Presented to

The Faculty of the Division of Graduate

Studies and Research

by

Edwin M. Hartley, Jr.

In Partial Fulfillment

of the Requirements for the Degree

Doctor of Philosophy in

The School of Chemical Engineering

Georgia Institute of Technology

September, 1973

SULFUR DIOXIDE REACTIONS WITH AQUEOUS SOLUTIONS OF MANGANESE AT HIGH TEMPERATURE AND WITH AMMONIA IN THE GAS PHASE

Approved:

[illegible]

Chairman

[illegible]

[illegible]

Date approved by Chairman: 11/11/73

Dedication

To Barbara

ACKNOWLEDGMENTS

I am deeply indebted to my thesis advisor, Dr. Michael J. Matteson for his assistance with this endeavor. His expertise in the field, his constant activity in staying abreast of new developments and enquiring into innovative ideas and techniques have been a continual source of motivation.

To Dr. G. L. Bridger, Director of the School of Chemical Engineering, I am very grateful for his advice and assistance throughout my stay at Georgia Tech. His making available to me a part time instructorship is most appreciated as well as the other essential sources of assistance such as the Work Study Program, NSF Traineeship, Dow and DuPont Fellowships.

The helpful and constructive critique of Reading Committee Member Dr. C. W. Gorton is appreciated as well as his friendship during the past few years.

The assistance received from Dr. Henry Neumann and Dr. W. T. Ziegler was essential to the completion of this work. Their liberal sharing of their time is acknowledged with gratitude as is the helpful comments of Dr. Joseph Smrekor.

The Staff of the Price Gilbert Library were never too busy to provide help regardless of the time and effort required. To Jim Nabors many thanks for his technical competence and cooperation in maintaining the laboratory instrumentation and equipment and thanks also to Bob Shucker for his expert help with the Univac Computer.

TABLE OF CONTENTS

TABLE OF CONTENTS (Continued)

LIST OF TABLES

LIST OF ILLUSTRATIONS

LIST OF ILLUSTRATIONS (Continued)

SUMMARY

The kinetics of the reaction of SO_2 in the aqueous phase forming sulfuric acid by manganous ion catalysis was investigated experimentally by dispersing a constant flow of air - SO_2 gas mixture into a continuous phase of water and dissolved manganese sulfate. Experimental tests were made with an SO_2 gas concentration in the range of 3000 - 5000 PPM, .001 and .003 molar $MnSO_4$, and a temperature range from 1° to 65°C. A semi-empirical rate equation describing the reaction is given which represents the experimental results within the estimated 10% accuracy of the experimental data. The rate decrease observed with increasing sulfuric acid concentration was found not to be caused primarily by the decrease in SO_2 solubility as had been reported by others. A minor but observable decrease in initial absorption rate was found when the humidity of the gas stream was reduced from saturated air to dry air.

The heterogeneous reaction of SO_2 and NH_3 gases in humid air at 23°C to form solid reaction products was studied experimentally. Results were similar to those reported by others on the reaction of anhydrous SO_2 and NH_3 gases to form solids in that a variety of products are formed depending on the concentrations of the reactants. With a large excess of H_2O vapor and O_2, e.g., air at 50% R.H., SO_2 and NH_3 gases in the initial concentration range of 4 to 60 millimoles per cu. meter and in the mole ratio of $\geq 1:1::[NH_3]:[SO_2]$ react to form crystalline ammonium sulfate. At equimolar concentration, a few percent of ammonium sulfamate is also formed. The reaction appears to be first order with respect to

both SO_2 and NH_3 and being irreversible, goes to completion. A differential rate equation and its integrated form are given which describes the experimental data within the estimated 7% accuracy of the experimental data. At lower concentrations of H_2O (trace to 31 $mM\text{-}m^{-3}$) the principle products are assumed to be $NH_3 \cdot SO_2$ and $(NH_3)_2 \cdot SO_2$ with minor amounts of NH_3SO_3, $(NH_4)_2S_2O_7$, NH_4N_3, and $N_3H_7SO_4$. Product identification of solid reaction products was by X-ray diffraction. At a lower concentration of O_2 (16 $mM\text{-}m^{-3}$) the reaction product was primarily $(NH_3)_2 \cdot SO_2$ with secondary products of $N_3H_7SO_4$ and NH_3SO_3. The aerodynamic diameter of particles produced from NH_3 and SO_2 gases in air containing a trace, 3-5 PPM water vapor, ranges from 1.2 μm to 2μm with a mean of 1.5 μm.

CHAPTER I

INTRODUCTION

General Introduction

This research consisted of a study of the kinetics of two types of reactions of sulfur dioxide. The first reaction, which is covered in the first part of this thesis, is the oxidation of SO_2 to sulfuric acid in an aqueous solution of manganese sulfate. The second reaction type, which is covered in the second part, is the formation of solid reaction products from NH_3 gas combining with SO_2 gas in the presence of O_2 gas and H_2O vapor in air. Both reactions are applicable to the general areas of the consequences of SO_2 gas emissions to the atmosphere, control of those emissions, and recovery of sulfur as its compounds. These reactions can and do occur both in concentrated stack gases and in the atmosphere removed from the SO_2 emitting sources where concentrations are lower. The products of SO_2 reactions (sulfates, sulfuric acid) compared to SO_2 gas are usually many fold more toxic to plant, animal and human life[45] and more corrosive. In addition to the interest in the reactions which occur spontaneously, there is application to planned reactions in order to convert SO_2 gas to its more easily handled compounds for recovery and control.

Introduction to SO_2 Reactions with Aqueous Solutions of Manganese

The first reaction studied was the system SO_2-air-water vapor

mixture contacting an aqueous solution containing dissolved manganese sulfate. The SO_2 and O_2 gases dissolve in part and are catalyzed by the manganous ion, reacting to form sulfuric acid. The stoichiometric equation is:

$$SO_2(aq) + \frac{1}{2} O_2(aq) + H_2O(\ell) \xrightleftharpoons{Mn^{++}\text{cat.}} H_2SO_4(aq) \qquad (I\text{-}1)$$

Formation of sulfuric acid by aqueous metal ion catalysis, of which Mn^{2+} has been found to be the most active,[5,9,19] has been of interest for many years. Early patents (1920's) exist for the manufacture of sulfuric acid by this method.[6] The method has been considered for removing SO_2 from waste gases of fossil fuel burning power plants, oil refineries, and from sulfuric acid contact plants[5] by use of catalyst containing aqueous solution in spray scrubbers, bubble washers and packed towers. A typical coal burning power plant will generate 100 lbs sulfur per ton of high sulfur coal burned, 95% of which is in the form of sulfur dioxide. Emissions in the range of 300 tons SO_2/day from a single plant point out the potential for sulfur recovery or pollution effect.[32]

The reaction is of interest in the general area of atmospheric chemistry and air pollution. Sulfur dioxide and metallic particulates (which can act as aerosol condensation nuclei) are found throughout the atmosphere both from man made and natural sources. Sulfuric acid aerosol has been found to be partly responsible for reduced visibility in smog.[17] Sulfur dioxide in concentrations commonly found in the atmosphere, even in heavily polluted areas, is classified toxicologically only as a mild respiratory irritant. The danger is in the potential

conversion to sulfuric acid. In the 1930 disaster in the Meuse Valley, Belgium, a number of people were killed by sulfuric acid mist inhalation which is suspected to have resulted by this reaction made possible by the combination of geographical, meteorological, and industrial emission factors. The SO_2 and metal contaminants of industrial stack gases combined with water aerosols and fog droplets in the atmosphere, and were held in prolonged contact by a tunnel effect of a temperature inversion over the valley. The resulting mass of sulfuric acid mist slowly drifted down the valley to an inhabited area. Similar catastrophes have occurred in Donora, Pa.,[8] and in London.[16]

The reaction is of interest as a possible explanation for atmospheric phenomena such as the world wide stratospheric layer of aerosol particles that are predominantly ammonium sulfate.[10] Reaction of sulfuric acid aerosols and atmospheric ammonia could in part account for this layer.

There are other mechanisms of interest in which SO_2 is oxidized in the atmosphere. The photochemical reaction of SO_2 and O_2 has been found to proceed at a very slow rate.[11,21,22] However, in the presence of nitrogen oxides and hydrocarbons the rate is markedly increased.[2,12,13,20] The reactions of NH_3, SO_2, O_2, H_2O gases to crystalline ammonium sulfate is the subject of the second part of this thesis and will be discussed below. The reaction of $SO_2 + O_2 = SO_4^=$ is extremely slow in absence of a catalyst and is of negligible effect. Considering the complexity of the atmosphere, the number of constituents and contaminants of diverse concentrations, the ranges of temperature, humidity, radiation, and turbulence, the true role of sulfur dioxide may never be known. Obser-

vations and experimental evidence have indicated the above reactions are significant.

Through the years investigators have studied the aqueous metal ion catalysis of SO_2 in regard to the relative effectiveness of the various metal ions,[5,6,9,14,15,19] effect of catalyst concentration,[4,5,6,9,14,18] performance of various types of contacting equipment,[5] effect of sulfuric acid concentration,[4,9,14] and possible intermediate complexes.[4,15] Not until the work of Matteson, Stober, and Luther[4] (MSL) was published in 1969 was there a definite kinetic model proposed for the reaction. The four step reaction proposed is as follows:

$$SO_2 + Mn^{2+} \underset{k_2}{\overset{k_1}{\rightleftharpoons}} Mn{\cdot}SO_2^{2+} \qquad \text{(I-2)}$$

$$2\ Mn{\cdot}SO_2^{2+} + O_2 \underset{k_4}{\overset{k_3}{\rightleftharpoons}} [(Mn{\cdot}SO_2^{2+})_2{\cdot}O_2] \underset{k_5}{\overset{k_5}{\rightleftharpoons}} 2Mn{\cdot}SO_3^{2+} \qquad \text{(I-3)}$$

$$Mn{\cdot}SO_3^{2+} + H_2O \underset{k_7}{\overset{k_6}{\rightleftharpoons}} Mn^{2+} + HSO_4^- + H^+ \qquad \text{(I-4)}$$

$$HSO_4^- + H^+ \rightleftharpoons H_2SO_4 \qquad \text{(I-5)}$$

Kinetic expressions were derived from this model and rate constants were evaluated for 298°K based on experimental data.

There are a wide range of concentrations encountered in the full scope of interest in this reaction. Sulfur dioxide concentrations vary from a few PPB in "clean air" to 2,000 PPM in the off gases of coal burning power plants. Water aerosols and fog droplets will vary typically from 0 to 1 gm water per cubic meter of air and these droplets can

contain from 0 to saturation PPM dissolved metal concentrations depending on the relative humidity and whether the droplets are increasing in size from the effect of water absorption by a deliquescent particle or decreasing in size by evaporation. The oxygen content of the carrier gas will vary from 21% of air down to 5% in power plant gas, depending on excess air in the combustion process.

The MSL model is in theory applicable to all of the above concentration ranges although it was developed by experimental concentrations of 5 PPM to 130 PPM SO_2, and manganese concentrations from .065 to 1.1 millimoles/cc liquid. The SO_2-air water vapor mixture was held in contact with aqueous-$MnSO_4$ aerosols in a reaction chamber for varying periods of time. Other investigators have used various techniques for experimental determinations including exposing gases to fogs,[6] drops,[6,17] a single drop,[17] bubbling gas through liquid,[5,9,15] mixing liquids in which the gases were dissolved,[14,18] and exposing gases to aerosols deposited on teflon beads.[18] The MSL model has been shown to adequately explain the results obtained by other investigations using other concentrations and techniques.

Scope of this Work

This research in part is an extension of the MSL work wherein rate constants for the MSL model were determined at other temperatures (32°F to 150°F) and at higher concentrations (2000-5000 PPM SO_2). This data is needed to predict and evaluate rates of acid formation in flue gases and stack plumes where temperatures and concentration are higher than normal atmospheric conditions.

Matteson, et al.,[4] and Cheng, et al.,[19] have shown comparable results among the various experimental methods in that the reaction in the aqueous phase is rate controlling rather than gas or liquid diffusion. Therefore, rather than using the MSL method of contacting aqueous manganese sulfate aerosol with SO_2-air mixture, the relatively uncomplicated technique of bubbling the gas mixture through a liquid solution was used. Rate constants at temperatures of 33°F, 77°F, 100°F, 150°F were determined, and calculated H_2SO_4 concentration vs. time was compared with experimental values.

The effect of gas stream humidity on SO_2 absorption was investigated at 298°K to determine how sensitive the reaction is to water vapor in the gas phase. The humidity data is of value in regard to operation of bubble type washers. Data on the solubility of SO_2 in H_2SO_4 solutions of varying concentration and temperature was developed for use in interpreting the experimental results.

CHAPTER II

LITERATURE SURVEY

Johnstone[5] in 1933 published a comprehensive study on the use of metal ion catalysis to remove SO_2 from coal burning power plant stack gas. Johnstone reviewed the tests made by the London Power Company in 1930[63] wherein it was observed that water used to wash the power plant gas absorbed more SO_2 than the solubility data indicated was possible, and that hot water absorbed more SO_2 than cold water which was the reverse of the solubility law. The conclusion reached was that the dust in the gas dissolved in the water and catalyzed a chemical reaction. The reaction rate increased with temperature. Johnstone determined that the oxidation of SO_2 was taking place in the liquid phase, not in the gas phase as is practiced in sulfuric acid manufacturing plants. Of the common types of absorption equipment, spray washers, bubble washers and packed columns, he found bubble washers to be most efficient in terms of contact time and volume of washing space. Manganese was found to be the most active catalyst of the several metal ions tested, followed by iron. A manganese concentration of .025% was optimum with little increase in absorption at higher Mn concentrations, due to the limiting absorption rate of oxygen. Manganese solution was up to 200 times more effective in absorbing SO_2 than pure water. Forty percent sulfuric acid was the highest acid concentration obtained. In tests on power plant gas the reaction was severely inhibited by dust components such as phenol

and copper compounds which acted as permanent inhibitors and tin salts which acted as temporary inhibitors. No economical means were found to remove or counteract the effect of the inhibitors.

In 1933 Copson and Payne[62] covered much of the same ground as Johnstone. They confirmed the maximum effective catalyst is manganese, with optimum .025% concentration and obtained the same results with manganese nitrate as with manganese sulfate. They also obtained a maximum of 40% sulfuric acid before the increasing hydrogen ion concentration reduced the reaction rate to essentially zero. Better efficiency was realized by introducing the gas into the liquid through a fine porous plate than by absorption in a packed tower. The heat of reaction raised the temperature of the solution from room temperature to 65°C with an increase in reaction rate with increased temperature. The volume of water evaporated matched the water absorbed from the gas stream (60% relative humidity) so the liquid volume remained nearly constant. Copson and Payne also concluded that the reaction rate is controlled by the catalyst concentration up to the optimum .025% manganese above which the absorption rate of oxygen is limiting. They claim that the reaction proceeds at the same rate at 20% acid concentration whether the acid is produced by the reaction or initially in the catalyst solution before the reaction starts. Contrary to the experience of Johnstone with coal burning power plant gas, Copson and Payne were successful in scrubbing SO_2 from oil refinery waste gases. They added mercury to the list of permanent inhibitors and determined several ions having no adverse effect on the catalytic activity of the manganese ion. They are antimony, arsenic, chromium, cobalt, lead, magnesium, molybdenum, nickel, vanadium,

and zinc.

Hoather and Goodeve,[14] 1934, using a dilatometric technique, studied the oxidation of sulfurous acid with manganese sulfate catalyst. At 35°C the reaction rate was proportional to the 1.7 power of the catalyst concentration over a catalyst concentration range of $.3 \times 10^{-5}$ to 8×10^{-5} molar. The reaction was zero order with respect to both SO_2 and O_2. From experiments at both 30°C and 35°C the ratio of reaction velocities was found to be 2.09. Adding .002 normal sulfuric acid while the reaction was in progress was found to depress the velocity by about one-third. Hoather and Goodee concluded the reaction mechanism is complex and the constant velocity indicated a chain mechanism.

Bassett and Parker,[15] 1951, studied the oxidation of sulfurous acid by oxides of manganese, ferric and cupric salts, and by molecular oxygen in the presence of various dissolved salts with special reference to the proportions of sulfate and dithionate formed. Dithionic acid, which is stable towards oxidation is an end product and not an intermediate in the formation of sulfuric acid. The oxidation of sulfurous acid in the presence of manganese sulfate produced a negligible amount of dithionate. They also concluded the oxidation of sulfurous acid by molecular oxygen in the presence of salts follows a chain mechanism. The formation of complex sulfite ions carrying co-ordinated oxygen molecules such as $(O_2 \rightarrow Mn(SO_3)_2)''$ which rapidly undergo self-oxidation and reduction is suggested. Of historical interest, Bassett and Parker cite L. Meyer (Ber., 1887, 20, 3058) as the first observer of the effect of dissolved salts on sulfurous acid oxidation. Meyer listed a number of

salts in order of their influence on the reaction. Sulfates and chlorides of manganese were followed by sulfates and chlorides of copper, iron, and cobalt.

Junge and Ryan,[9] 1957, bubbled air and SO_2 gas through very dilute water solutions of metal ion catalysts with reference to the final H_2SO_4 concentration reached when reaction decreased to a negligible rate. The final acid concentration was a linear function of the SO_2 partial pressure for a given catalyst concentration. He concluded the hydrogen ion concentration retards the reaction, finally reaching a point of zero rate which is not a reaction equilibrium but rather the result of a negative self-catalytic reaction. The possible explanation that hydrogen ion concentration stops the reaction because it stops the solubility of SO_2 was discounted because direct measurements showed dissolved SO_2 was still present in the solution after oxidation had come to a stop. Again manganese was the most active catalyst (Junge and Ryan used $MnCl_2$) followed by $CuCl_2$ and $FeCl_2$ and final acid concentration increased with increased catalyst concentration. Junge and Ryan concluded the observed sulfate concentrations in rain, fog, and smog could be accounted for only if some neutralizing cation or NH_3 was absorbed by the water droplets and held the pH from reaching a low value. This was demonstrated by combining NH_3 with the SO_2-air gas stream just before entering the bubbler. The reaction continued for thirty hours until a pH of 2.47 was reached whereas, without the NH_3, the reaction stopped after three hours.

Johnstone and Coughanowr,[17] 1958, studied the rate of absorption of SO_2 (20 - 200 PPM) into a single drop of catalyst solution (250 -

1000 PPM). Theoretical equations based on mass transfer and chemical reaction rate agreed well with experimental results. The reaction of SO_2 to sulfuric acid in manganese sulfate solution was found experimentally to be zero order with respect to SO_2 and O_2 and the rate constant was proportional to the square of the catalyst concentration up to 15 PPM catalyst concentration. The drop was considered quiescent and mass transfer took place by molecular diffusion. The resistance to absorption was entirely within the drop and the concentration of the dissolved SO_2 at the surface of the drop was assumed to be its solubility at the partial pressure of the SO_2. According to the authors, at low catalyst concentration and high partial pressure SO_2, the SO_2 penetrated into the drop and the reaction took place throughout the drop whereas at higher catalyst concentration, 250 PPM, the SO_2 penetrated only to the outer shell of the drop where it was entirely consumed by the reaction. For this latter case the absorption rate R, moles/min-cm^2 is given by the simple expression:

$$R = \sqrt{2C_i D_l k_o} \qquad \text{(II-1)}$$

where C_i = concentration of SO_2 at surface of drops, moles/cm^3

D_l = diffusivity of solute in liquid, cm^2/min

k_o = reaction rate constant, millimoles/liter-minute

From their results they estimated that for .2 gm water per cubic meter of fog containing 20 μm droplets each of which contains 1 micron manganese sulfate the rate of oxidation is 1% per minute for 1 PPM SO_2 concentration. This is 500 times the rate of photochemical oxidation found by Gerhard and Johnstone.[11]

Johnstone and Moll,[6] 1960, measured sulfuric acid formation in artificial fogs containing dissolved manganese sulfate. SO_2 concentrations simulated diluted gases from the combustion of sulfur-bearing fuels, 200 - 500 PPM. Sampling times corresponded to stack plumes discharged into winds 2 - 10 miles per hour or plume travel of .25 to several miles. Sulfuric acid formation was of the order of .1 to 6 mg per cubic meter. Tests on nuclei other than $MnSO_4$ yielded reduced acid formation with no acid formed from NaCl nuclei.

Coughanowr and Krause,[18] 1965, extended the work of Johnstone and Coughanowr[17] to include reaction rate determinations for $MnSO_4$ catalyst concentrations from 0 to 10,000 PPM at 25°C. Their method involved mixing oxygenated solutions of sulfur dioxide and manganese sulfate in a batch system for low catalyst concentration (0 - 15 PPM) and in a flow system for higher catalyst concentrations. For all catalyst values, the reaction was found to be zero order with respect to SO_2 and O_2. The reaction rate constant was proportional to the square of the catalyst concentration up to 100 PPM above this value, k_o increases less rapidly up to 500 PPM after which it increases very slowly.

Cheng, Corn, and Frohliger,[19] 1971, used a novel approach to the reaction. They passed SO_2 (3 - 18 PPM) in air through a flow reactor filled with Teflon beads which were coated with the dissolved catalyst. They tested NaCl and the sulfate and chloride of manganese and copper. Data from several tests were presented which indicate that the overall absorption rate of SO_2 was controlled by the rate of chemical reaction and not by mass transfer in the gas or liquid phases. As so many other researchers had done in the past, they found manganese salts were the

most effective catalyst. The reaction proceeded in three stages. Initially all the SO_2 was removed from the gas stream. Then followed a transition period where reaction rate fell off to the third stage which was a steady low rate. Relative humidity was very influential. When relative humidity was reduced to 60% the reaction rate was barely discernible. For manganese sulfate catalyst the reaction rate was first order with respect to SO_2 concentration in the air stream. Based on their results they estimated SO_2 absorption by natural fog to be 2% - $hour^{-1}$ for .1 PPM SO_2 in a fog of 15 μm droplets, half of which contain 500 PPM $MnSO_4$. Fog concentration was assumed at .2 gm water per cubic meter of air.

Matteson, Stober, and Luther,[4] 1969, took perhaps the most realistic approach to studying the rate of SO_2 absorption at atmospheric conditions. They passed a mixture of SO_2, humid air and aqueous $MnSO_4$ aerosol up through a vertical flow reactor for periods of up to 15 minutes. SO_2 concentrations ranged from .23 millimole - $meter^{-3}$ to 5.2 mM - m^{-3} and $MnSO_4$ concentrations from .065 to 1.1 mM/cc. The four step reaction and the kinetic rate equations derived therefrom reproduced experimental data not only of aerosol - gas reactions but also of bulk solution reactions of others. The induction period observed by Hoather and Goodeve, Johnstone and Coughanowr, and Coughanowr and Kraus was explained by this model and the length of time of the induction period calculable. The apparent reaction rate of others which was proportional to the square of the catalyst concentration is also explained by the MSL model. Rate constants for the rate expressions were determined at room temperature.

CHAPTER III

EXPERIMENTAL

Matteson, Stöber, and Luther[4] point out that the reaction of SO_2 catalyzed to $SO_4^=$ by aqueous manganese ions at 25°C can be described by the same mechanism whether the system be gas - aerosol or bulk solutions. For this reason, when considering a study of the reaction at various temperatures, the relatively uncomplicated method of dispersing an air - SO_2 gas mixture into a water - manganese continuous phase was used.

The equipment is shown schematically in Figure 1. Equipment details are found in Appendix D. Compressed air was reduced in pressure to about 10 psig, and filtered through a 1.2 micrometer membrane filter. The air flow was regulated by a double port micro needle valve to about 1 liter/minute as measured by a gas rotameter. The water manometers and immersion thermometer provided data to insure duplicate conditions for each run and for wet test meter rotameter calibration. The air supply which had a dew point of about 266°K was bubbled through water which could be heated slightly higher than the system temperature to insure 100% humidification. A bypass around the humidifier, containing a gas rotameter and silica gel drying tube allowed humidity control of from near 0 relative humidity to saturation. Humidity monitored by a Cambridge Systems Model 880 Dew Point Hygrometer which had a rated accuracy of ±2°F. From the hygrometer the humid air was mixed with SO_2 gas. SO_2 was supplied from a Matheson Company SO_2 cylinder and was

filtered through a 0.4 micro meter membrane filter and flow was regulated by forcing it through a high pressure drop capillary coil. Flow rate was controlled by varying the approximately 25 psig pressure at the cylinder pressure regulator. The SO_2 flow rate was measured by running the air-SO_2 mixture through a by-pass around the reaction tube to the IR SO_2 analyzer where the PPM SO_2 was read. After the SO_2 was mixed into the air stream the mixture was introduced into the water - manganese liquid mixture in the reaction tube. The gas was dispersed in the liquid through a fritted glass gas dispersion tube which had been modified so that the gas bubbles emerged into the liquid at the very bottom of the reaction tube in order to provide maximum contact time and as complete mixing as possible. A fritted gas diffuser was chosen over other methods of contacting the gas with the liquid because of the results of Johnstone,[5] Andersen and Johnstone,[52] and Copson and Payne.[62] Bubbling the gas through a fritted disperser was found to be best for absorbing a relatively insoluble gas such as oxygen into a liquid. Bubbles dispersed from a frit were more efficient for gas absorption into liquid than packed towers, spray washers, or Venturi atomizers.

From the reaction tube the gas was passed through a glass wool filter and an acetone - water ice freeze out trap to remove most of the water vapor before the SO_2 content of the gas was measured by the Beckman Model 215A Infra-red Analyzer(IR). The water vapor had to be removed because of its significant absorbance of infra red energy near the frequency absorbed by SO_2. A test was made to evaluate the error, if any, caused by the condensed water absorbing SO_2 and giving IR readings which were falsely low. Dry air containing SO_2 added at a constant, controlled

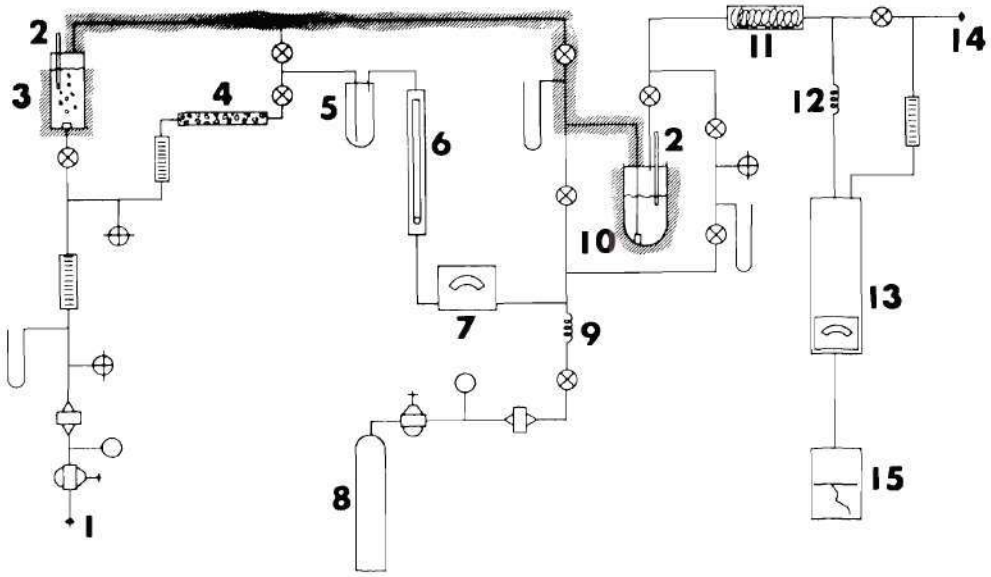

1. Compressed Air
2. Thermometer
3. Humidifier
4. Drying Tube - Silica Gel
5. Trap
6. Total Immersion Thermometer
7. Dewpoint Hygrometer
8. SO_2 Bottle
9. High Pressure Drop Capillary Coil
10. Back Mix Reactor with Constant Temp Bath
11. Glasswool Filter
12. Freeze-out Trap
13. Infrared SO_2 Analyzer
14. Drain
15. Strip Recorder

Symbols

- Pressure Regulator
- Valve
- Pressure Indicator
- Needle Valve
- Rotameter
- Manometer
- Insulation and Temperature Control
- Membrane Filter

Figure 1. Experimental Apparatus for Kinetic Studies of SO_2 Oxidation by Mn^{++} Catalysis.

rate was flowed through the IR which indicated the SO_2 content. Dry air and SO_2 at the same flow rates and concentration were humidified, then passed through the acetone ice cold trap to remove the water vapor and flowed through the IR. If the condensate absorbed appreciable SO_2, the SO_2 concentration indicated by the IR would have been less than when dry air, unhumidified, was used. The IR indicated the same SO_2 concentration in each case, showing there was no problem with SO_2 absorption by the condensate.

All runs at temperatures other than the constant lab temperature of 298°K were made with saturated air. For these runs the hygrometer line was by-passed, and the air from the humidifier was run directly to the SO_2 mixing tee and reaction tube. This section of the system including the humidifier, mixing tee and reaction tube was wrapped with controlled voltage heating tape and insulation to provide for testing above 298°K. For tests below 298°K, this section was immersed in a constant temperature water bath. Ice and water were used for the tests at 274°K. The reaction tube was fitted with a thermometer which could be lowered into the liquid for a temperature check then raised above the liquid so as not to interfere with the gas liquid dispersion pattern. Several tests at 298°K with the gas humidity varying from near zero to saturated indicated very little difference in initial reaction rate. After a period of time, low humidity gas will lower the liquid volume by evaporation. For this reason all other tests were made with saturated air and the volume of the liquid was measured after each test to check for evaporation loss or gain by condensation. The higher temperature tests required very close control to avoid liquid volume change from evaporation or

condensation.

As discussed above, to insure adequate surface area between the gas and liquid phases in the reaction tube, a fritted glass diffuser was used to provide many small bubbles. This resulted in some back pressure in the gas upstream from the reactor. As a compromise between flow rate and pressure drop, a flow of approximately 1 liter/min was chosen. Initial exploratory runs with about 50 cc water containing the optimum catalyst concentration of .05 mMole Mn^{2+} per cc (as reported by Matteson,[4] et al.) and SO_2 concentration in the gas stream in the range of 4500 PPM, resulted in all the SO_2 being removed from the gas stream for the first several minutes. Since the method used to study the reaction calls for an experimental value of initial reaction rate, the liquid volume and catalyst concentration were reduced until the reaction was slowed to a point where there was measurable SO_2 concentration in the initial gas out of the reaction tube. Finally a volume of 10 cc liquid was indicated as optimum with Mn^{2+} initial concentrations varying from .001 to .005 mMole/cc. At higher initial manganese concentration or lower SO_2 concentration, all the SO_2 was removed which meant initial reaction rate was controlled by the rate at which SO_2 was supplied rather than by the rate of the reaction. At lower liquid volume or higher gas rate, the gas to liquid ratio was too high for good mixing and the gas was observed to blow through rather than to produce a turbulent mixture of swirling bubbles. At the dilute concentrations of Mn^{2+} and SO_2 used the heat of the reaction caused an increase in solution temperature of 1 - 2°C maximum, and therefore an isothermal reaction was not difficult to maintain. Specifications of the gases and of the

$MnSO_4$ used are given in Appendix C.

A typical sequence of operations in making a run as follows: The air flow rate and desired humidity and temperature were adjusted with the air flow by-passing the reaction tube to the freeze-out trap and IR analyzer. The by-pass line contained a needle valve set to produce a back pressure identical to that caused by the diffuser in the reaction tube. The IR reading from the water vapor in the air which was not removed by the freeze-out trap was recorded. This usually was in the range of 30 PPM. The SO_2 was then opened up to the gas stream and set to the desired concentration as read by the IR. The true SO_2 concentration was the value read at this time less the reading caused by the water vapor. It would be possible to use a colder mixture for the freeze out trap such as dry ice - acetone (212°K) but a larger volume trap would be required which in turn would cause a higher error in the IR reading by dilution of the gas out of the reaction tube in the lines and vessels ahead of IR analyzer. After the SO_2 concentration was set, the SO_2 was cut off and the air stream was switched to the reaction tube. If the SO_2 - air stream were to be diverted to the reaction tube, the surge in back pressure caused by the initial flow through the wet diffuser would be unsettling to the flow parameters causing erratic readout of the initial reaction. In a few seconds, after flow through reaction tube to IR has steadied, the SO_2 was opened up again to the air stream. Part of the SO_2 into the reactor was absorbed into the liquid and the balance was in the gas stream emerging from the liquid and was continuously measured by the IR and recorded. The amount absorbed was then obtained by difference.

In a typical test, the recorder was started when only the air was flowing through the reaction tube. The recorder reading was the constant "background" reading, or reading of the unremoved water vapor in the air. After the SO_2 flow was started, the recorder line remained on the background level for a few seconds, then rose sharply to a point where it tended to level off depending on rate of SO_2 absorption at the particular conditions of temperature, catalyst concentration and SO_2 partial pressure in the air. A typical recorder output is shown in Figure 2.

In treating the data, the following nomenclature was used:

V = volume of liquid in reactor, cc liquid, constant

V_o = volumetric feed rate of SO_2 - air mixture, cc/min, constant

τ = space time, = V/V_o, cc liquid-min/cc gas, constant

CAO = concentration of SO_2 in gas feed, mM SO_2/cc gas, constant

BGR = "background reading," IR analyzer reading of water vapor in air stream, scale units

BGP = BGR converted to Parts Per Million by volume

AWIR = IR analyzer reading of air - SO_2 - H_2O mixture into reaction, scale units, constant

AWIP = AWIR converted to PPM

AIP = PPM SO_2 in air stream in gas going into reactor,
= AWIP - BGP

AWOR = IR analyzer reading of air - SO_2 - H_2O mixture out of reaction, scale units

AWOP = AWOR converted to PPM

AOP = AWOP - BGP, PPM SO_2 in gas leaving reactor

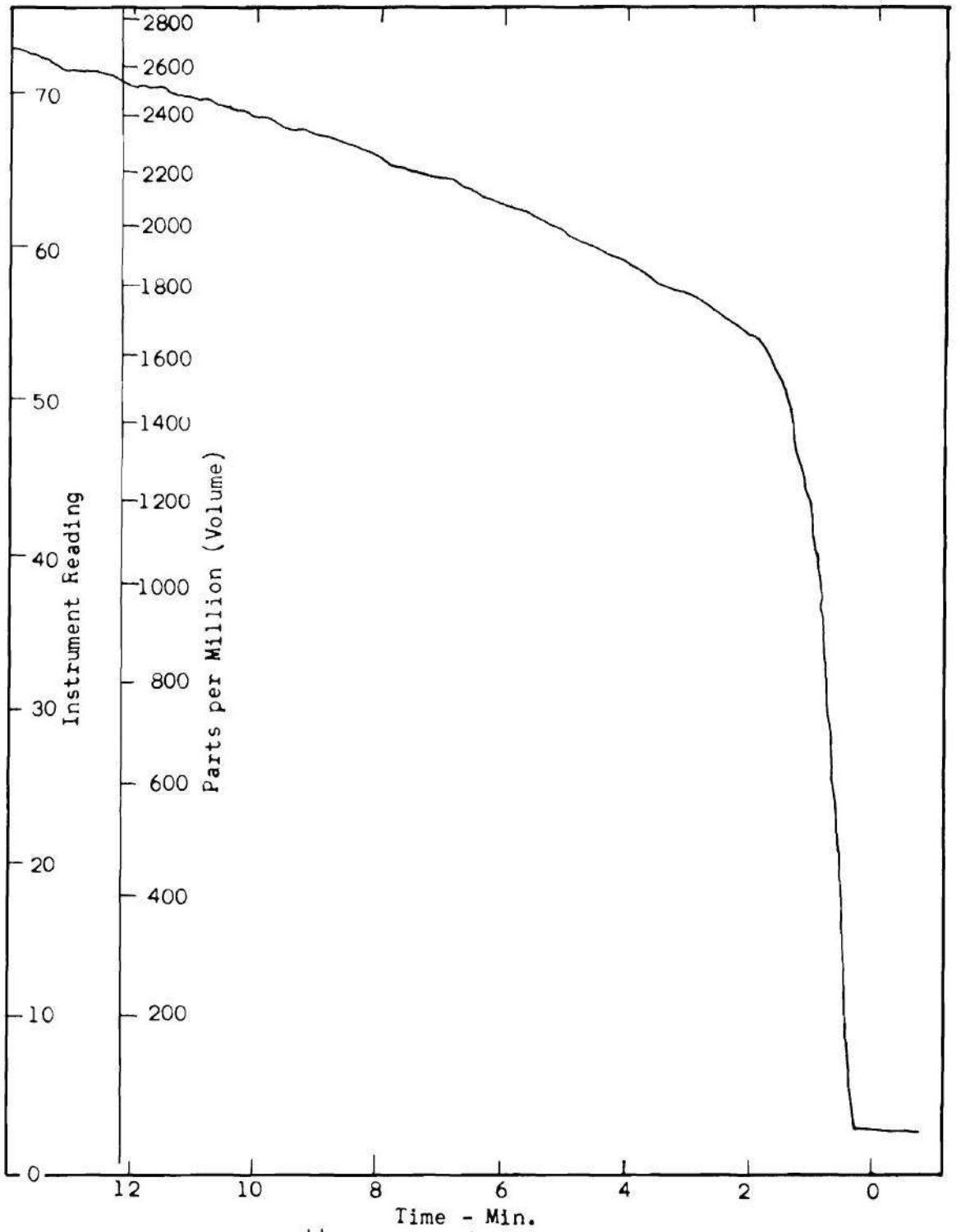

Run 49 - 25°C, $[Mn^{++}]$ = .003 mM/cc, $[SO_2]$ Input to Reactor = 4748 PPM

Figure 2. SO_2 Concentration in Reactor Off Gas, PPM.

RA = rate of total SO_2 transfer from the gas phase into the liquid phase, mM SO_2/cc liq.-minute

XA = fraction of SO_2 entering reactor which is absorbed out of gas stream

R = dissolved SO_2 concentration in liquid, mM SO_2/cc liquid

H = solubility constant, (mM SO_2/cc liquid)(mM SO_2/cc gas)$^{-1}$

CAG = SO_2 concentration in gas leaving reactor, mM SO_2/cc gas

X = concentration of manganese complex in liquid mM Complex/cc liquid

J = concentration, $[H^+] = [HSO_4^-]$ in liquid mM H_2SO_4/cc liquid

t = time, minutes

S = total SO_2 absorbed from gas stream at any time, t, mM SO_2/cc liquid

Bo = initial Mn^{2+} concentration in liquid, mM Mn^{2+}/cc liquid

The IR analyzer readings of SO_2 and H_2O in gas stream are converted to PPM (volume) by a graph supplied by the manufacturer. A computerized least squares program was used to convert the readings to PPM by curve fitting the manufacturers graph to a 4^{th} degree polynomial.

The rate of SO_2 absorption into the liquid is given by:

$$\frac{dS}{dt} = RA = \frac{CAO \cdot XA}{\tau} \frac{\text{mM } SO_2}{\text{cc liq.-min.}} \qquad \text{(III-1)}$$

where

$$CAO = \frac{AIP}{22.4 \times 10^6} \times \text{Press. Correction} \times \text{Temp. Corr.} \frac{\text{mM } SO_2}{\text{cc gas into rxn}} \qquad \text{(III-2)}$$

The ideal gas law was assumed in this calculation.

$$XA = \frac{AIP - AOP}{AIP} \qquad \text{(III-3)}$$

$$\tau = \frac{V}{V_o} \qquad \text{(III-4)}$$

The concentration of SO_2 dissolved in the liquid is assumed to be in equilibrium with the concentration of SO_2 in the gas stream leaving the reaction by the solubility relationship. The concentration of SO_2 dissolved in the liquid, R, is given by:

$$R \frac{\text{mM } SO_2}{\text{cc liq}} = H\left(\frac{\text{mM } SO_2}{\text{cc liq}}\right) \cdot \left(\frac{\text{mM } SO_2}{\text{cc gas}}\right)^{-1} \times CAG \frac{\text{mM } SO_2}{\text{cc gas out of rxn}} \qquad \text{(III-5)}$$

where

$$CAG = \frac{AOP}{10^6 \cdot 22.4} \times \text{Temp. Corr.} \times \text{Press. Corr.} \frac{\text{mM } SO_2}{\text{cc gas}} \qquad \text{(III-6)}$$

S, the total SO_2 removed from gas stream at any time t is:

$$S = \int_o^t RA \, dt \qquad \text{(III-7)}$$

Since all of the SO_2 absorbed from the gas stream is present in the liquid phase in three forms: dissolved SO_2, R; manganese - SO_2 complex, X; and HSO_4^-, J; the rate of acid production is:

$$\frac{dJ}{dt} = \frac{dS}{dt} - \frac{dR}{dt} - \frac{dX}{dt} = \left(RA - \frac{dR}{dt} - \frac{dx}{dt}\right) \frac{\text{mM } H_2SO_4}{\text{cc liq - min.}} \qquad \text{(III-8)}$$

The concentration of manganese - SO_2 complex is assumed constant, therefore

$$\frac{dJ}{dt} = RA - \frac{dR}{dt} \qquad \text{(III-9)}$$

where

$$\frac{dR}{dt} = \frac{\Delta R}{\Delta t} \qquad \text{(III-10)}$$

The total acid formed at any time is then:

$$J = S - R - X \frac{mM\ H_2SO_4}{cc\ liq.} \qquad \text{(III-11)}$$

A computer program with a subroutine for converting IR analyzer readings to PPM was used to facilitate the above calculations. A comparison of Simpson's Rule and the Trapezoidal Rule for evaluating the integral equation (III-7) showed no significant difference so the Trapezoidal Rule was used. The input to the program is:

(1) BGR, AWOR, AWIR, IR analyzer readings with AWOR readings taken from the continuous recording.

(2) Constants: temperature of reaction, pressure in reaction tube (assumed equal to atmospheric pressure), V_o, V, B_o.

(3) t values for the numerical integration and print out of values at various times.

Solubility of SO_2 in Dilute Sulfuric Acid

The experimental system described herein is well suited for determining the gross absorption value for SO_2 in dilute sulfuric acid - water mixtures. The SO_2 - air mixtures were bubbled through the water - sulfuric acid liquid mixture until the SO_2 concentration out of the liquid was the same as the concentration into the liquid, at which time the

concentration of dissolved SO_2 was in equilibrium with the gaseous SO_2 in the air mixture. By numerical integration of the difference in SO_2 rates into and out of the reaction tube, using equation (III-7), the total SO_2 dissolved was determined. Knowing the SO_2 gas concentration and liquid volume, the equilibrium value in terms of (mM SO_2/cc liquid) (mM SO_2/cc gas)$^{-1}$ was determined for several dilute H_2SO_4 concentrations and for the range of temperatures used in the study of the SO_2 catalyzed reaction. This method determines only the total SO_2 removed from the air stream with no accounting for any effects of SO_2 oxidation to HSO_4^-, nor reaction with water forming sulfurous acid, nor of the other dissolved gases from the air. The results are shown in Figure 3.

There is a maximum error of about 10% using this method in this work because of the assumption that all concentrations of SO_2 in the gas stream out of the reactor can be related to SO_2 concentration in the liquid by using Figure 3. Actually only the un-ionized dissolved SO_2 follows a Henry's Law relationship and at dilute concentrations of H_2SO_4 a significant part of the total dissolved SO_2 is ionized: $H_2O \cdot SO_2 \rightleftharpoons H^+ + HSO_3^-$. As the concentration of H_2SO_4 increases, the hydrogen ion concentrations reduces the HSO_3^- concentration and the dissolved SO_2 is progressively present in the un-ionized form. Therefore, at low concentrations of H_2SO_4 the solubility relationship is a function not only of temperature and H_2SO_4 concentration, but also of partial pressure of SO_2 in the gas.

In summary, the experimental method used in this work has the advantage of simplicity, good control, and continuous recorded data, eliminating the need for any chemical analysis. The main disadvantage

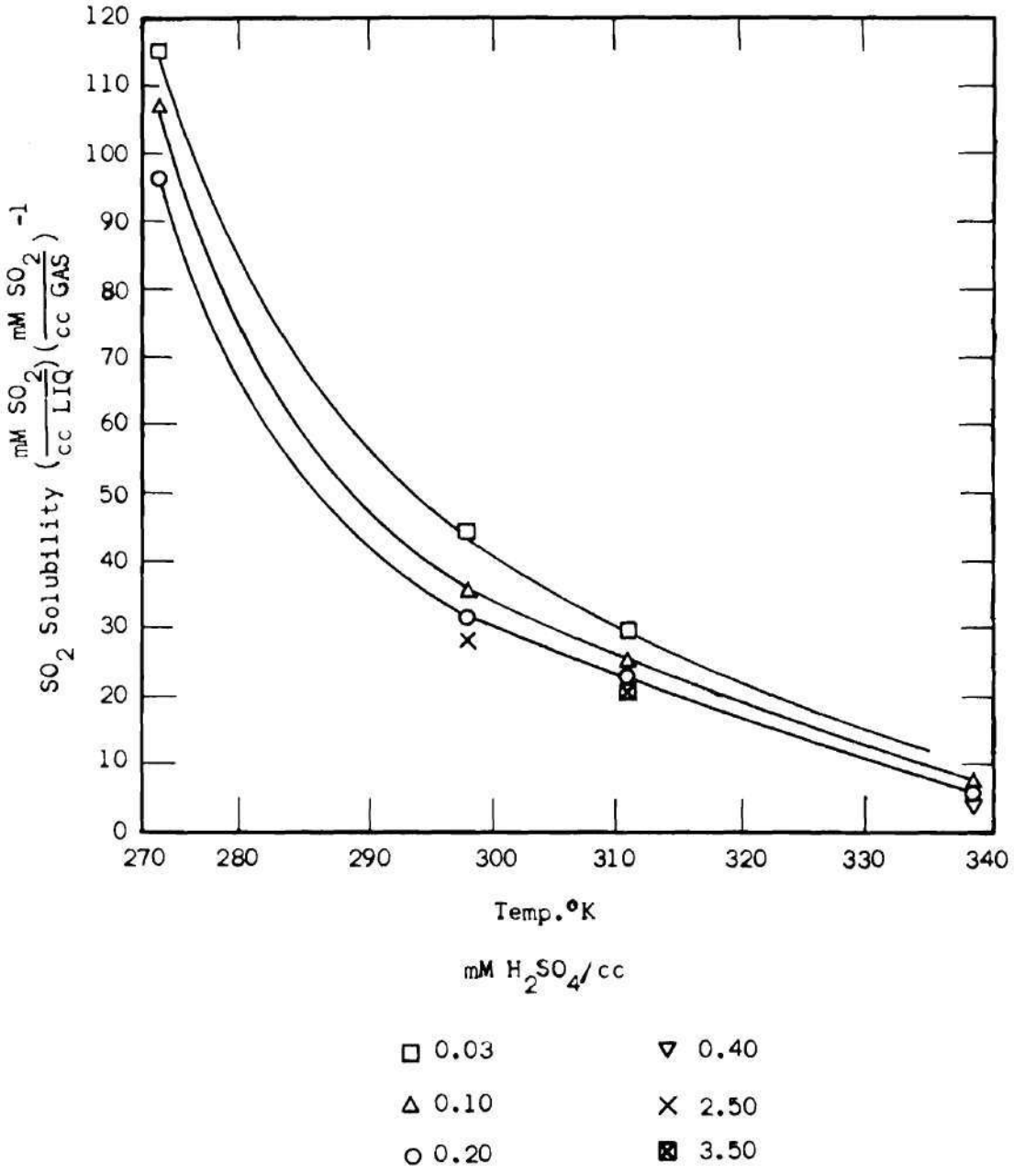

Figure 3. Solubility of SO_2 Gas in Sulfuric Acid Solution at Various Temperatures.

is in the restriction on maximum manganese concentration in the liquid phase on the order of .005 millimoles/cc and in the restriction on the minimum SO_2 concentration in the gas phase of 2000 PPM. These limits exist in the sense that if higher Mn^{++} concentration is used or lower SO_2 concentration is used, all the SO_2 is removed from the gas stream for the initial period of the run and initial reaction rate determinations are thereby unavailable.

CHAPTER IV

RESULTS AND DISCUSSION

To determine the effect of temperature on reaction rate, tests were made at five temperatures, 1°C, 11°C, 25°C, 38°C and 65°C. Air and SO_2 in the range of 3000 - 5000 PPM SO_2 was bubbled through 10 cc of .001 to .003 mM/cc Mn^{++} solution isothermally at the rate of 1 liter/min. The SO_2 in the gas out of the liquid was continuously monitored by a recorder on the infrared SO_2 analyzer. By difference between the SO_2 concentration of the gas out of the liquid and the constant SO_2 concentration of the gas into the liquid, continuous data was obtained on the rate and quantity of SO_2 absorbed by the liquid. Details of each experimental test are listed in Appendix A. The concentration of sulfuric acid vs. time for an initial manganese concentration of .003 mM - cc^{-1} and SO_2 concentration in the gas of 4200 PPM is shown in Figure 4. As is apparent from Figure 4, there is a large increase in reaction rate with increased temperature up to 25°C, above which temperature the reaction rate increase is much less. At each of the temperatures below 66°C there is a decrease in reaction rate with time, whereas at 65°C the reaction rate is constant with time over the time range tested. This is shown more clearly in Figure 5, a plot of reaction rate vs. time at the various temperatures. Three runs were made at 1°C, 25°C, and 38°C for an extended period of time, several hundred minutes, to determine decrease in reaction rate with increase of sulfuric acid concentration. Volume control was

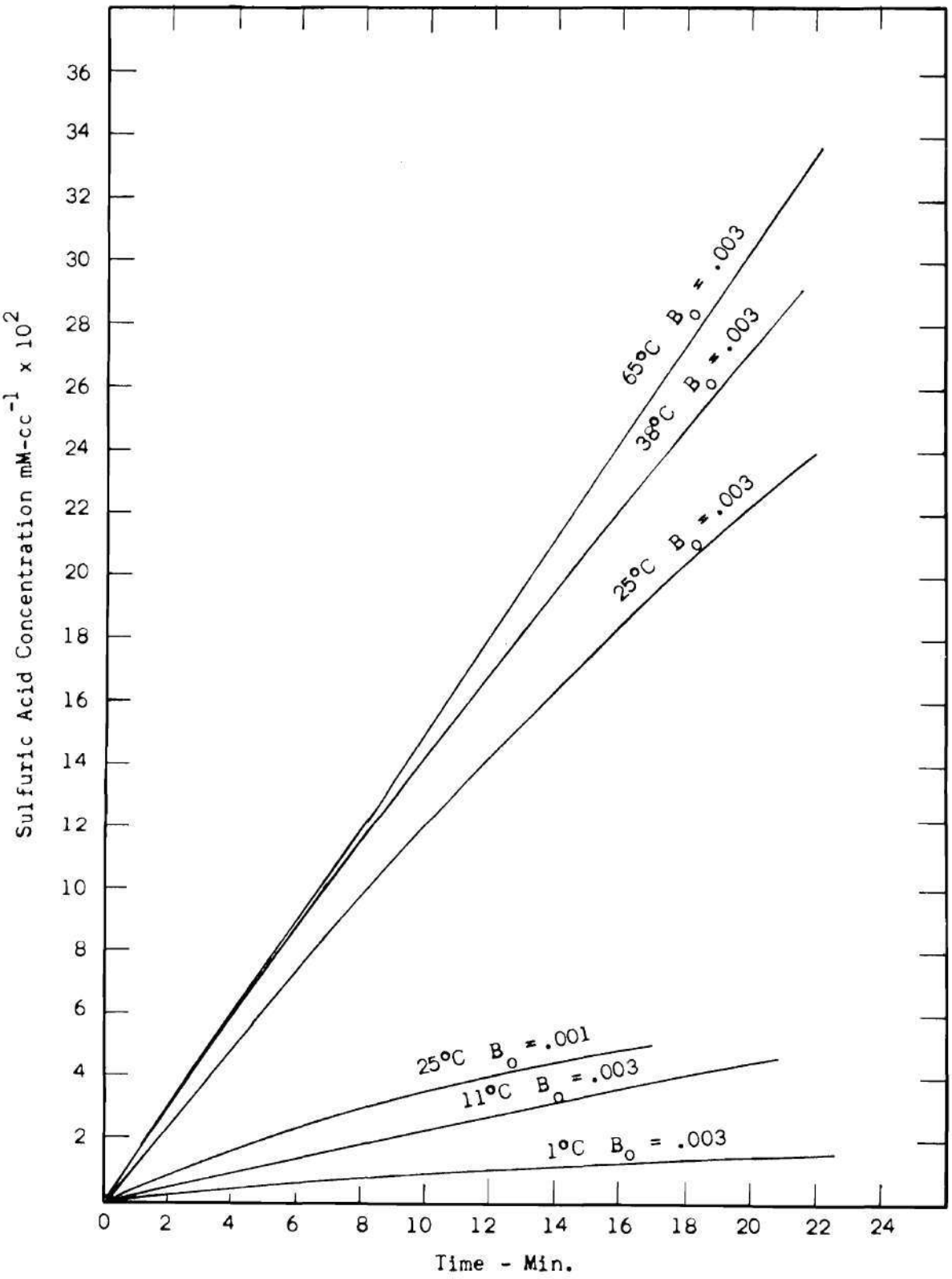

Figure 4. Sulfuric Acid Concentration vs. Time for Various Temperatures.

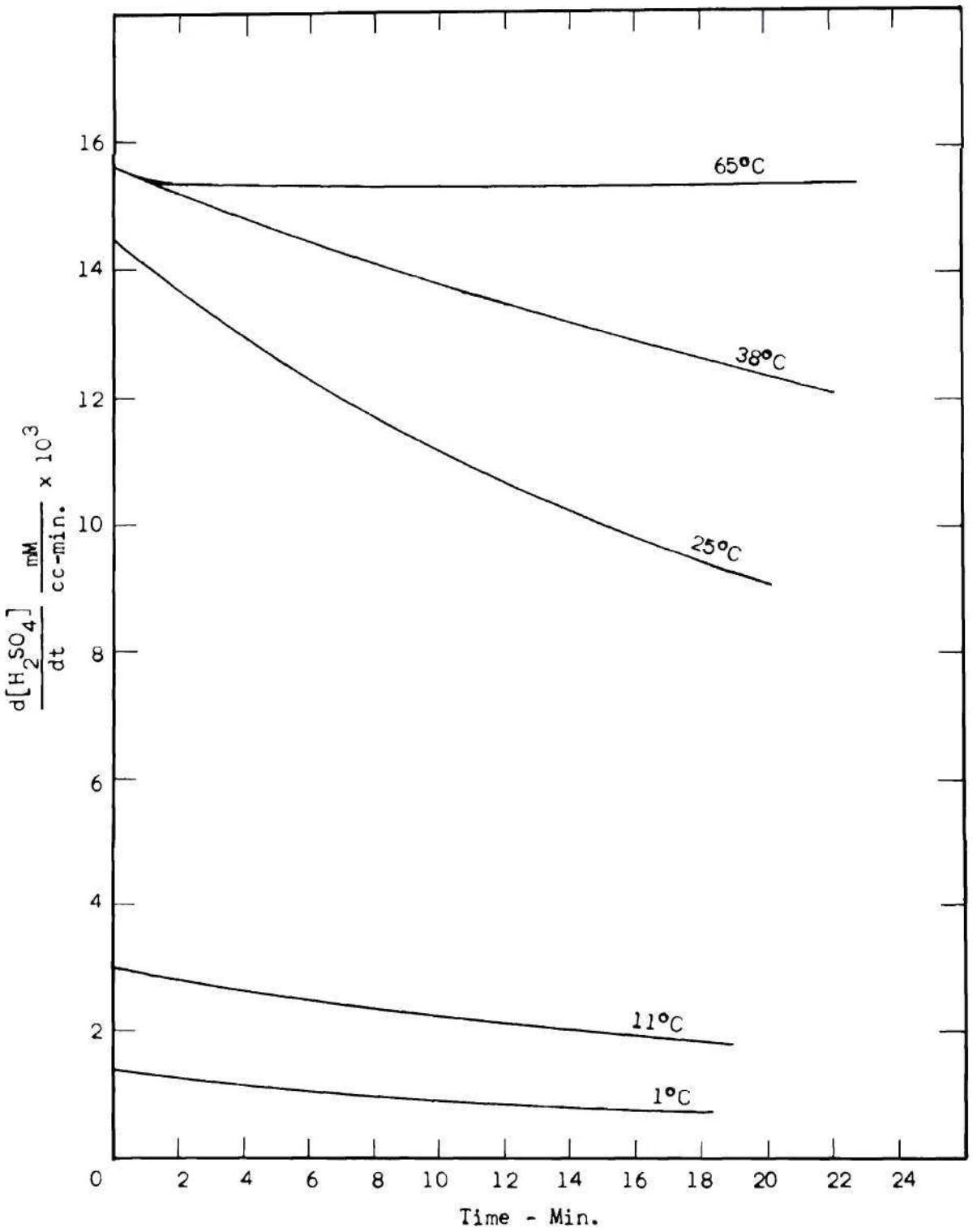

Figure 5. Sulfuric Acid Formation Rate vs. Time For Various Temperatures.

difficult over the extended runs because of the constantly changing equilibrium vapor pressure of water vapor over the sulfuric acid solution. For this reason the accuracy of this data plotted in Figure 6 is probably on the order of ±10%. Volume control was so erratic at 65°C (the water vapor content of saturated air at 65°C is 8 fold higher than at 25°C) that a run of over 40 minutes at this temperature was considered too inaccurate.

Rate Constant Determinations

Rate constants k_1, k_2', k_6', and k_7 in the reaction series below were evaluated for each of the five temperatures. The significance of the primed value will be explained later.

$$SO_2 + Mn^{2+} \underset{k_2}{\overset{k_1}{\rightleftharpoons}} Mn\cdot SO_2^{2+} \qquad \text{(IV-1)}$$

$$2Mn\cdot SO_2^{2+} + O_2 \underset{k_4}{\overset{k_3}{\rightleftharpoons}} (Mn\cdot SO_2^{2+})_2\cdot O_2 \underset{k_5'}{\overset{k_5}{\rightleftharpoons}} 2Mn\cdot SO_3^{2+} \qquad \text{(IV-2)}$$

$$Mn\cdot SO_3^{2+} + H_2O \underset{k_7}{\overset{k_6}{\rightleftharpoons}} Mn^{2+} + HSO_4^- + H^+ \qquad \text{(IV-3)}$$

$$HSO_4^- + H^+ \rightleftharpoons H_2SO_4 \qquad \text{(IV-4)}$$

The following is a description of the procedure used to arrive at an estimated value for each of the rate constants.

Concentrations of the components are designated by the following symbols. All concentrations are millimoles per cc of liquid solution.

$B_o = [Mn^{2+}]_o$, initial catalyst concentration

$R = [SO_2]$, conc. of SO_2 dissolved in liquid

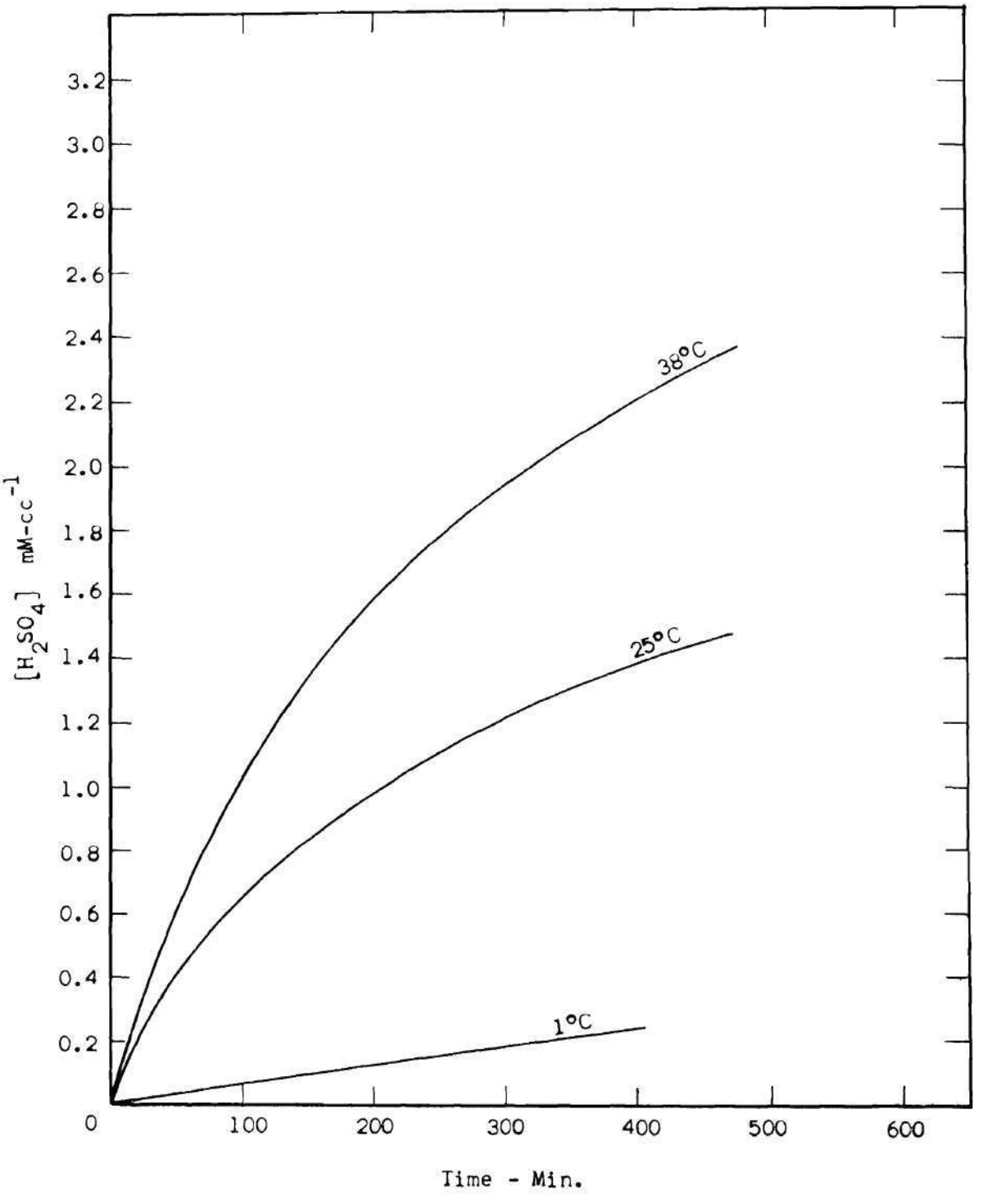

Figure 6. H_2SO_4 Concentration vs. Time at 1°C, 25°C, and 38°C for Extended Periods of Time.

$$J = [HSO_4^-] = [H^+]$$

$$D = [Mn{\cdot}SO_2^{2+}]$$

$$E = \frac{1}{2}[(Mn{\cdot}SO_2^{2+})_2{\cdot}O_2]$$

$$F = [Mn{\cdot}SO_3^{2+}]$$

$$X = D + E + F$$

$$B = [Mn^{2+}] = B_o - X \text{ by Stoichiometry}$$

Rates of formation of the manganese complexes:

$$\frac{dD}{dt} = k_1R[B_o - X] - k_2D - 2k_3[O_2]D^2 + 2k_4E^2 \qquad \text{(IV-5)}$$

$$\frac{dE}{dt} = 2k_3D^2[O_2] - 2k_4E^2 - 2k_5E^2 + 2k_5'F^2 \qquad \text{(IV-6)}$$

$$\frac{dF}{dt} = 2k_5E^2 - k_6[H_2O]F - 2k_5'F^2 + 2k_7[B_o - X]J^2 \qquad \text{(IV-7)}$$

since $$X = D + E + F, \quad \frac{dX}{dt} = \frac{dD}{dt} + \frac{dE}{dt} + \frac{dF}{dt} \qquad \text{(IV-8)}$$

$$\frac{dX}{dt} = k_1R[B_o - X] - k_2D - k_6[H_2O]F - 2k_7[B_o - X]J^2 \qquad \text{(IV-9)}$$

Assuming that the proportion of each complex to the total complex concentration is constant,

$$D = \left(\frac{D}{D+E+F}\right)X \qquad \text{(IV-10)}$$

$$F = \left(\frac{F}{D+E+F}\right)X \qquad \text{(IV-11)}$$

and

$$k_2D = k_2'X \qquad \text{(IV-12)}$$

$$k_6[H_2O]F = k_6'X \qquad \text{(IV-13)}$$

$$\frac{dX}{dt} = k_1R(B_o - X) - k_2'X - k_6'X + 2k_7(B_o - X)J^2 \qquad \text{(IV-14)}$$

From equation (IV-3)

$$\frac{dJ}{dt} = k_6'X - 2k_7(B_o - X)J^2 \qquad \text{(IV-15)}$$

Equations (IV-14) and (IV-15) lend themselves to analysis by the slope-intercept technique. At time zero when sulfuric acid concentration is zero, the reciprocal rate of acid formation is a linear function of R_o^{-1} and the rate constants k_6' and K_s' can be determined by the slope and the intercept. The development of the slope intercept technique for this application is detailed below.

Setting dX/dt equal to zero (steady state hypothesis) and considering the initial reaction near time zero when J = 0

$$\frac{dX}{dt} = 0 = k_1R_o(B_o - X_o) - k_2'X_o - k_6'X_o \qquad \text{(IV-16)}$$

$$X_o = \frac{k_1R_oB_o}{k_1R_o + k_2' + k'_6} \qquad \text{(IV-17)}$$

Divide through by k_1R_o and let $K_s' = (k_2' + k_6')/k_1$: (IV-18)

$$X_o = \frac{B_o}{1 + K_s'/R_o} \qquad \text{(IV-19)}$$

From equation (IV-15):

$$\frac{dJ}{dt} = k_6'X - 2k_7(B_o - X)J^2 \qquad \text{(IV-15)}$$

Initially

$$\left(\frac{dJ}{dt}\right)_o = k_6' X_o = \frac{k_6' B_o}{1 + K_s'/R_o} \qquad \text{(IV-20)}$$

For 25°C, four tests were made at an initial manganese concentration of B_o = .003 mM/cc and each at a constant but different SO_2 gas concentration into the reaction with the four tests covering the range from 3460 PPM to 4748 PPM which resulted in R_o varying from 6.2×10^{-4} to 2.6×10^{-3} mM/cc. Seven tests were made at an initial manganese concentration of .001 with SO_2 gas concentrations such that R_o covered the range from 1.6×10^{-3} to 6.6×10^{-3}. All of the above tests were at 25°C. From the experimental values for $(dJ/dt)_o$ and R_o from these tests, k_6', and K_s' were determined. By inverting equation (IV-20)

$$\frac{1}{(dJ/dt)_o} = \frac{1}{k_6' B_o} + \frac{K_s'}{k_6' B_o} \cdot \frac{1}{R_o} \qquad \text{(IV-21)}$$

and plotting $\frac{1}{(dJ/dt)_o}$ vs. $\frac{1}{R_o}$, k_6' is determined by the intercept; $k_6' = ((\text{intercept})(B_o))^{-1}$, and K_s' is determined by the slope; $K_s' = (\text{slope})\ (k_6')(B_o)$. A graph of $\frac{1}{(dJ/dt)_o}$ vs. R_o for 25°C is shown in Figure 7.

Similar treatment at other temperatures yielded results as listed in Table 1 below.

Table 1. Slope-intercept Data for k_6' and K_s'

Temp.	B_o	Intercept	k_6'	Slope	K_s'
1°C	.003	600	.56	1.95	3.25×10^{-3}
11°C	.003	256	1.3	1.89	7.35×10^{-4}
25°C	.001	238	4.2	1.23×10^{-2}	5.16×10^{-5}
25°C	.003	84.4	4.0	3.12×10^{-3}	3.74×10^{-5}
38°C	.003	67.8	4.9	3.4×10^{-4}	5×10^{-6}
65°C	.003	51	6.6	1.01×10^{-5}	2×10^{-7}

Figure 8 is a plot of log k_6' vs. $1/T°K$. Two significant facts emerge at this point: k_6' vs. $1/T$ is not a straight line and the value of k_6' at 25°C varies from the value obtained by MSL[4] by an order of magnitude, 0.22 min^{-1} by MSL[4] compared to 4.1 by this work. Since k_6' contains the assumed constant F/X there is no irrevocable reason why k_6' should have a linear relationship to reciprocal absolute temperature. The nonlinearity could be explained by a variation of F/X with temperature. The higher value of k_6' could be similarly explained by a difference in F/X at the same temperature, possibly caused by the difference in SO_2 concentrations; 100 PPM in gas by MSL[4] and 3000 - 5000 PPM in this work.

The method planned for determining k_7 was to continue a test until the SO_2 concentration was the same in the exit gas stream as it was in the feed stream. At this point ($dJ/dt = 0$) and k_7 can be determined from Equation (IV-15)

$$\frac{dJ}{dt} = 0 = k_6'X_o - 2k_7(B_o - X_o)J^2_{\frac{dJ}{dt}=0} \qquad \text{(IV-22)}$$

$$k_7 = \frac{k_6'X_o}{2J^2_{\frac{dJ}{dt}=0}(B_o - X)} \qquad \text{(IV-23)}$$

By substituting $X_o = \frac{B_o}{1 + K_s'/R_o}$ into Equation (IV-23)

$$k_7 = \frac{k_6'R_o}{2J^2_{\frac{dJ}{dt}=0}K_s'} \qquad \text{(IV-24)}$$

or

$$J^2_{\frac{dJ}{dt}=0} = \frac{k_6' R_o}{2k_7 K_s'} \qquad \text{(IV-25)}$$

Equation (IV-25) indicates the acid concentration at ($dJ/dt = 0$) is independent of the catalyst concentration.

Consequently, tests of several hours duration were made at 1°C, 25°C and 38°C with a SO_2 gas concentration of ~4200 PPM. Very low values of acid formation rate were reached which were nearly constant and zero rate was obtained by adding concentrated sulfuric acid to the liquid. The liquid was then titrated with standard NaOH to determine the value of J at $dJ/dt = 0$, enabling k_7 to be determined from Equation (IV-24). The subsequent calculated values of k_7 are given in Table 2 and plotted on Figure 9.

Table 2. Estimated Rate Constant k_7 at Various Temperatures

Temp.	k_6'	K_s'	R_o	$J_{\frac{dJ}{dt}=0}$	k_7	
1°C	0.56	3.25×10^{-3}	0.01956	0.58	4.2	
11°C	1.3	7.35×10^{-4}	0.00957	1.1	7.9	(interpolated)
25°C	4.1	4.45×10^{-5}	0.00249	2.5	18.4	
38°C	4.9	5×10^{-6}	0.0012	4.0	36.8	
65°C	6.6	2×10^{-7}	0.000631	9.0	14.0	(extrapolated)

The question which arises at this point is whether the acid concentration at $dJ/dt = 0$ represents approximate reaction equilibrium or is it merely the result of a negative self catalytic reaction as observed by Junge and Ryan. To settle this matter an attempt was made to calculate the acid equilibrium concentration by Equation (IV-27) and (IV-28) below for the overall reaction:

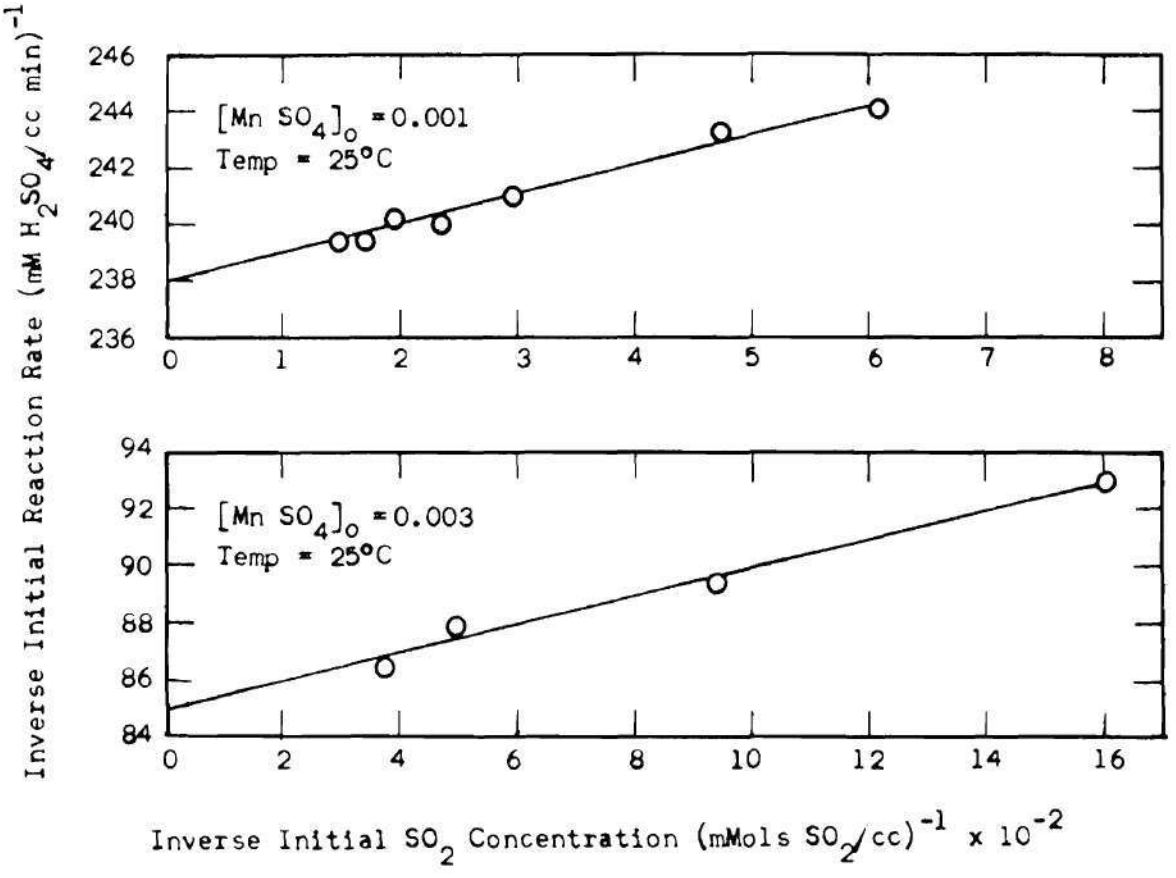

Figure 7. Inverse Initial Reaction Rate vs. Inverse Initial SO_2 Concentration for Determination of Rate Constants k_6' and K_s' at 25°C.

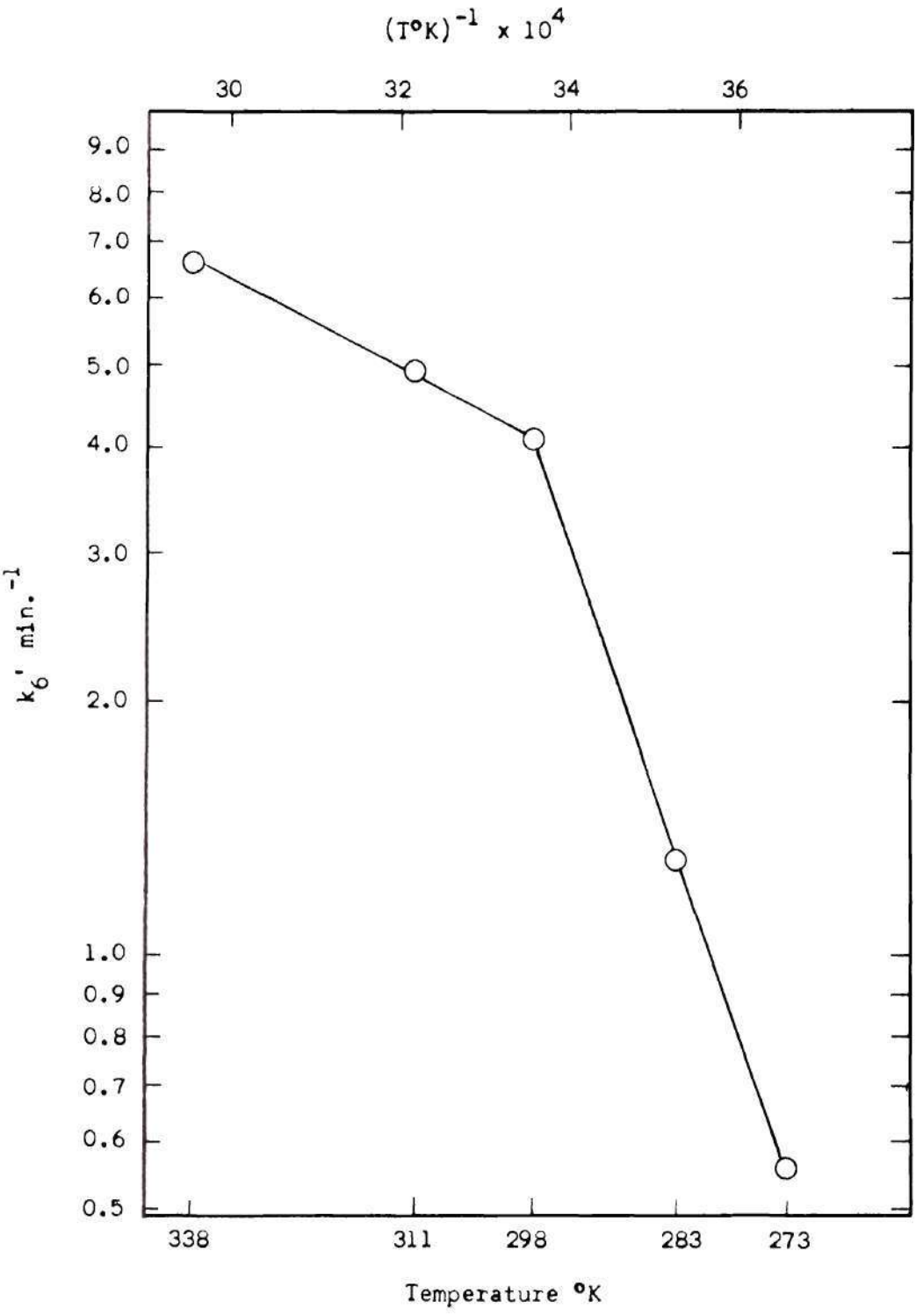

Figure 8. Log k_6' vs. $(T°K)^{-1}$.

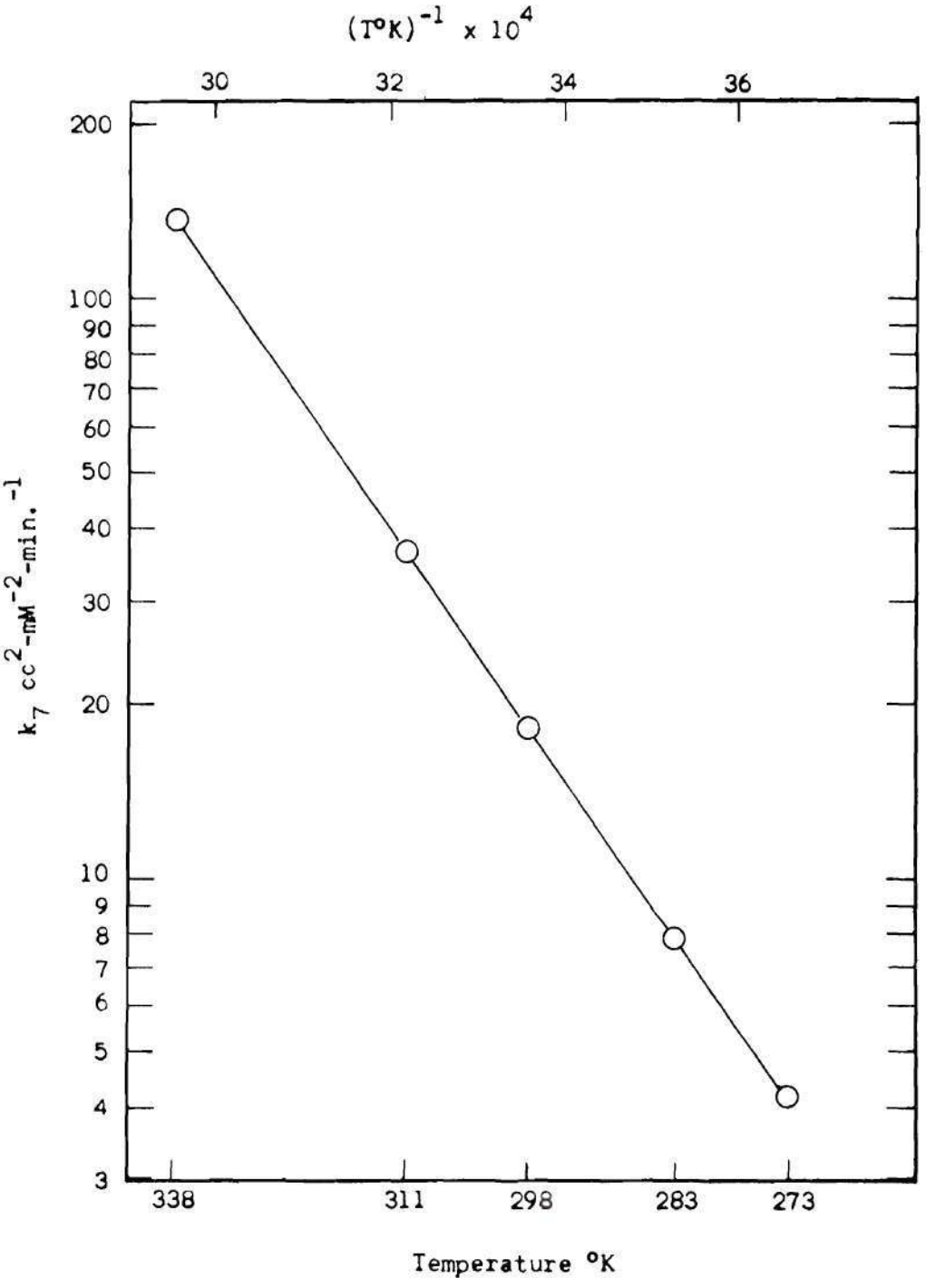

Figure 9. Log k_7 vs. $(T°K)^{-1}$.

$$SO_2(aq) + \frac{1}{2} O_2(aq) + H_2O(\ell) \xrightarrow{Mn^{++}} H_2SO_4(aq) \qquad \text{(IV-26)}$$

$$\sum \nu_i \mu_i = 0 \qquad \text{(IV-27)}$$

$$- RT \ln \frac{\gamma_{\pm}^{\nu} \, m_{H^+}^{\nu_{H^+}} \, m_{HSO_4^-}^{\nu_{HSO_4^-}}}{P_{SO_2} \, P_{O_2}^{1/2} \, P_{H_2O}} = \nu_{H^+}\mu^{\square}_{H^+} + \nu_{HSO_4^-} \mu^{\square}_{HSO_4} - \mu^{o}_{SO_2} - \frac{1}{2}\mu^{o}_{O_2} - \mu^{o}_{H_2O} \qquad \text{(IV-28)}$$

where

R = gas constant

T = temperature, °K

$\gamma_{\pm}$ = mean activity coefficient of sulfuric acid in aqueous solution

ν = number of ions obtained by dissociation of one molecule of electrolyte

m = molality

$\mu^{\square}$ = chemical potential of ion in a hypothetical ideal solution in which molality of ion is unity

μ^{o} = chemical potential of pure substance at 25°C and 1 atm

Equation (IV-28) incorporates the following assumptions: the effect of the manganese ion and complexes is ignored since in this work the initial Mn^{++} concentration was quite low, .001 - .003 mM/cc. The fugacity of the species in the gas phase is equal to the fugacity in the liquid phase at equilibrium, so the fugacity in gas phase was used. At pressure of 1 atm and temperature of 298°K, ideal gas law assumption is reasonable so partial pressures of gases were used for fugacity. As will be discussed below a molality of H_2SO_4 of 17.5 was chosen because the

degree of second ionization is low, .14, and was ignored for simplicity of calculation.

The method chosen in which to use Equation (IV-28) to test the 2.5 mM/cc H_2SO_4 concentration for thermodynamic equilibrium was to select a value for molality of H_2SO_4, substitute into Equation (IV-28), solve for p_{SO_2}, compare calculated p_{SO_2} with actual $p_{SO_2} = 4.3 \times 10^{-3}$ atm. The first value chosen for H_2SO_4 molality was 17.5 which corresponds to 11.4 mM/cc, a value considerably higher than the 2.5 mM/cc value being tested. Therefore, if 2.5 mM/cc is truly an equilibrium value, the calculated p_{SO_2} for 17.5 molal should be much higher than experimental p_{SO_2} of 4×10^{-3} atm. The calculated p_{SO_2} was 10^{-31} atm, considerably lower than experimental p_{SO_2}. The only conclusion to be drawn, therefore, is that both 2.5 mM/cc and 11.4 mM/cc are lower than the value at equilibrium. The values for $\gamma_\pm$ and concentration of H_2O vapor in equilibrium with $H_2SO_4(aq)$ for stronger solutions were not found in the literature, but as H_2SO_4 concentration increases, $\gamma_\pm$ increases and p_{H_2O} decreases rapidly, giving a higher calculated p_{SO_2}. The details of the calculation are given in Appendix B. It should be noted here that the water vapor concentration in the gas stream can not be arbitrarily specified because as is indicated by the phase rule, too many variables are specified:

$$D = C - R + 2 - \varphi$$

D = number of intensive variables that can be specified

C = number of species = 7, SO_2, N_2, O_2, H_2O, H^3O^+, HSO_4^-, H_2SO_4

R = number of reactions = 2

φ = number of phases = 2

D = 7 - 3 + 2 - 2 = 4; temp., press., P_{SO_2}, P_{N_2}/pO_2

In the calculation, therefore, the water vapor concentration that is in equilibrium with the sulfuric acid concentration was used.

Constants k_1 and k_2' were estimated by solving Equation (IV-18)

$$K_s' = \frac{k_2' + k_6'}{k_1} \qquad \text{(IV-18)}$$

simultaneously with a rate equation for the change in dissolved SO_2 concentration developed as follows:

$$SO_2 + Mn^{++} \underset{k_2}{\overset{k_1}{\rightleftharpoons}} Mn \cdot SO_2^{2+} \qquad \text{(IV-29)}$$

$$\frac{dR}{dt} = -k_1 R(B_o - X) + k_2' X \qquad \text{(IV-30)}$$

where

$$k_2' = k_2 \frac{D}{X} \qquad \text{(IV-31)}$$

Equation (IV-30) does not describe the dissolved SO_2 situation completely. The reaction does not start with a fixed concentration of SO_2 which is diminished by reaction to sulfuric acid. Instead the SO_2 supply to the reaction is the constant flow of air - SO_2 gas into the liquid phase. As the reaction slows with decreasing acid concentration of the solution, the concentration of the SO_2 in the off gas increases which in turn tends to increase the liquid phase concentration which is in equilibrium with the off gas concentration by the solubility relationship. Offsetting

this trend is the decrease in solubility of the SO_2 in the liquid phase with increasing sulfuric acid concentration. The net result can be either a positive or negative rate of dissolved SO_2 concentration with time. A rate balance on the dissolved SO_2 in the liquid phase, equation (IV-32) is used.

Rate of dissolved SO_2 accumulation in liquid = Rate SO_2 into liquid by gas stream + Rate SO_2 generation in liquid by reaction - Rate SO_2 out of liquid by gas stream - Rate SO_2 depletion in liquid by reaction. (IV-32)

where

$$\text{Rate } SO_2 \text{ accumulation} = dR/dt \tag{IV-33}$$

$$\text{Rate } SO_2 \text{ in} = CAO \tag{IV-34}$$

$$\text{Rate } SO_2 \text{ generation} = k_2'X \tag{IV-35}$$

$$\text{Rate } SO_2 \text{ out} = CAG \tag{IV-36}$$

$$\text{Rate } SO_2 \text{ depletion} = k_1 R(B_o - X) \tag{IV-37}$$

Combining equations (IV-34) and (IV-36), rate SO_2 into liquid - rate SO_2 out of liquid = RA = rate of SO_2 transferred to liquid phase.

$$\frac{dR}{dt} = RA + k_2'x - k_1R(B_o - x) \tag{IV-38}$$

From the continuous data on SO_2 concentration in gas out of reaction, dR/dt is known. Equation (IV-18) together with equation (3-38) can be used to estimate k_1 and k_2' at each temperature. The results are shown in Figures 10 and 11 and Table 3.

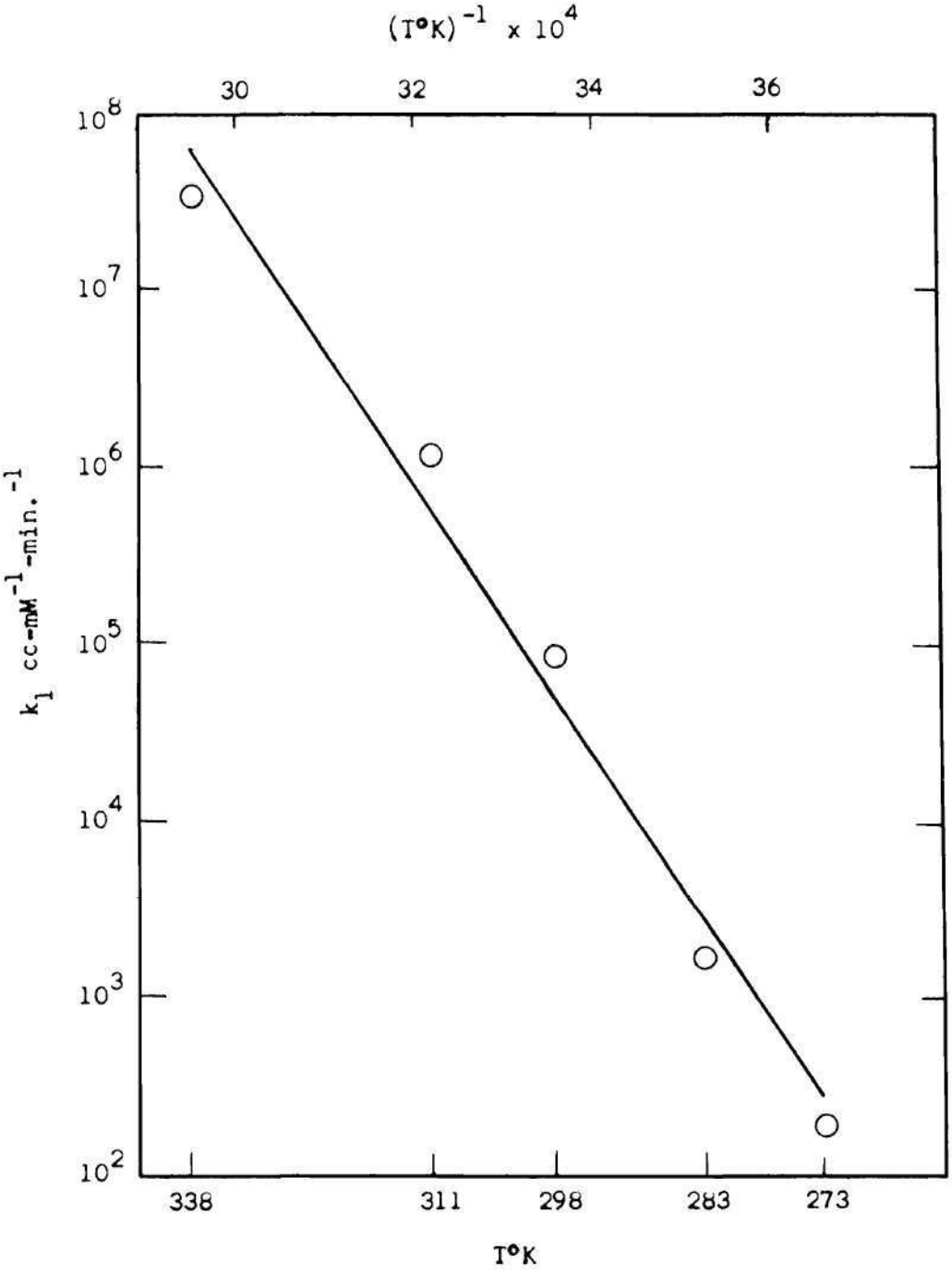

Figure 10. Log k_1 vs. $(T°K)^{-1}$.

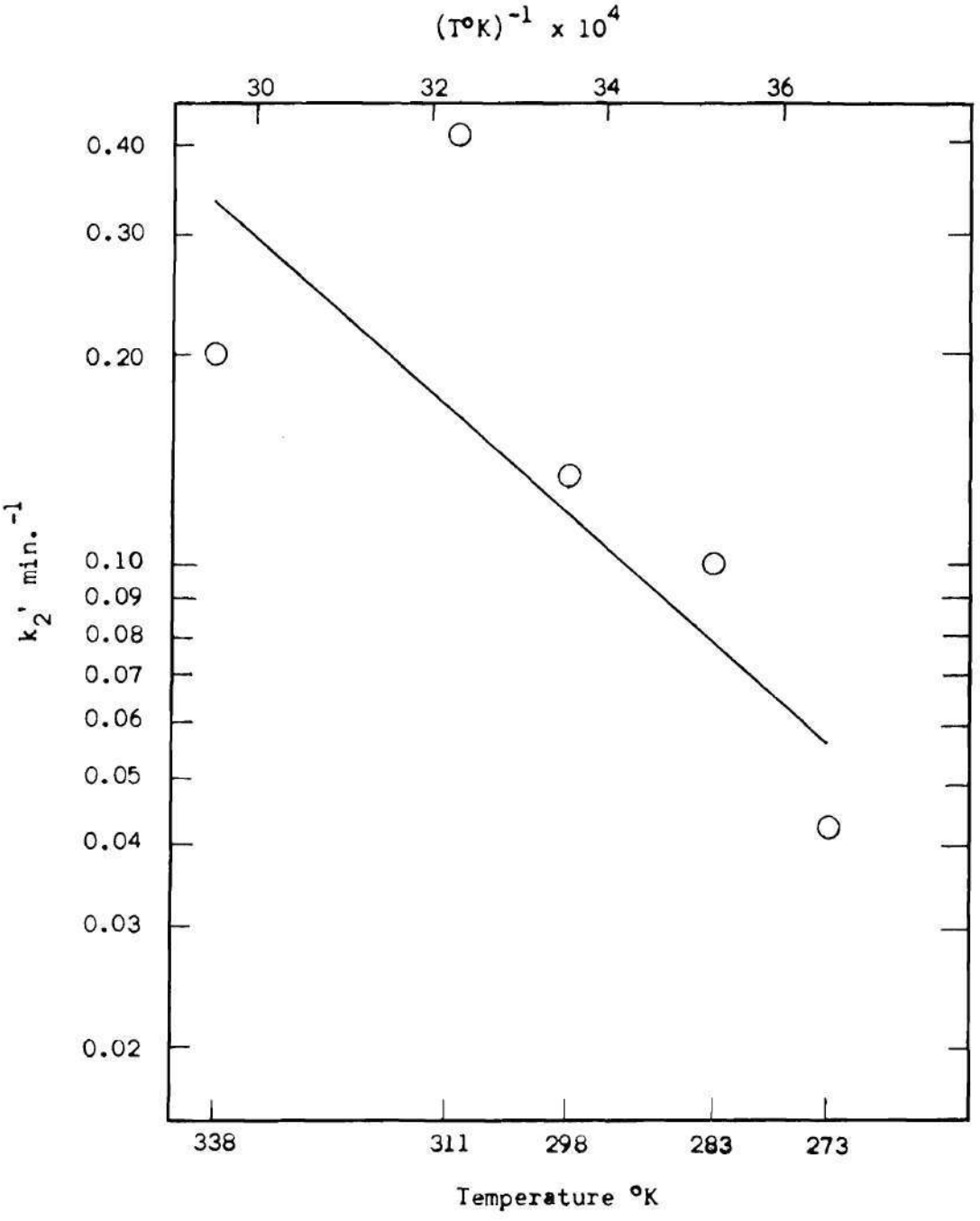

Figure 11. Log k_2' vs. $(T°K)^{-1}$.

Table 3. Estimated Rate Constants k_1 and k_2' at Various Temperatures

Temp.	k_1	k_2'
1°C	1.85×10^2	0.04
11°C	1.8×10^3	0.10
25°C	9.5×10^4	0.13
38°C	1.1×10^6	0.60
65°C	3.4×10^7	0.20

Calculated vs. Experimental Results

Equation (IV-15), the rate equation for the formation of sulfuric acid, can be integrated analytically, if X is considered constant:

$$\frac{dJ}{dt} = k_6'X - 2k_7(B_o - X)J^2 \qquad \text{(IV-15)}$$

$$J = \left[\frac{k_6'X}{2k_7(B_o - X)}\right]^{1/2} \text{TANH}\left[\{2k_6'k_7X(B_o - X)\}^{1/2}t\right] \qquad \text{(IV-39)}$$

Substituting

$$X_o = \frac{B_o}{1 + K_s'/R_o} \qquad \text{(IV-19)}$$

$$J = \left[\frac{k_6'R_o}{2k_7K_s'}\right]^{1/2} \text{TANH}\left[\frac{B_o(2k_6'k_7R_oK_s')^{1/2}t}{R_o + K_s'}\right] \qquad \text{(IV-40)}$$

Equation (IV-40) can be used to calculate acid concentration vs. time and incorporates the following assumptions:

1. The ratio of each complex to the sum of the complexes is constant; D/X, E/X, F/X are constant.

2. The rate of change of the sum of the complexes is zero, $dX/dt = 0$.

The second assumption is not necessary if Equations (IV-14) and (IV-15) are solved simultaneously.

These equations were solved by 4^{th} order Runga Kutta numerical integration for temperatures of 25°C and 38°C and the results compared with the experimental acid concentration and that calculated by Equation (IV-40). The results are shown in Table 4 and Figures 12 and 13. Figure 14 is a comparison of experimental acid conc. vs. time and calculated values by Equation (IV-40). The value for R was obtained by fitting the experimental R for each run to a polynomial function of time by the method of least squares. When the argument of the tanh function, equation (IV-40) is a low value such as when time, t, is a low value, the tanh function is approximately equal to its argument. In this case, J is a linear function of time and the plot of J vs. t is straight line and this is verified experimentally. That is, the reverse reaction rate is negligible when the sulfuric acid concentration is low, and dJ/dt is essentially constant, $k_6'X$. Since k_6' was determined from experimental initial reaction rates, a plot of calculated J vs. t for the first few minutes coincides exactly with the experimental curves, Figure 4.

As can be seen from the data, the assumption of constant complex concentration, X, introduces an error of up to 10% below values for sulfuric acid concentration calculated by equations (IV-14) and (IV-15). However, the calculated acid concentrations by these equations are approximately 70% higher than the experimental concentrations after the initial time when acid concentration is low. Although the accuracy of the experimental results was adversely affected by the volume control difficulties, this factor is not a sufficient explanation for the

Table 4. Calculated and Experimental Acid Concentration vs. Time for 1°C, 25°C, 38°C

Run 127
Temp: 25°C
$[Mn^{++}]_o$ = .003 mM-cc^{-1}
$[SO_2]_o$ = .0025 mM-cc^{-1}
X_o = .002947 mM-cc^{-1}

	$[H_2SO_4]$mM-cc^{-1}				
Time min.	Exp.	Eq. (40)	Eq's (14)+(15)	X, Eq's (14)+(15)	R, Exp.
0	0	0	0	0	0.0024910
25	0.27	.31	0.31	0.002955	0.0029966
54	0.43	.66	0.66	0.0029602	0.0034812
174	0.86	1.73	1.82	0.0029600	0.0045832
234	1.02	1.99	2.12	0.0029562	0.0047552
294	1.16	2.22	2.35	0.0029507	0.0048218
354	1.29	2.34	2.43	0.0029507	0.0047800
414	1.39	2.41	2.44	0.0029449	0.0046974
456		2.44	2.44	0.0029438	0.0046386
474	1.49				

Run 147
Temp: 38°C
$[Mn^{++}]_o$ = .003 mM-cc^{-1}
$[SO_2]_o$ = .0012 mM-cc^{-1}
X_o = .0029875 mM-cc^{-1}

	$[H_2SO_4]$mM-cc^{-1}				
Time min.	Exp.	Eq. (40)	Eq's (14)+(15)	X, Eq's (14)+(15)	R, Exp.
0	0	0	0	0	.0012
25	0.34	0.38	0.38	.0029906	.001602
53	0.64	0.78	0.78	.0029923	.001976
173	1.48	2.22	2.40	.0029942	.0029633
233	1.72	2.76	3.08	.0029941	.0031639
293	1.92	3.17	3.65	.0029936	.0032497
306	1.95	3.22	3.74		
353	2.09	3.40			
413	2.25	3.61			
473	2.37	3.7			

Table 4. (Continued)

Run 31
Temp: 1°C
$[Mn^{++}] = .003\ mM\text{-}cc^{-1}$
$[SO_2]_o = .0196\ mM\text{-}cc^{-1}$
$X_o = .0025741\ mM\text{-}cc^{-1}$

		$[H_2SO_4]$
Time, min.	Exp.	Eq. (40)
0		0
20	0.029	0.029
60	0.060	0.086
100	0.100	0.142
140	0.130	0.195
200	0.171	0.270
240	0.196	0.315
300	0.228	0.376
340	0.247	0.411
400	0.272	0.457
440		0.483
500		0.515

discrepancy between calculated and experimental results. There is no readily apparent reason why the model is accurate at an SO_2 concentration range of 10 - 100 PPM[4] but a discrepancy exists between the calculated rates and this experimental data at SO_2 gas concentration range of 3000 - 5000 PPM. Because the rate constant were estimated by methods involving possible inaccuracies, trial and error adjustments to the rate constants were attempted with results shown in Figure 15 and Table 5 for 25°C.

To solve equations (IV-14) and (IV-15) by Runga Kutta numerical integration required very small time increments. For the run at 25°C the time increment was .005 minutes, and .0005 minutes for 38°C. Since

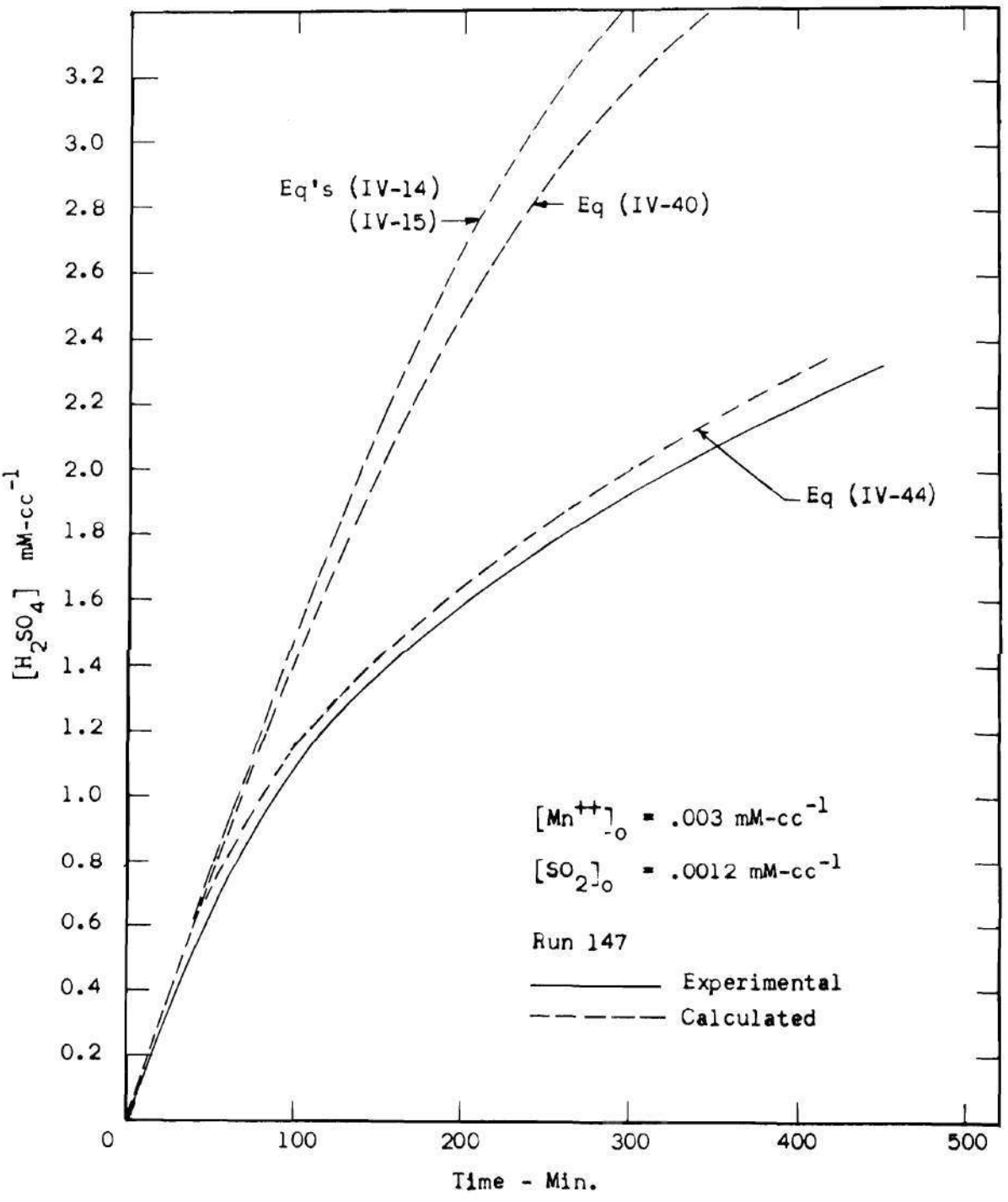

Figure 12. Sulfuric Acid Concentration vs. Time, 38°C.

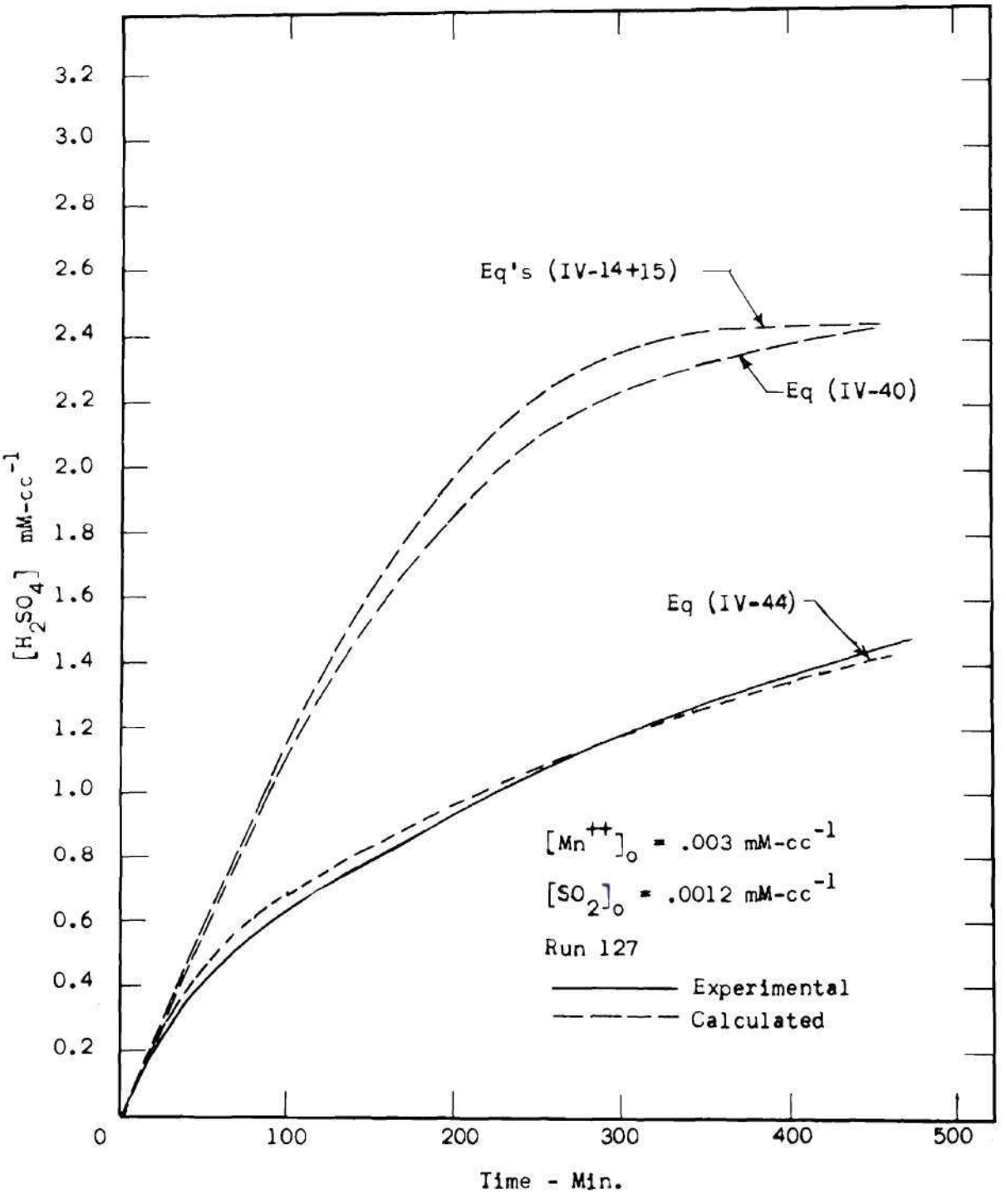

Figure 13. Sulfuric Acid Concentration vs. Time, 25°C.

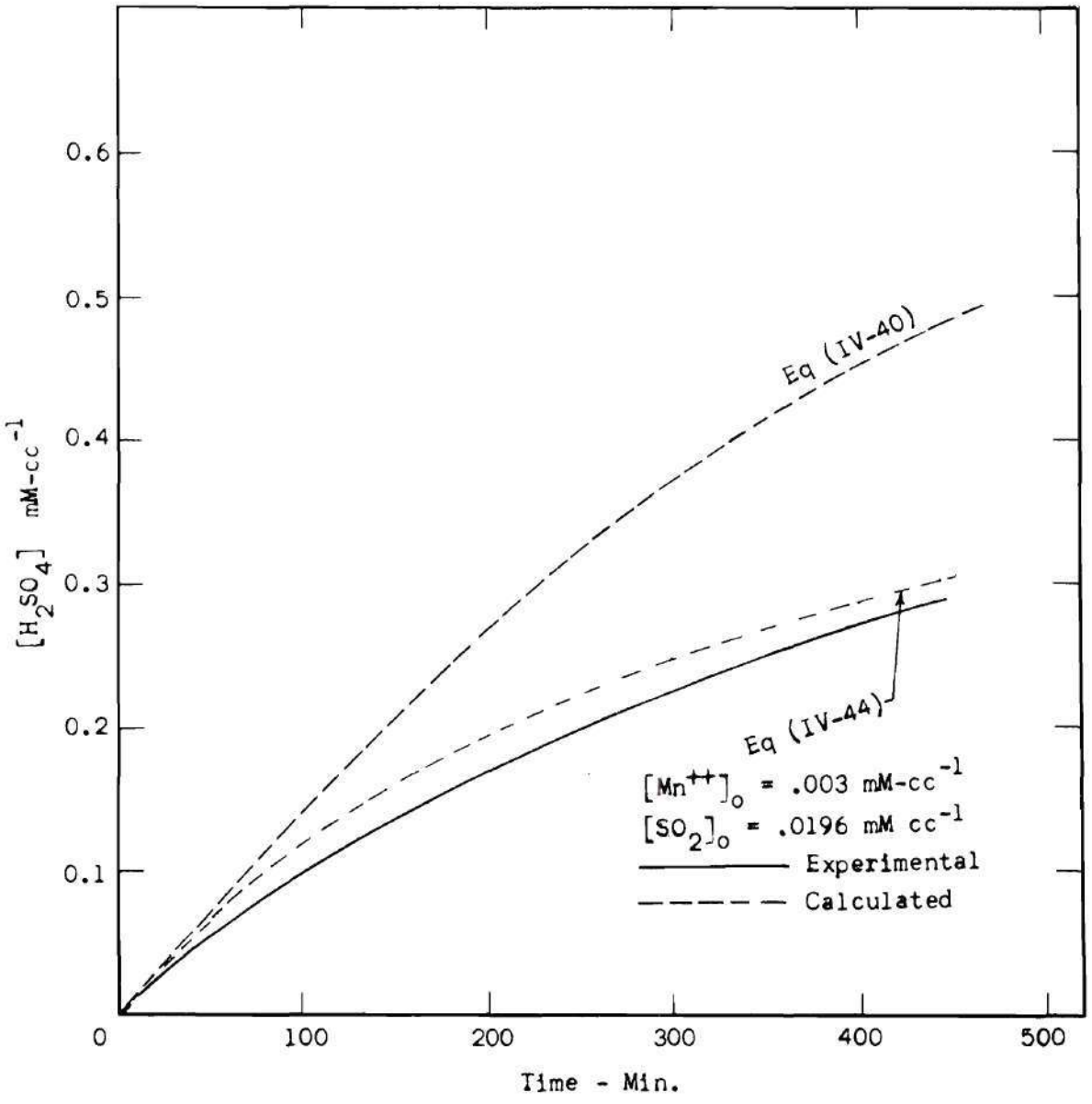

Figure 14. Sulfuric Acid Concentration vs. Time, 1°C.

the computer time per run was in the range of 2 - 5 minutes because of the required small time increment, and since there was little difference in results from solving the simultaneous differential equations and the single equation (IV-40), equation (IV-40) was used exclusively for all calculations other than the two Runga Kutta computer runs described above.

Table 5. Rate Constant Variations on Figure 15

Figure 10 Designation	k_6'	k_7	K_s'	Comment
Exp				Experimental
0	4.1	18.4	4.45×10^{-5}	Original estimated values
A	10.0	18.4	4.45×10^{-5}	k_6' varied independently - higher
B	0.4	18.4	4.45×10^{-5}	k_6' varied independently - lower
C	4.1	30.0	4.45×10^{-5}	k_7 varied independently - higher
D	4.1	60.0	4.45×10^{-5}	k_7 varied independently - higher
E	4.1	18.4	4.45×10^{-6}	K_s' varied independently - lower
F	4.1	18.4	4.45×10^{-4}	K_s' varied independently - higher

The small time increment is necessary apparently because the value of X is very close to B_o since $K_s' \ll R_o$. When X is incremented by the numerical integration procedure, the terms involving $(B_o - X)$ will go negative and the program blows up unless the increment of X is held to a low value by a small time increment. For a lower range of SO_2 concentration there should be much less of a problem.

The MSL model appears to describe the reaction very well in two respects: the zero order rate with respect to SO_2, and the initial rate proportional to catalyst concentration. It is qualitatively correct in predicting rate retardation with accumulation of sulfuric

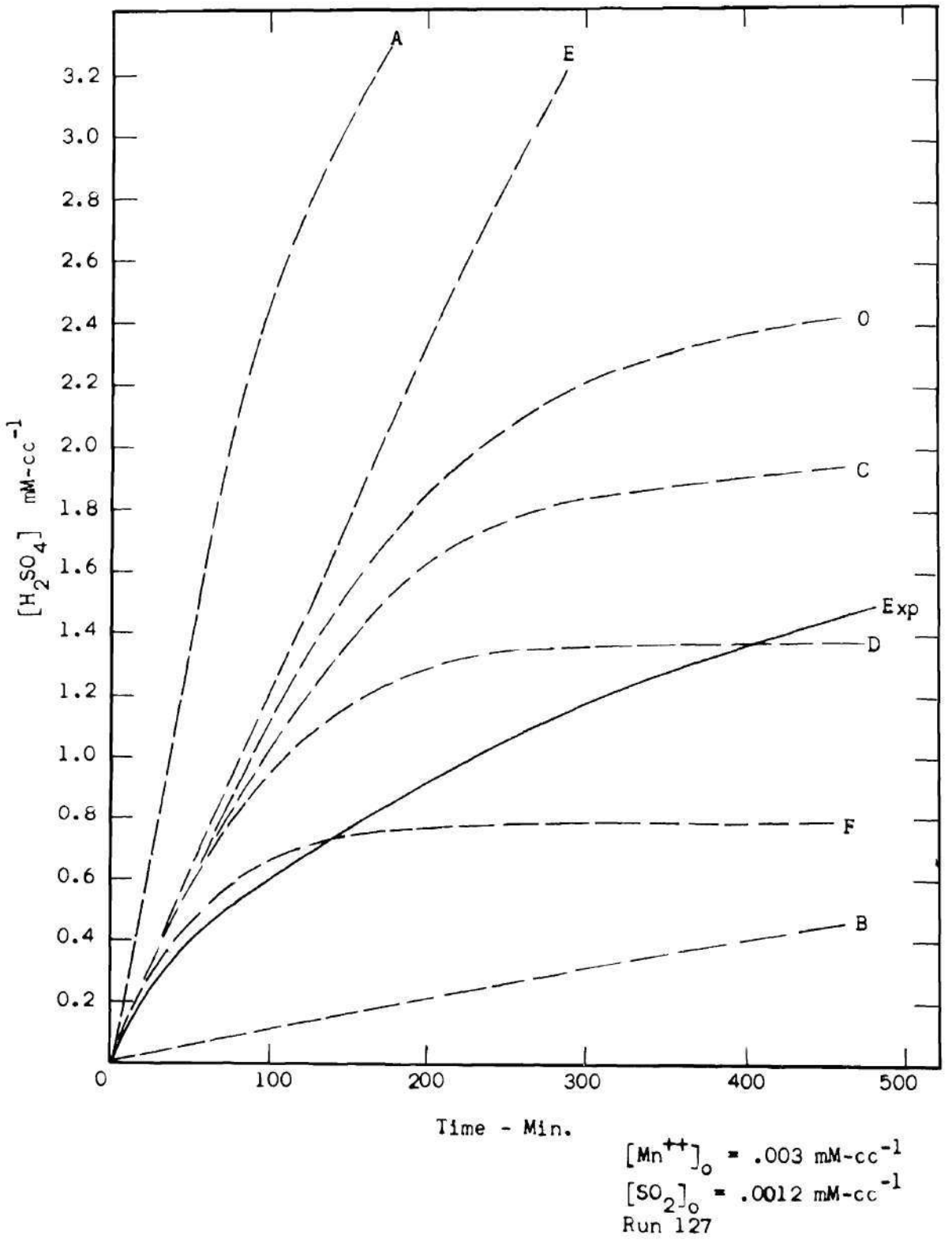

Figure 15. Sulfuric Acid Concentration vs. Time at 25°C with Rate Constant Variations.

acid, but does not give a quantitative fit to the data. By trial and error curve fitting it was found that the experimental data is modeled very closely by the expression:

$$\frac{dJ}{dt} = K \frac{1}{J} \qquad \text{(IV-41)}$$

Integration of Eq. (IV-41):

$$\int_o^J JdJ = K \int_o^t dt \qquad \text{(IV-42)}$$

$$J^2 = 2Kt \qquad \text{(IV-43)}$$

Table 6 and Figures 16, 17, and 18 show the straight line relationship obtained in plotting J^2 vs. t thus validating Eq.'s (IV-41) and (IV-43)

Table 6. Experimental Values of J and t Used in Figures 16, 17, and 18.

Temperature: 1°C

Time, min.	J mM/cc	J^2	J calc. by Eq (IV-44)
0	0	0	
20	0.029	0.0008	
60	0.060	0.0036	
100	0.100	0.0100	0.144
140	0.130	0.0169	
200	0.171	0.0292	0.204
240	0.196	0.0384	
300	0.228	0.0520	0.248
340	0.247	0.0610	
400	0.272	0.0740	0.288

Table 6. (Continued)

Time, min.	J mM/cc	J^2	J calc. by Eq (IV-44)
Temperature: 25°C			
0	0	0	
25	0.27	0.073	
54	0.43	0.185	
100			0.695
174	0.86	0.740	
200			0.981
234	1.02	1.04	
294	1.16	1.35	
300			1.20
354	1.29	1.66	
400			1.35
414	1.39	1.93	
474	1.49	2.22	
Temperature: 38°C			
0	0	0	
25	0.34	0.116	
53	0.64	0.410	
100			1.16
173	1.48	2.19	
200			1.642
233	1.72	2.96	
293	1.92	3.69	
300			2.01
306	1.95	3.80	
353	2.09	4.37	
400			2.32
413	2.25	5.06	
473	2.37	5.62	

The slope of the J^2 vs. t line in Figures 16, 17, and 18 yields values for K as follows:

Temperature	Slope = 2K	K $mM^2\text{-}cc^{-2}\text{-}min^{-1}$	$K' = \frac{K}{B_o}$ $\frac{mM}{cc\text{-}min}$
1°C	2.080×10^{-4}	1.040×10^{-4}	3.467×10^{-2}
11°C			1.4×10^{-1} (interp)
25°C	4.825×10^{-3}	2.412×10^{-3}	8.04×10^{-1}
38°C	1.350×10^{-2}	6.75×10^{-3}	2.25
66°C			24.0 (extrap.)

Calculated values of J vs t using Eq. (IV-44) are shown on Figures 12, 13, and 14 and Table 6

$$J = (2Kt)^{1/2} \qquad \text{(IV-44)}$$

In the range of initial concentrations of Mn^{++} of this work, .001 to .003 mM/cc the reaction rate has been found to be proportional to $[Mn^{++}]_o$ which is confirmed by the data of Coughanowr and Krause.[18] Therefore for this range of B_o, the acid concentration at any time t can be accurately expressed by Eq. (IV-45) with values of K' as shown above

$$J = (2K'B_o t)^{1/2} \qquad \text{(IV-45)}$$

K' for the other temperatures by interpolation and extrapolation are as shown above and in Figure 19. Figure 19, a graph of log K' vs $\frac{1}{1^oK}$, shows a fairly good linear relationship.

Humidity Effects

Air - SO_2 streams of varying humidity were bubbled through the aqueous Mn^{++} solution at 25°C to observe the effect of water evaporation into the gas bubbles on SO_2 gas diffusion within the gas bubble to the liquid interface. The results, Table 7 and Figure 17 indicate an approximate 14% decrease in SO_2 absorption rate as relative humidity of the gas stream is decreased from 100% relative humidity to near zero humidity for the first 15 minutes of the test. As the test proceeds for an extended time, evaporation into the gas stream of low humidity would cause an increase in both Mn^{++} and H_2SO_4 concentration with opposite effects on reaction rate.

Table 7. Effect of Humidity on SO_2 Absorption at 25°C

B_o = .003 V = 10 cc liq.
R_o = .002 V_o = 1018 cc/min

		mM SO_2 Absorbed per cc liq.			
Run No.	% Rel. Hum.	1 Min.	5 Min.	10 Min.	15 Min.
44	0	0.016	0.069	0.121	0.162
40	12.4	0.016	0.069	0.19	0.159
47	48.5	0.016	0.070	0.124	0.168
127	100.0	0.016	0.070	0.129	0.177

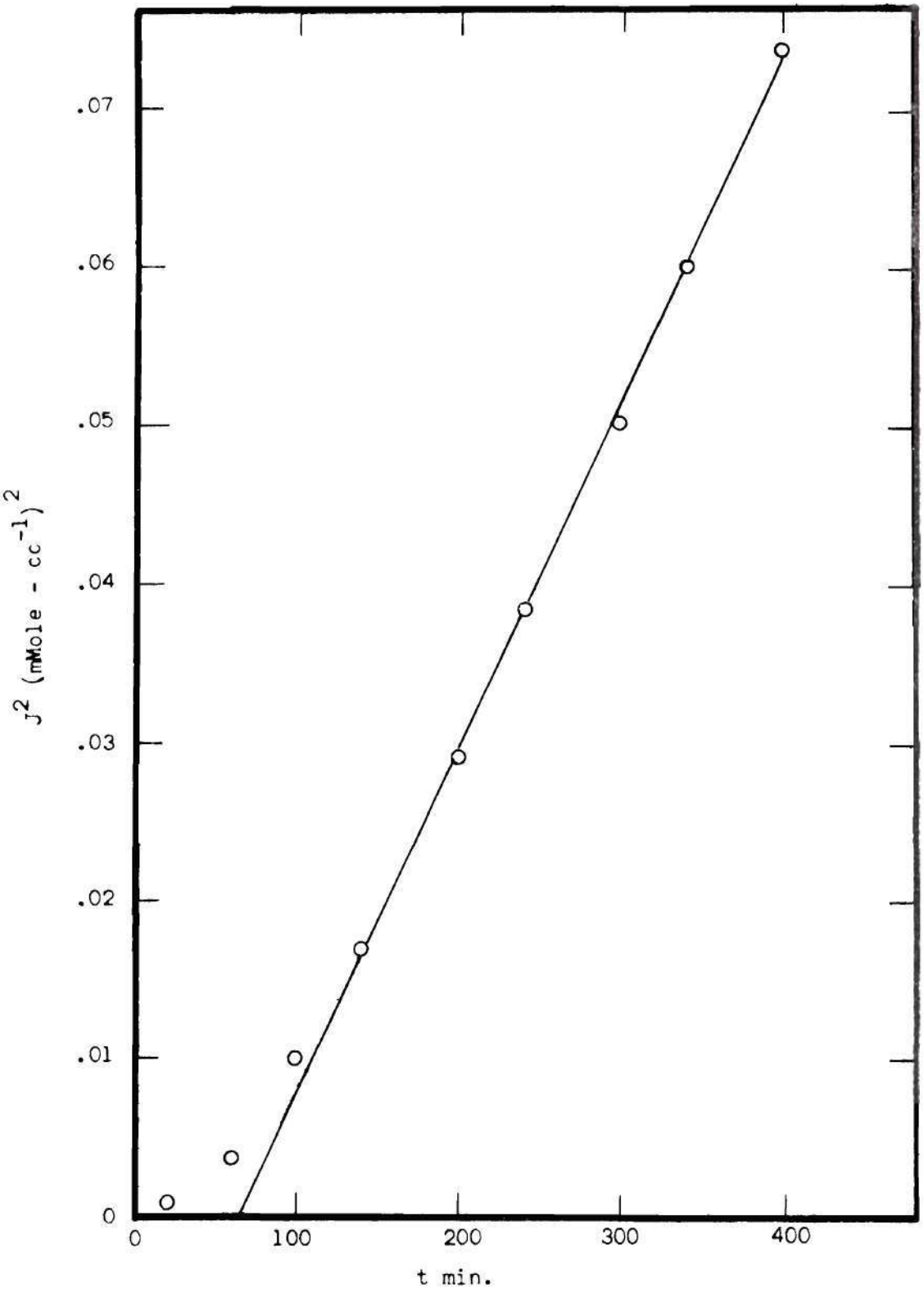

Figure 16. (Sulfuric Acid Conc.)^2 vs. Time for 1°C.

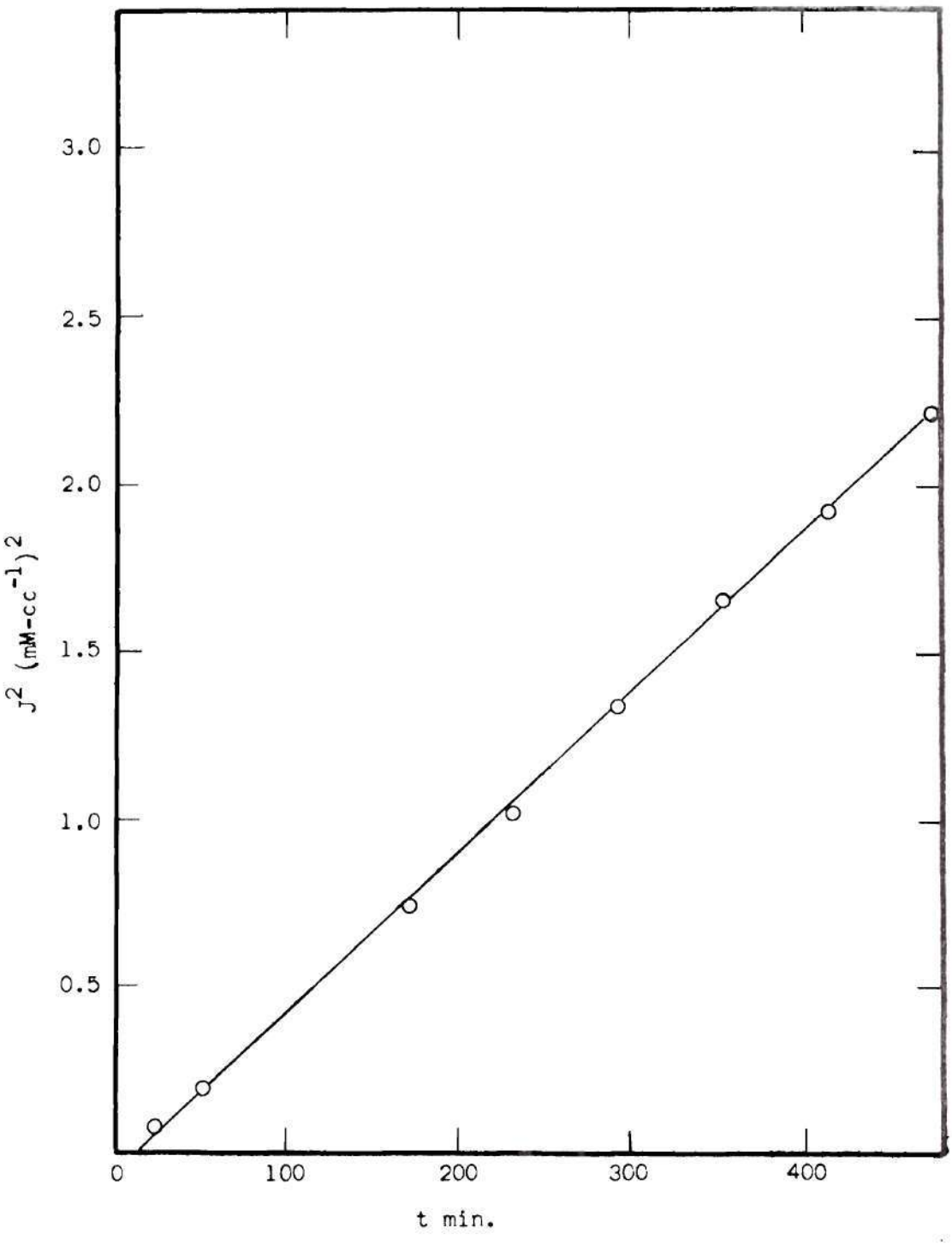

Figure 17. (Sulfuric Acid Conc.)^2 vs. Time, 25°C.

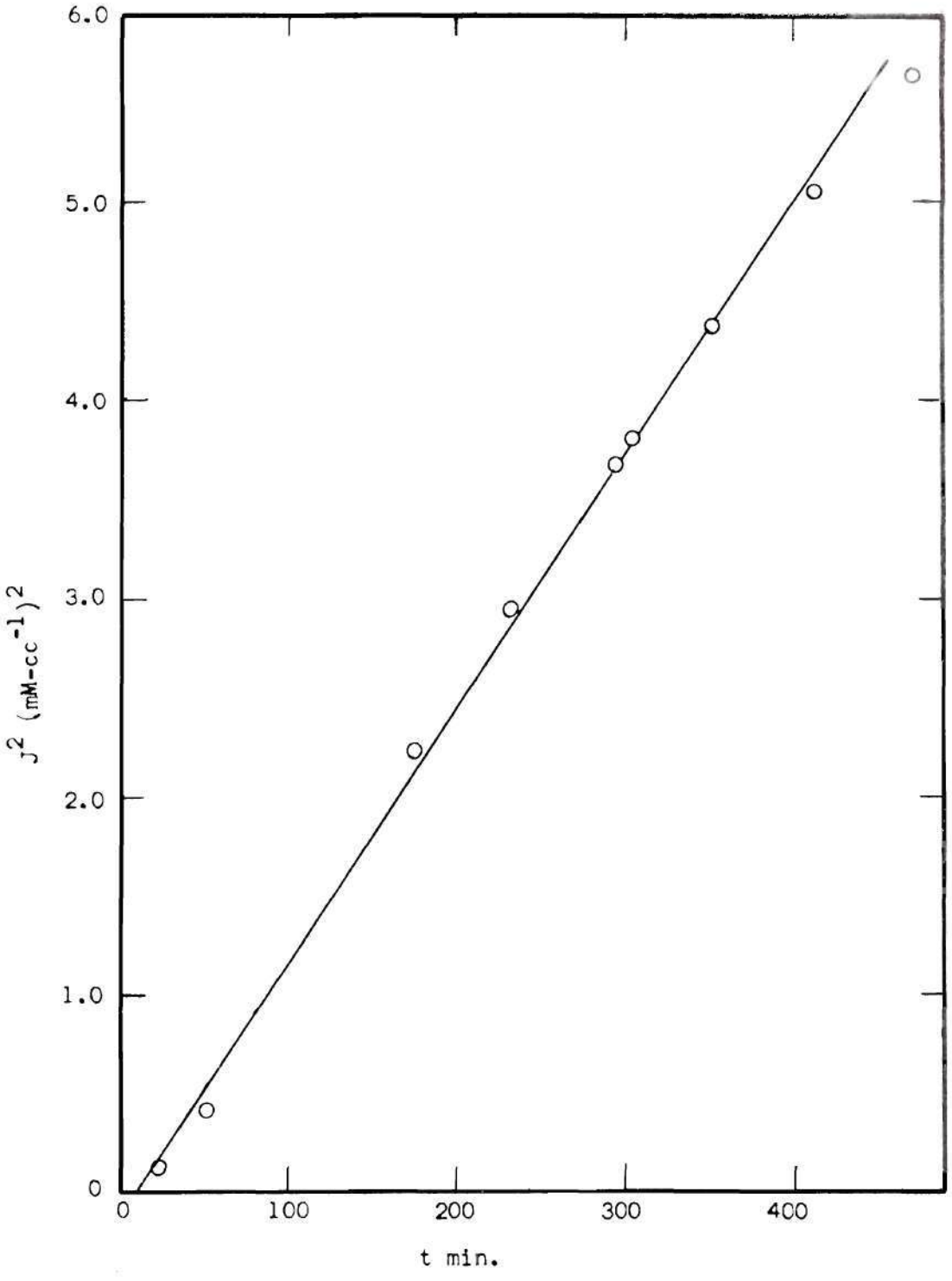

Figure 18. (Sulfuric Acid Conc.)^2 vs. Time for 38°C.

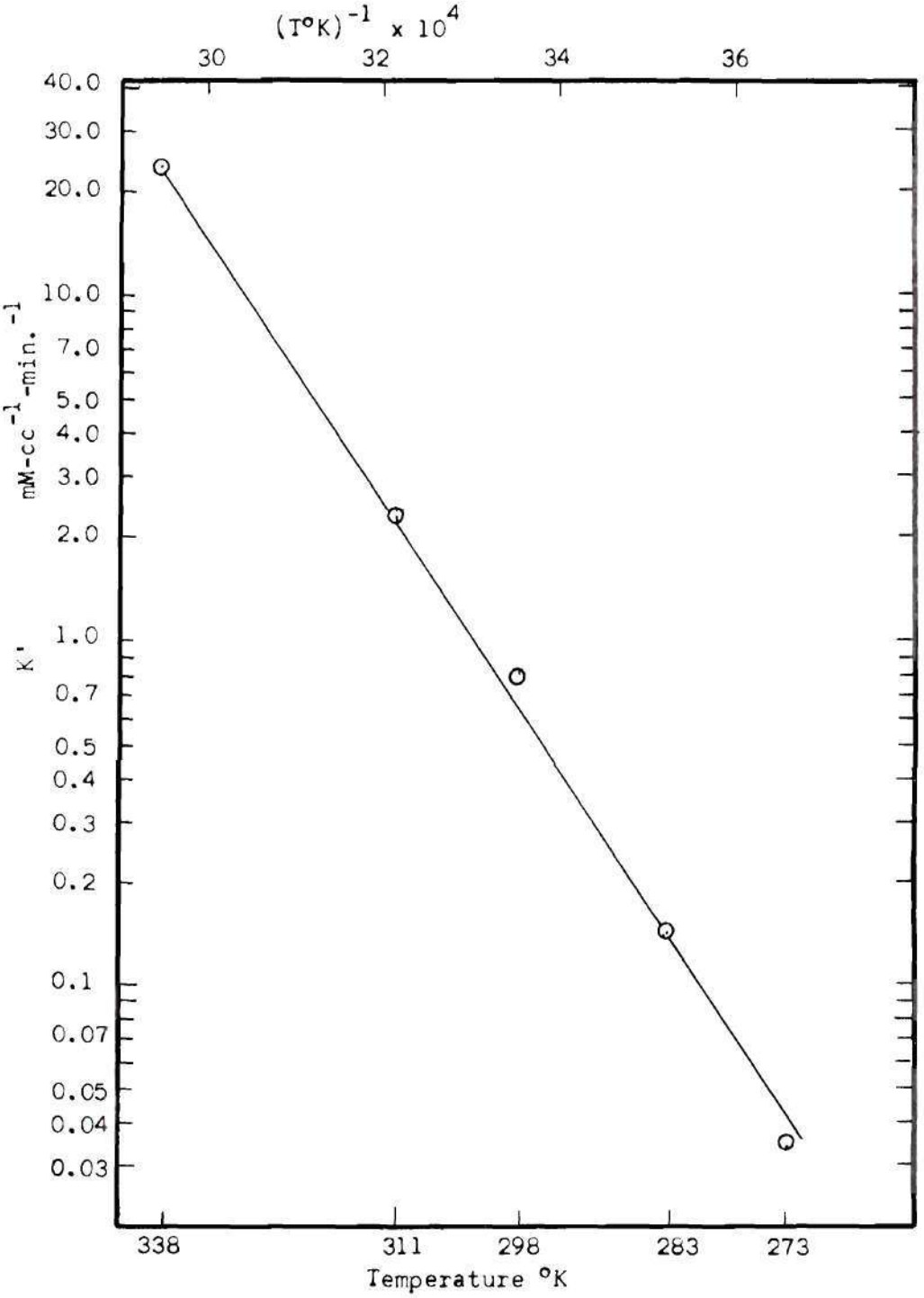

Figure 19. Log K' vs. $(T°K)^{-1}$.

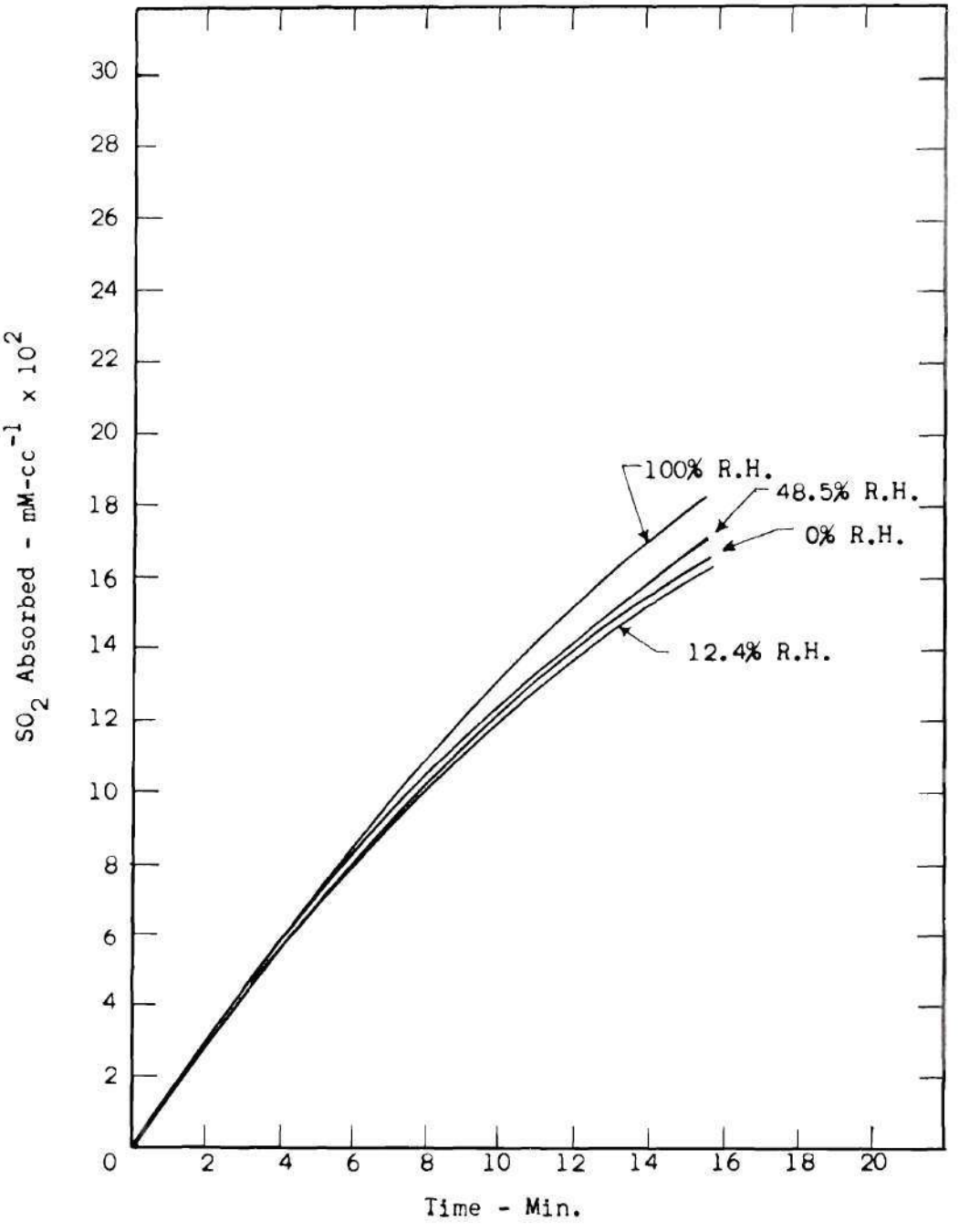

Figure 20. Effect of Gas Stream Humidity on SO_2 Absorption at 25°C.

CHAPTER V

CONCLUSIONS AND RECOMMENDATIONS

Conclusions

The rate of oxidation of SO_2 to sulfuric acid in aqueous solution of Mn^{++} ion can be described by equations (V-1) and (V-2).

$$\frac{d[H_2SO_4]}{dt} = \frac{K'[Mn^{++}]_o}{[H_2SO_4]} \qquad (V\text{-}1)$$

$$[H_2SO_4] = (2K'B_o t)^{1/2} \qquad (V\text{-}2)$$

This equation was tested for $[SO_2]_{liq}$ in equilibrium with an air -SO_2 gas mixture in the range of 3000 - 5000 PPM SO_2 and initial Mn^{++} concentration of .001 - .003 mM - cc^{-1}. Rate constants for Equation (V-1) and Equation (V-2) are as follows:

Temp.	K'
1°C	3.467×10^{-2}
11°C	1.4×10^{-1}
25°C	8.04×10^{-1}
38°C	2.25
66°C	24.0

The reaction rate decrease with increased sulfuric acid concentration is definitely not caused by the decreased solubility of SO_2. To demonstrate this point, the reaction rate at 25°C was found to decrease in the range of acid concentration from 0.2 to 2.0 mM - cc^{-1} where the

SO_2 solubility is nearly constant. The data throws some doubt on the rate called for by the reversible reaction of the MSL[4] model at the reactant concentrations of this work.

The humidity of the SO_2 - air gas mixture sparged into the liquid decreases initial absorption rate by as much as 14%.

Recommendations

1. The nearly constant initial reaction rate shown in Figure 5 for 65°C suggest the possibility that the solubility of the reactant gases has an effect on the rate i.e. the rate is no longer zero order with respect to SO_2 and O_2. The role of the oxygen transfer from gas phase to liquid phase should be investigated at the higher temperatures.

2. A model for the reaction which takes into account the variable volume of the liquid should be developed to more accurately describe the actual physical situation where volume is changed by acid formation and by evaporation or condensation of water to or from the gas in equilibrium with the acid solution.

3. For purely reaction rate studies at higher temperature better control is needed of the liquid volume or better measurement techniques of the volume if a variable volume model is used.

4. Equations (V-1) and (V-2) should be tested at the higher temperature and at other manganese concentrations to investigate the dependency on higher and lower initial Mn^{++} concentrations.

CHAPTER VI

INTRODUCTION TO SO_2 REACTIONS WITH NH_3 IN THE GAS PHASE

The reaction studied was the combination of NH_3 gas with SO_2 gas in air with and without the presence of H_2O vapor to form solid products. Of particular interest was the reaction to form ammonium sulfate:

$$2NH_3(g) + SO_2(g) + H_2O(g) + \frac{1}{2} O_2(g) \longrightarrow (NH_4)_2SO_4(s) \qquad (VI\text{-}1)$$

The reactions of NH_3 gas and SO_2 gas have been virtually unmentioned in text books. One is led to believe the only route to reaction products of NH_3 and SO_2 is by aqueous solutions and an acid-base neutralization. This is a bit surprising in view of the fact that NH_3-SO_2 gas reactions have been known since Priestly's observation in 1790[35] and have been studied at intervals since that time. Perhaps one reason for the scarcity in the texts is the diversity of reaction products. The product composition depends on the absence or presence (and concentration) of O_2 gas and H_2O vapor, the relative concentration of NH_3 and SO_2, the temperature, and probably other factors as yet unknown. Various researchers have found either $NH_3 \cdot SO_2$ or $(NH_3)_2 \cdot SO_2$ result as primary products of the reaction between anhydrous SO_2 and NH_3 gases[25,36,37] with a host of secondary products[25] such as imides, polythionates, sulfates, thiosulfates, etc. (depending on the temperature). Other researchers have found no reaction at all in the absence of at least a "trace" of water vapor. In

the presence of sufficient O_2 and H_2O vapor, ammonium sulfates and sulfites result.

With the event of the discovery of the "Junge Layer" of statospheric ammonium sulfate particles previously mentioned, interest in the NH_3-SO_2 gas reactions has intensified. The exact mechanism of the reaction has been, and remains, controversial.

The reaction has been pertinent to the removal of SO_2 from flue gases although scrubbing by aqueous solutions has been far more popular.

The $NH_3 \cdot SO_2$ and $(NH_3)_2 \cdot SO_2$ compounds are difficult to work with. When exposed to the atmosphere they tend to either sublime directly into their constituent gases or to combine with the O_2 and H_2O in the air to form other compounds.

Scope of This Work

The kinetics involved in the formation of $(NH_4)_2SO_4$ was the primary goal of this part of the study. A reaction scheme was proposed and rate constants evaluated for conditions at 298°K, excess H_2O and O_2. Sulfur dioxide and NH_3 concentrations were in the range 100-1000 PPM, so again application is slanted more towards areas of high concentrations such as flue gas emissions.

The effect of using H_2O vapor concentration at the stoichiometric value for ammonium sulfate formation was studied. Some work was done on product formation in the system NH_3 - SO_2 - O_2 - H_2O trace and the range of aerodynamic diameters were determined by the aerosol centrifuge developed by Preining.[39]

CHAPTER VII

LITERATURE SURVEY

Early research, beginning with the observations of John Priestly[35] in 1790, on the reactions of NH_3 and SO_2 gases forming solid reaction products was performed on dry gases in the absence of oxygen. A variety of reaction product descriptions and proposed compositions were reported. Dobereiner[40] in 1826, Forchhammer[41] in 1837, and Rose[42] in 1844 observed the product to be a waxy solid which when dissolved in water gave tests for NH_4^+, $SO_3^=$, $SO_4^=$, $S_2O_3^=$, and polythionates. Dobereiner[44] observed a yellow brown vapor which condensed to a bright brown solid. Schumann[37] in 1900 observed the formation of $NH_3 \cdot SO_2$ with an excess of SO_2, and $(2\ NH_3) \cdot SO_2$ with an excess of NH_3. Temperatures above 0°C and even traces of moisture partially decomposed the $NH_3 \cdot SO_2$. Divers and Gawa[43] in 1900 found that the thoroughly dried gases do not react and that moisture is necessary to catalyze the reaction. They also observed $(NH_3)_2 \cdot SO_2$ formed in an excess of NH_3 to which they assigned the structure $NH_2 - SO_2 - NH_4$ and named it ammonium amido sulfite. Ephraim and Piotrowski[36] in 1911 also found $NH_3 \cdot SO_2$ resulted from an excess of SO_2. In an excess of NH_3, either white $NH_4SO_2NH_2$ or a red substance formed, which they called triammoniumimidobisulfite:

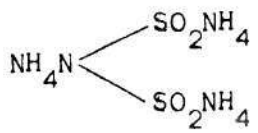

Ogawa and Aoyama[38] in 1916 prepared white $NH_4SO_2NH_2$ by mixing NH_3 and SO_2 in ether and passing dry ammonia over the separated white precipitate. The white salt when dissolved in ice cold water answered tests for pure ammonium sulfite. They also prepared a yellow salt from an excess of SO_2 which they analyzed as $NH_3 \cdot SO_2$.

Badar-ud-Din and M. Aslam[25] in 1953 made a study of the $NH_3 \cdot SO_2$ reaction over a temperature range from -10°C to 80°C. They stated that from 10°C to 80°C the gases do not react unless a trace of moisture is present. From 0°C - 10°C the product was white. Above 10°C the product color was light yellow to orange as reaction temperatures increased and above 80°C free sulfur was formed.

The products were unstable which caused severe problems in analyzing primary and secondary products. The products depended on (1) whether SO_2 or NH_3 was in excess and (2) temperature. At the higher reaction temperatures they found a higher proportion of secondary products.

Their results are summarized as follows:

Excess NH_3, primary product:

The ammonium salt of amido sulfurous acid, ammonium amido sulfite:

$NH_2 - \underset{\underset{O}{|}}{S} - ONH_4$ $(NH_3 : SO_2 :: 2 : 1)$

Excess NH_3, secondary products:

ammonium sulfate $(NH_4)_2SO_4$

diammonium amido sulfite $H_4N - SO_2 - NH - SO_2 - NH_4$

ammonium amido sulfonate $NH_4 - SO_3 - NH_3$

mono anhydride of ammonium trithionate $\begin{matrix} SO_2\,NH_2 \\ | \\ S \\ | \\ SO_2ONH_4 \end{matrix}$

di-anhydride of ammonium trithionate $\begin{matrix} SO_2NH_4 \\ | \\ S \\ | \\ SO_2ONH_2 \end{matrix}$

anhydride of ammonium thiosulfate $\begin{matrix} SO_2 \cdot NH_2 \\ | \\ S \cdot NH_4 \end{matrix}$

Excess SO_2, primary product:

amido sulfurous acid $NH_2 - \underset{\underset{O}{|}}{S} - OH$ $(NH_3 : SO_2 :: 1 : 1)$

Excess SO_2, secondary products: generally, secondary products were the corresponding free acids of the secondary product ammonium salts formed from an excess of NH_3.

ammonium hydrosulfate NH_4HSO_4

free acid of diammonium - imido sulfite $H - SO_2 - NH - SO_2 - H$

amido sulphonic acid $NH_2 - SO_3 - H$

thio and thionic compounds

Scott, Lamb, and Duffy[31] determined the equilibrium vapor pressure over the solid products from -70°C to -10°C. This data indicated the anhydrous reaction could be of importance in the formation of the stratospheric ammonium sulfate aerosol layer. Infrared spectra of the equilibrium vapor over the solid implied that the solid products reversibly decompose into NH_3 and SO_2 gas, rather than sublime directly. Their observations corroborated previous work wherein at low temperatures (0°C) and an excess NH_3, a white compound of the type $(NH_3)_2 \cdot SO_2$ is formed and with an excess of SO_2, a light yellow compound of the type $NH_3 \cdot SO_2$ is formed. These compounds are also formed at higher temperatures with an

increasing proportion of multicolored secondary products.

Scott and Lamb[30] and Lamb[29] developed a thermodynamic model in which the reaction products were assumed to be an ideal solid solution of the 1:1 and 2:1 compounds. They presented charts of vapor pressure vs. reciprocal temperature with composition as parameter. Enthalpies and entropies of decomposition were calculated. The thermodynamic properties for the 1:1 compound suggested the structure 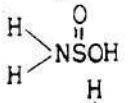 which on dissolving in water transforms into a zwitterion 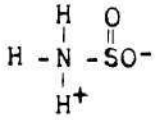

The suggested ionic structure for the 2:1 solid is:

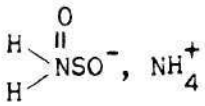

Kushmir, et al.[26] have undertaken a three phase experimental program as follows:

Phase I - Confirmation of products formed under a wide range of conditions between ammonia and sulfur dioxide and an evaluation of the physical and chemical properties.

Phase II - Determination of whether or not reactions involving NH_3, SO_2, H_2O, O, etc. could lead to formation of ammonium sulfate. Included in this phase was reactions at conditions of the Junge Layer: 50 torr total pressure, -50°C, concentrations of NH_3 and SO_2 in the PPB range.

Phase III - A study of the kinetics of the reaction between NH_3 and SO_2 to determine its importance to the formation of ammonium sulfate in the atmosphere.

Results to date, contained in their interim report are summarized as follows:

The reaction occurs between the anhydrous gases from -70°C to 30°C with a trace of water vapor not being needed. Over this temperature range, what appeared to be the same solid product was observed to have formed.

Depending on which gas was in excess the solid was yellow (excess SO_2) or white (excess NH_3) which confirmed the results of others.

Infrared spectra suggested both white and yellow compounds are similarly associated and the association is of a hydrogen bonding nature. The only difference between the two solids is the molecular size, that is, the solids are polymeric in nature. The nature of the product depends only on the extent of polymerization.

X-ray diffraction analysis on a sample of the yellow material gave no well defined lines, indicating the material is amorphous. After the yellow material was exposed to ambient moist air it turned white. The x-ray diffraction pattern indicated a similarity to ammonium sulfate with the non corresponding lines similar to the strong lines of ammonium bisulfite. The authors concluded therefore that the material formed by reaction of anhydrous NH_3 and SO_2 when exposed to H_2O and O_2 converts to ammonium sulfate by way of ammonium bisulfite, $NH_4H\ SO_3$. This suggests the product of an NH_3-SO_2-H_2O gas reaction (no O_2) would be NH_4HSO_3.

The anhydrous reaction at the "Junge Layer" conditions produced particles of what the authors called $(NH_3 \cdot SO_2)_n$ in the micron size range.

The reaction of $NH_3 + SO_2$ was found to occur in the gas phase, not on the walls of the reaction vessel.

Friend[46] experimented with trace quantities of H_2O, SO_2, NH_3 and O_2 in air of varying proportions and with various conditions of radiation with ultraviolet light. Their objective was information on the photo-oxidation of SO_2, mechanism of formation of stratospheric aerosols, and the roll of trace organic gases in atmospheric nucleation processes. In one series of their experiments they observed formation of condensation nuclei and large particles from the system NH_3, SO_2, H_2O, air, unfiltered light or UV radiation of wave length 2200-5000 Å. The large particles were seen to be colorless, hygroscopic crystals which were "probably ammonium sulfate." The reaction occurred readily at room temperature and at -55°C. In the dark or with UV radiation of 2500-4000 Å wavelength there was no reaction from the same system of gases. UV light of 2500-4000 Å wavelength excludes radiation that is absorbed by O_2 (2450 Å) to produce O atoms. Both wavelengths mentioned above, 2200-5000 Å and 2500-4000 Å, are absorbed by SO_2. Their interpretation of these results was that if the addition compounds of NH_3 and SO_2 did form, they did not lead to the formation of ammonium sulfate and that they are not precursors to the formation of ammonium sulfate in the stratosphere. They proposed a three stage mechanism:

1. production of H_2SO_4-H_2O embryonic nuclei from oxidation of SO_2 by O atoms, and combinations of SO_3 with H_2O.
2. neutralization of acid embryos by NH_3.
3. oxidation of SO_2 in the embryonic salt solution, catalyzed by NH_4^+. Continued addition of NH_3 to give particles of ammonium sulfate.

To sum up the research reported in the literature; there is agreement that NH_3 and SO_2 gases under certain conditions will form solid reaction products. It is generally agreed that at least a trace of water vapor and light are sufficient conditions for the reaction to take place but it is not agreed that these conditions are necessary. Ammonia and SO_2 gases upon reaction condense out of the gas phase in an approximate ratio of 1:1 NH_3 to SO_2 with an excess of SO_2 gas, and in an approximate ratio of 2:1 NH_3 to SO_2 with an excess of NH_3 but there is no agreement or overwhelming evidence to support any of the various claims as to the nature of the solid product, be it an ionic salt or polymer, etc.

The reaction between NH_3 and SO_2 gases has had some application industrially, mainly in the areas of ammonium sulfate production and for recovering or removing SO_2 from flue gas streams. A 1923 British Patent by West and Jaques[28] describes a process wherein a mixture of ammonium sulfite and ammonium sulfate is prepared by reacting a mixture of $NH_{3(g)}$ and $H_2O_{(g)}$ with a mixture of $SO_{2(g)}$ and air in proportions such that the temperature does not exceed 100°C and the product is obtained in a dry condition. The sulfate-sulfite mixture is precipitated on cooling the reaction gases to 40°C or below. The sulfite fraction is converted to sulfate by exposure to air. According to Smith and Finlayson[47] (1925) an ammonium sulfate manufacturing plant in the North of England was in operation using the process in the patent.

Variations of the process described above are to be found in the literature. U. S. Patent 2,912,304,[49] 1959, describes a process of mixing NH_3, SO_2, H_2O, gases and air in the presence of a finely divided, suspended

solid to produce ammonium sulfate which is free of sulfite. The solid is to contain at least a fraction of Vanadium Pentoxide which increases the speed of the reaction, and catalyzes the oxidation of part of the ammonia to oxides of nitrogen which contribute to the formation of ammonium sulfate. The solid particles are essential for transferring the heat of the reaction (125 K cal/mol) to the walls of the reactor. Temperature is specified at 200-350°C and pressure at 1 atmosphere. If water vapor is present in less than the stoichiometric amount the di- and tri- ammonium imidodisulfonates are formed:

$$2\,SO_2 + O_2 + 3NH_3 \rightarrow (NH_4SO_3)_2\ NH \qquad \text{(VII-1)}$$

$$2\,SO_2 + O_2 + 4NH_3 \rightarrow (NH_4SO_3)_2\ NH_4 \qquad \text{(VII-2)}$$

If the ratio of SO_2:NH_3 is greater than 2:1, ammonium sulfamate is formed:

$$SO_2 + \tfrac{1}{2}\,O_2 + 2NH_3 \rightarrow NH_4SO_3NH_2 \qquad \text{(VII-3)}$$

Hungarian Patent 150,852[50] (1962) describes a process for converting a gas fume of 0.3% SO_2 and 4.0% O to $(NH_4)_2\ SO_4$ by mixing with 0.6% NH_3 at 160° and passing over a cylindrical tube where a field strength of 15 kv/cm is maintained. Kiyoura[48] describes a process where V_2O_5 catalyst is used at 380-450° to convert SO_2 to SO_3, followed by injection of NH_3 at 220-260° forming 98.5-99.6% pure agglomerates of $(NH_4)_2SO_4$.

In a process developed by two French companies,[51] flue gases are treated with gaseous ammonia and subsequently washed to remove 93 to 97%

of the sulfur compounds in the form of ammonium sulfite, bisulfite, and sulfate. The wash liquors are treated to recover and recycle the ammonia and to recover the SO_2. An experimental unit was installed on an oil burning power plant in 1967. It was concluded that if the SO_2 could be sold for $40/ton the operation would break even.

A process patented by E. D. Cann treats SO_2 containing flue gas at 220°F with ammonia to form either ammonium sulfite or ammonium bisulfite depending on the ratio of NH_3 injected to SO_2 in the flue gas.

$$2NH_3 + SO_2 + H_2O \rightarrow (NH_4)_2SO_3 \qquad \text{(VII-4)}$$

$$NH_3 + SO_2 + H_2O \rightarrow NH_4HSO_3 \qquad \text{(VII-5)}$$

The sulfite-bisulfite is separated and treated with either zinc oxide or an aqueous alkaline earth metal oxide to liberate the NH_3 for recycle and form an insoluble metal sulfite:

$$ZnO + (NH_4)_2SO_3 \rightarrow ZnSO_3 \cdot H_2O\downarrow + 2NH_3 \qquad \text{(VII-6)}$$

The alkaline earth metal sulfite is decomposed thermally to liberate a concentrated stream of SO_2 and an alkaline earth metal oxide for recycle.

To sum up the industrial aspects of the reaction for the production of ammonium sulphate, which is mainly used as a fertilizer, the principal problem is the avoidance of sulfite, bisulfite and sulfamate. Sulfite and bisulfite require additional operations devoted to the oxidation to sulfate. The additional cost of manufacturing is increased to a prohibitive figure. According to Mellor,[53] the rate of oxidation of sulfite solutions by atmospheric oxygen decreases markedly with increasing

concentration of the solution. Oxidation of solid sulfite by air is very slow and even at the optimum temperature of 60-70°C an apparent equilibrium is reached in 2-3 hours with only 30% conversion. Ammonium sulfamate is to be avoided because of its herbicidal properties.

For the removal of SO_2 from flue gases with subsequent recovery of SO_2 and NH_3, it is important to reduce production of the sulfate since the decomposition energy requirements are exhorbitant. The main problem then is to prevent air from contacting the sulfite while it is being processed to recover the NH_3 and SO_2.

CHAPTER VIII

EXPERIMENTAL

The scope of the study was to be limited to investigating concentration dependency of the reaction at room temperature and 1 atm. Temperature dependency, pressure effects, and effects of radiation were not intended to be covered by this work, except for possibly some qualitative determinations.

An experimental arrangement was needed in which the quantity of solid reaction product or the concentrations of reactants could be measured at various times during a reaction in order to obtain kinetic rate data. The apparatus was to be flexible in that the concentrations of the reacting gases, NH_3, SO_2, O_2 and H_2O could be individually varied. Preliminary experiments and information from the literature indicated that the reaction is extremely rapid. Scott et al.,[31] for example, found the NH_3 and SO_2 reactants which were frozen on the walls of the reaction vessel reacted violently upon warming the chamber to -10°C. During the experimentation covered in Part I, an experiment was planned wherein approximately 4000 PPM each SO_2 and NH_3 gases in moist air were to be sparged into the manganese sulfate solution. Upon introducing the NH_3 air stream into the SO_2 air stream, the mixing tee almost instantaneously plugged with a white crystalline solid. A preliminary run of 500 PPM SO_2 and 500 PPM NH_3 in moist air indicated the reaction had proceeded to over 50% completion in less than two seconds. Because of the

speed of the reaction and the low partial pressures of the limiting reactants, a constant volume batch type reactor, where the reactants concentrations are followed by pressure measurements, was judged impractical. For an example, a typical run of high concentration initial reactants was 500 PPM SO_2, 1000 PPM NH_3, and air of about 50% relative humidity. If the residence time were high enough for all of the SO_2 and NH_3 to react, the drop in total pressure would be only .19 torr or .225% for a 760 torr initial total pressure. On the other hand, if higher concentrations of reactants were to be used, the reaction would be too rapid to follow.

The method selected was a steady state flow reactor shown in Figure 21. The gases were introduced to the reactor through two concentric nozzles. Through one of the nozzles flowed humid air and SO_2, and humid air - NH_3 through the other. The solid reaction product which formed in the reactor was either deposited on the surfaces of the reactor or caught by the membrane filter on the end of the reactor.

Before the final decision was made on this system to study the kinetics of the reaction, a test was made to determine if the reaction was a "surface" dependent type. As is commonly used as a method of investigation,[56] duplicate runs were made with the only difference being the ratio of surface area to volume of the reactor. This was achieved by packing the reactor with glass wool and resulted in the run with the packed reactor yielding less reaction product. Based on these results and the findings of Mohnen[26] that the reaction occurs in the gas rather than on the walls of the reaction vessel, the reaction was assumed not to be of the "surface" type.

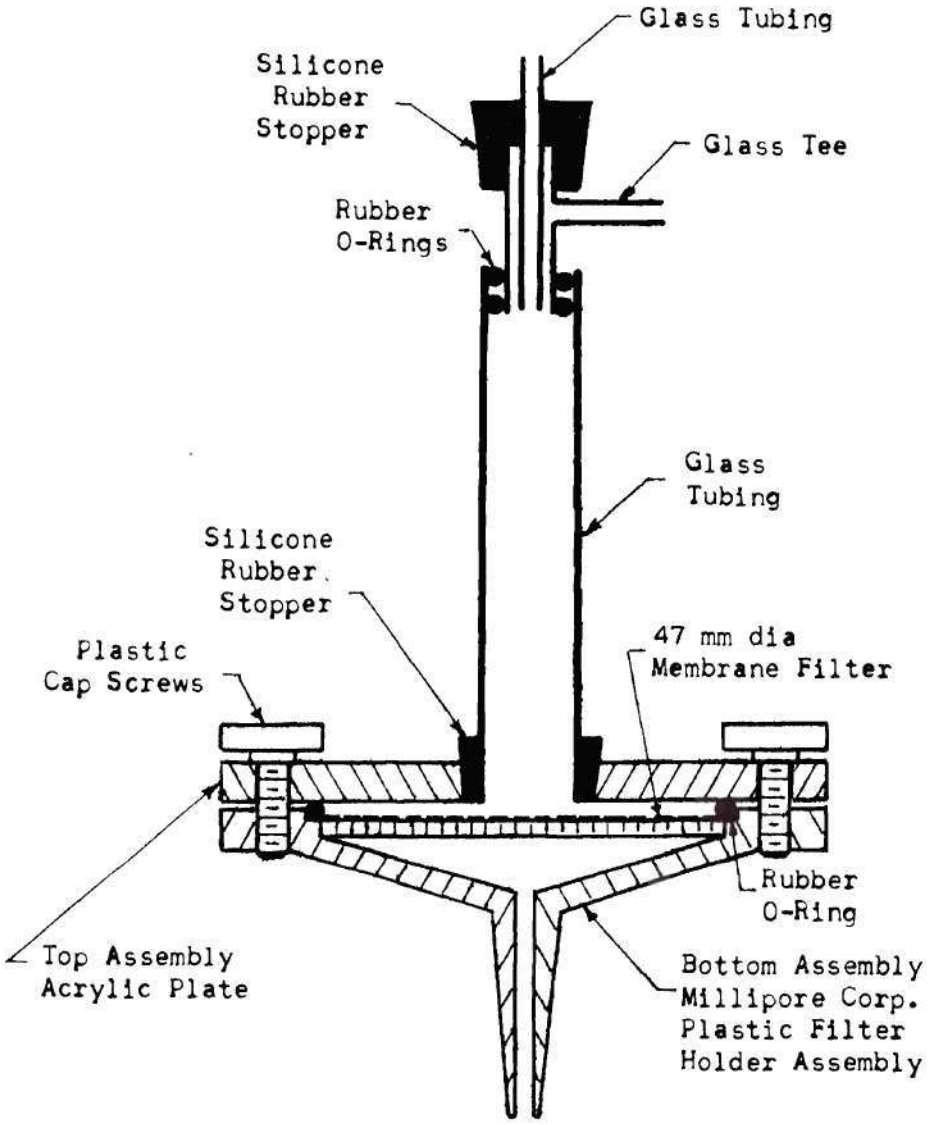

Figure 21. Flow Reactor for NH_3 -SO_2 Reactions.

Since the pressure change through the reactor was so slight, constant density was assumed throughout and the equations describing the flow reactor reduce to the simpler equations for batch type, constant volume.[54] With plug flow assumed for the flow reactor, the space time (or residence time) was simply determined by the volume of the reactor and the total flow rate of gas through the reactor:

$$\tau, \text{ space time, sec.} = \frac{V}{v_o} \begin{matrix} \text{total vol. of reactor, } cm^3 \\ \text{volumetric flow rate, } \frac{cm^3}{sec} \end{matrix} = t, \text{ residence time, sec.} \qquad \text{(VIII-1)}$$

Although the Reynolds Number was low both at the nozzle exit, 450, and in the flow tube, 200, molecular diffusion and nozzle exit effect turbulence were assumed sufficient to produce adequate mixing. Solid deposition on the flow tube slightly behind the nozzle end and complete deposition on the entire surface of the flow tube support the supposition. By varying the length of the tube i.e., the volume of the reactor, or by varying the total flow rate, various residence times were obtained for a series of runs at a given set of concentrations. Residence times of from .02 seconds to 1 second were found appropriate. Total flow rates varied from 2 to 3 liters per minute. The quantity of reaction product formed during a run was determined by weighing the reactor (less bottom assembly) before and after the run. Identification of reaction product was by X ray diffraction. Based on desired initial concentrations of reacting gases and residence time, the length of time of each test was decided. The test was to be of sufficient duration to form the maximum product weight, which would reduce the error in weighing, but not so long as to increase pressure by plugging the filter to the point that flow

control was erratic and density increase changed residence time significantly. Duration of tests varied from 12 minutes for high concentrations and long residence times to 60 minutes for low concentrations and short residence times. These same considerations dictated filter size. The same size, membrane filter, 1.2 micrometers pore size (Millipore Corp., Bedford Mass.), was used throughout and represented a compromise between low pressure build up but initial loss of small grains of product through the pores, and maximum product retention, but high pressures and faster pressure build up. To test the effectiveness of the 1.2 μm filter, duplicate runs were made with 1.2 μm and .45 μm filters. The .45 μm filter yielded a 4% increase in weight of product retained; all concentrations, flow rates etc. being equal. Four per cent represented a larger increase than can be accounted for by the density increase but was within experimental error of the system as a whole. Duplicate runs to determine reproducibility resulted in from 1.2% to 7.1% variation based on the lowest weight.

The filter undoubtedly allowed some of the solid to pass through for the first few minutes until a bed had been built up. The plug flow assumption through the reactor introduced some error in the residence time.

The large weight of the reactor top assembly and tube (the parts of the reactor that are weighed) compared to the weight of the reaction product necessitated extreme care in technique. To insure that errors in weighing were minimal, the following procedure was followed. The filter reactor assembly were installed in place in the apparatus and air of test conditions of flow rate and H_2O vapor content were passed through

the reactor for five minutes. The purpose was to allow time for the inside of the reactor to reach an equilibrium with the air and water vapor which would flow through it during a test. Simultaneously the exterior of reactor reached an equilibrium with the atmosphere in the lab. After five minutes, the reactor assembly and filter were weighed to obtain a tare weight. The parts were handled with metal tongs to minimize handling contamination. At the conclusion of a run, the assembly, filter and reaction product were weighed. The reactor was cleaned, a new filter paper installed, and after five minutes exposure of the same flow conditions under which the original tare weight was obtained, the assembly was weighed again. If the two tare weights (taking into account differences in filter paper weights) varied by more than 5% of the net weight of the reaction product, the run was discarded. The tare weights and net product weights for each run are listed in Appendix F. This method was more successful than anticipated considering the reactor weights are in the range of 50 - 70 gm and the net reaction product weight was in range of 0.01 - 0.1 gm. Care in technique and the inert, non absorbent materials of construction of the reactor are credited for the degree of accuracy attained. Other problems that would probably have an effect, regardless of the method used, are the hygroscopic nature of the solid product. After one of the runs in which ammonium sulfate was formed, the solid was left exposed to the atmosphere overnight and a 1.9% increase in weight resulted. The sulfites and products of the anhydrous gases would be much more of a problem. The complete apparatus is shown in Figure 22. Compressed air was filtered through a membrane filter and, as experimental conditions dictated, all of part of the air could be dried to a dew point of ~ -70°C by a silica gel drier

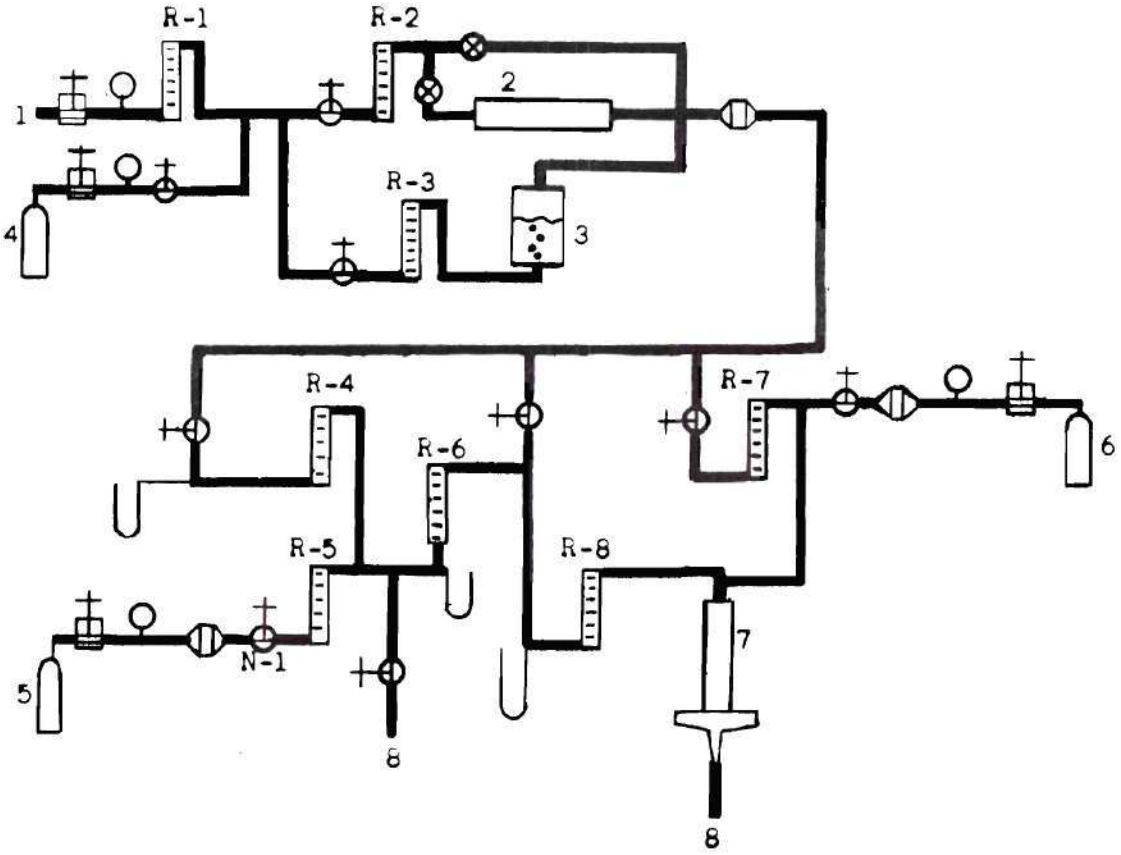

Pressure Regulator

Pressure Indicator

Membrane Filter

Rotameter

Valve

Needle Valve

Manometer

1. Compressed air
2. Drying Tube, silica gel
3. Humidifier
4. Nitrogen bottle
5. Ammonia bottle
6. Sulfur dioxide bottle
7. Reactor
8. Drain

Figure 22. Experimental Apparatus for SO_2-NH_3 Reactions.

in series with an acetone-dry ice cold trap. Part or all of the air could be humidified to saturation by sparging into distilled water. Desired H_2O vapor concentration was obtained by a measured ratio of the dry air with the H_2O saturated air. Nitrogen, sulfur dioxide and ammonia were from commercially supplied cylinders. Each gas was filtered through a membrane filter, regulated by a double port Nupro Co. micro needle valve and flow rate measured by Matheson Co. gas rotameters. The gases (except air) were commercial grade, generally of 99.9% purity or higher. The specifications are given in Appendix C. Since reactions involving absolutely anhydrous gases were not planned, the few PPM H_2O impurities in the cylinder gases was of no consequence. SO_2 concentration was set prior to a run by adjusting the flow rates to test conditions (with the exception that air was substituted for NH_3) and diverting part of the gas stream through the IR SO_2 analyzer. The recorder was used for an indicator since it has a higher accuracy than the indicator on the IR. The ammonia concentration was set by a "double dilution" method. Pure ammonia measured through a rotameter was mixed with measured air stream. A measured part of this combined flow was then combined with another measured air flow. By this method the original flow of ~20 cc/min was diluted down to a concentration in the range of ~1000 PPM or ~3 cc/min NH_3 per ~3000 cc/min total gas flow.

All gas rotameters were calibrated at actual conditions of flow, pressure and temperature by a wet test meter. The IR SO_2 analyzer was calibrated with a mixture of N_2 and SO_2 of known SO_2 concentration before each series of runs or twice daily. The ammonia rotameter was calibrated by running a measured ammonia flow into concentrated H_2SO_4 for a

measured period of time. Total ammonia flow was determined by weighing the sulfuric acid before and after the ammonia flow into it. The rotameter calibrations agreed within a maximum of 6% of the manufacturers calibration curves.

Equipment details, the operation of a typical test and a sample calculation are given in Appendices D and E.

Experimental conditions are summarized as follows:

SO_2 conc. PPM - 100 to 500

NH_3 conc. PPM - 250 to 1500

O_2 conc., 21% (air), 500 PPM

H_2O conc. PPM - 500 to large excess (16,500 PPM)

Total gas flow rates	2000 to 3000 cc/minute
Reactor volume	1 cc to 32.3 cc
Residence time in reactor	.02 to 1 second
Filter size (membrane)	1.2 micrometer pore size
	47 mm dia.
Product weight	0.006 - 0.135 gm
Temperature	296°K
Pressure	~750 torr

CHAPTER IX

RESULTS AND DISCUSSION

Twelve series of tests were made, designated Series A to L, with initial concentrations (millimoles - meter^{-3}) of reactants as follows:

Table 8. Initial Reactant Concentrations, NH_3-SO_2 Reactions

Series	A	B	C	D	E	F
$[SO_2]_o$	3.98	6.05	9.95	27	10.14	20.6
$[NH_3]_o$	27.0	27.0	27.0	27.0	35.65	47.3
$[H_2O]_o$	668	682	682	682	682	668
$[O_2]_o$	← 8530 (Air) →					
$[NH_3]_o$:$[SO_2]_o$	6.78:1	4.47:1	2.72:1	1:1	3.52:1	2.3:1

Series	G	H	I	J	K	L
$[SO_2]_o$	20.9	20.9	20.9	20.9	20.6	20.0
$[NH_3]_o$	40.4	20.9	40.4	60.1	47.3	45.2
$[H_2O]_o$	31.0	16.0	16.0	16.0	668	0.1
$[O_2]_o$	← 8530 →				31	8530
$[NH_3]$:$[SO_2]_o$	1.93:1	1:1	1.93:1	2.88:1	2.3:1	2.26:1

All runs were made at a temperature of 23°C ± 1°C and 750 torr ± 5 torr pressure. The results of the tests in millimoles of solid reaction product per meter^3 of total gas through reactor vs. time in seconds, are listed in Table 11 at the end of the chapter. This data is also plotted in Figures 24 to 34. Complete details of each series of tests are given in Appendix F.

In series A to F the SO_2 concentration ranged from 3.98 to 27 millimoles per cubic meter ($mM\text{-}m^{-3}$) and the NH_3 initial concentrations were 27 to 47.3 $mM\text{-}m^{-3}$. The ratios of NH_3 initial concentration to SO_2 initial concentrations were 1 : 1 up to 6.78 : 1. Water vapor, 682 $mM\text{-}m^{-3}$, and oxygen, 8530 $mM\text{-}m^{-3}$ which is taken as the oxygen content of air, were in large enough excess that their concentration was considered constant. The kinetics, therefore, were simplified to the concentration dependency of SO_2 and NH_3. A sample of solid reaction product produced under identical conditions to Series F, $[NH_3]_o : [SO_2]_o :: 2.3 : 1$ was determined by x-ray diffraction analysis to be ammonium sulfate. A sample of solid reaction product produced under conditions identical to Series D, $[NH_3]_o : [SO_2]_o :: 1 : 1$, was determined by x-ray diffraction to be predominantly ammonium sulfate with an estimated 2 - 3% $NH_4SO_3NH_2$, ammonium sulfite amide, or ammonium sulfamate.

This result is consistent with the statements of Vian-Ortuno,[49] et al., in their description of a process for production of ammonium sulfate wherein they state that ammonium sulfamate is formed when SO_2 is in excess. From these results and from consideration of the results in the literature, the reaction product identification is assumed as follows: for $[NH_3]_o : [SO_2]_o$ ratios of 2 : 1 the product is essentially

ammonium sulfate; as the $[NH_3]_o$: $[SO_2]_o$ ratio is reduced from 2 : 1 to 1 : 1, the secondary product of ammonium sulfamate is formed in increasing concentration reaching 2 - 3% at a 1 : 1 ratio. This work did not cover reactions with $[NH_3]_o$: $[SO_2]_o$ of <1 : 1, although a logical prediction would be a higher concentration of sulfamate. Since Series A to F were all run with a ratio of > 1 : 1 the reaction product is assumed to be primarily ammonium sulfate for each. As stated previously, ammonium sulfamate formation is significant because of its toxicity to plane life. From the standpoint of SO_2 removal from a gas stream, the same efficiency of one mole of SO_2 per mole of reaction product is realized.

The apparent ease with which ammonium sulfate was produced was unexpected in light of the experience of others as reported in the literature wherein sulfites were formed unless special provisions were made to prevent their formation. In neither of the samples were sulfites detected and as will be discussed below, sulfites were not detected in any of the various samples of this work. Precise data on the type of compound formed as a function of temperature and concentration, etc. was not found in the literature, however, generalized statements can be made which possibly could explain the nonoccurrence of sulfites in this work. In the case of those processes described in the literature for the production of ammonium sulfate, concentrations were much higher than those used in this work and higher temperatures from the exothermic reaction (125 K cal/mole) were also encountered. In the case of flue gas treatment, the temperatures were much higher and the oxygen concentrations usually 1/3 - 1/2 of the normal content of air.

In Series G to J $[NH_3]_o$ was in the range of 20 - 60 mM-m^{-3}, $(SO_2)_o$ at 20.9 mM-m^{-3} and air was the carrier gas. The water vapor content was reduced to 80% and 150% of the stoichiometric requirement for ammonium sulfate production. $[NH_3]_o$: $[SO_2]_o$ ratios were 1 : 1, 2 : 1 and 3 : 1. A sample of reaction product produced under conditions identical to Series G was analyzed by x-ray diffraction and the results were quite indefinite. The sample contained an estimated 7% NH_3SO_3 - amide : sulfonic acid, 5% NH_4N_3, 20% amorphous material, and the balance was a crystalline substance which matched none of the diffraction patterns. Since the substance $NH_3 \cdot SO_2$ is known to show up as an amorphous material by x-ray diffraction analysis, the assumption was so made here. A natural suspect for the unknown crystalline material was $(NH_3)_2 \cdot SO_2$. With these assumptions, the mM-m^{-3} of product reported in Tables 10 - 12 were calculated from the weights of product formed using an average molecular weight of 93.

Series L was attempted with an $[NH_3]_o$: $[SO_2]_o$ ratio of 2 : 1, in air, but with only a trace (3 - 5 PPM) of H_2O vapor. This was accomplished by conducting the carrier air through an acetone - dry ice cold trap. The temperature of the air at the exit to the cold tran was measured at -70°C. The x-ray diffraction analysis of this reaction product was not well defined, indicating crystals of $(NH_4)_2SO_4$ - ammonium sulfate, $(NH_4)_2 S_2O_7$ - ammonium pyrosulfate, $NH_3 SO_3$ - amide: sulfonic acid, and $N_3H_7SO_4$ - amide : sulfate hydrazine. The possibility of $(NH_3)_2 \cdot SO_2$ was not excluded since there were no standards for this substance. Results in terms of grams of solid reaction product were also erratic in that for three identical tests, a variation in grams of product

of 300% was obtained. A sample of product formed from a large excess of $[SO_2]_o$ relative to $[NH_3]_o$ in air with a trace of water vapor was analyzed and the results indicated mostly $N_3H_7SO_4$ - amide: sulfate hydrozine, and some amorphous material. Again the amorphous material is suspected of being $NH_3 \cdot SO_2$. These samples may also have been exposed to air, since they were collected and analyzed before the technique for preventing atmospheric contamination was perfected.

Series K was designed to indicate the oxygen concentration dependency of the reaction. An $[NH_3]_o$: $[SO_2]_o$ ratio of 47.3 : 20.6 or 2.3 : 1 $mM\text{-}m^{-3}$ was used with a large excess of water vapor but only enough air bled into the nitrogen carrier gas to produce an oxygen concentration of 31 $mM\text{-}m^{-3}$, or 1.5 times stoichiometric requirement for ammonium sulfate. A sample produced under these conditions was analyzed and found to be an estimated 10% $N_3H_7SO_4$ - amide : sulfate hydrazine, 5% NH_3SO_3 - amide: sulfonic acid, and the balance was a crystalline substance which again matched none of the diffraction patterns and is assumed to be $(NH_3)_2 \cdot SO_2$. With this assumption the average molecular weight of the product is taken to be 103.

The results of all the x-ray diffraction analysis are summarized in Table 9.

The data of Series A to F, where H_2O and O_2 concentration were high enough to be considered constant, indicated a second order reaction, first order with respect to SO_2 and first order with respect to NH_3. The rate expression for an irreversible second order reaction as given below appeared to fit the experimental data fairly well.

$$-\frac{d[SO_2]}{dt} = K[SO_2][NH_3] \qquad \text{(IX-1)}$$

By stoichiometry:

$$[SO_2] = [SO_2]_o - [(NH_4)_2SO_4] \qquad \text{(IX-2)}$$

$$[NH_3] = [NH_2]_o - 2[(NH_4)_2SO_4] \qquad \text{(IX-3)}$$

By the integral method of analysis, a plot of $\ln \frac{[NH_3][SO_2]_o}{[SO_2][NH_3]_o}$ vs. time should yield a straight line with slope of $K([NH_3]_o - [SO_2]_o)$. The experimental data of Series C is given as an example of this analysis.

$[SO_2]_o = 9.95$ mM-m^{-3}

$[NH_3]_o = 27$ mM-m^{-3}

Time, Sec.	$[(NH_4)_2SO_4]$	$[SO_2]$	$[NH_3]$	$\frac{[NH_3][SO_2]_o}{[SO_2][NH_3]_o}$
0.029	3.4	6.55	20.2	1.14
0.057	4.98	4.97	17.04	1.27
0.119	6.41	3.54	14.18	1.52
0.190	8.12	1.83	10.76	2.16

Log $\frac{[NH_3][SO_2]_o}{[SO_2][NH_3]_o}$ vs. time is plotted on Figure 23. A straight line through the data yields a slope of 4.52.

$$K = \frac{2.303\ (\text{slope})}{[NH_3]_o - [SO_2]_o} = \frac{2.303(4.52)}{27.0 - 9.95} = .61\ \frac{\text{meter}^3\text{-sec.}}{\text{mg mole}} = .61 \times 10^6\ \frac{\text{liter-sec.}}{\text{g. mole}} \qquad \text{(IX-4)}$$

Table 9. Summary of X Ray Diffraction Analysis

Sample No.	Series	$[NH_3]_o$	$[SO_2]_o$	$[H_2O]_o$	$[O_2]_o$	Compound(s)
42	F	47.3	20.6	668	8530	100% $(NH_4)_2SO_4$ - ammonium sulfate
73	D	27	27	682	8530	97% $(NH_4)_2SO_4$ - ammonium sulfate 3% $NH_4SO_3NH_2$ - ammonium sulfamate
95	G	40.4	20.9	31	8530	68% $(NH_3)_2 \cdot SO_2$ 20% $NH_3 \cdot SO_2$ 7% NH_3SO_3 amide: sulfonic acid 5% NH_4N_3
1	L	45.2	20.0	0.1	8530	$(NH_4)_2SO_4$ ammonium sulfate $(NH_4)_2S_2O_7$ ammonium pyrosulfate NH_3SO_3 amide: sulfonic acid $N_3H_7SO_4$ amide: sulfate hydrazine
2	-	Large excess $[SO_2]_o$ to $[NH_3]_o$		0.1	8530	$N_3H_7SO_4$ amide: sulfate hydrazine
94	K	47.3	20.6	668	31	85% $(NH_3)_2 \cdot SO_2$ 10% $N_3H_7SO_4$ amide: sulfate hydrazine 5% NH_3SO_3 - amide: sulfonic acid
89	-	40.4	20.9	154	8530	95% $(NH_4)_2SO_4$ - ammonium sulfate 5% $(NH_3)_2 \cdot SO_2$

Assuming $-\frac{d[SO_2]}{dt} = \frac{d[(NH_4)_2SO_4]}{dt}$, $[(NH_4)_2SO_4]$ is calculated by integrating Equation (IX-1) using Equations (IX-2) and (IX-3)

$$\frac{d[(NH_4)_2SO_4]}{dt} = K([SO_2]_o - [(NH_4)_2SO_4])([NH_3]_o - 2[(NH_4)_2SO_4]) \quad \text{(IX-5)}$$

$$\int_o^{[(NH_4)_2SO_4]} \frac{d[(NH_4)_2SO_4]}{([SO_2]_o - [(NH_4)_2SO_4])([NH_3]_o - 2[(NH_4)_2SO_4])} = Kt \quad \text{(IX-6)}$$

$$= \frac{1}{[NH_3]_o - 2[SO_2]_o}\left[\ln \frac{2[(NH_4)_2SO_4] - [NH_3]_o}{2[(NH_4)_2SO_4] - 2[SO_2]_o} - \ln \frac{[NH_3]_o}{2[SO_2]_o}\right] = Kt \quad \text{(IX-7)}$$

when $[NH_3]_o \neq 2[SO_2]_o$.

Equation (IX-7) can be rearranged to solve for $((NH_4)_2SO_4)$ explicitly

$$[(NH_4)_2SO_4] = \frac{Exp\{Kt([NH_3]_o - 2[SO_2]_o)\} - 1}{Exp\{Kt([NH_3]_o - 2[SO_2]_o)\}/[SO_2]_o - 2/[NH_3]_o} \quad \text{(IX-8)}$$

Calculated values of $((NH_4)_2SO_4)$ are included in Table 11 and Figures 24 to 34. Included in each of the graphs is a dotted line opposite the maximum possible concentration of product based on the limiting reactant and based on the reaction going to completion. On Figures 25, for example, the Series B experimental ammonium sulfate concentration of 6.45 $mM\text{-}m^{-3}$ is higher than possible from the limiting 6.05 $mM\text{-}m^{-3}$ $(SO_2)_o$. The possible causes of this error will be discussed later.

A possible reaction scheme that was investigated during the course of the research was a series of reactions for the production of ammonium

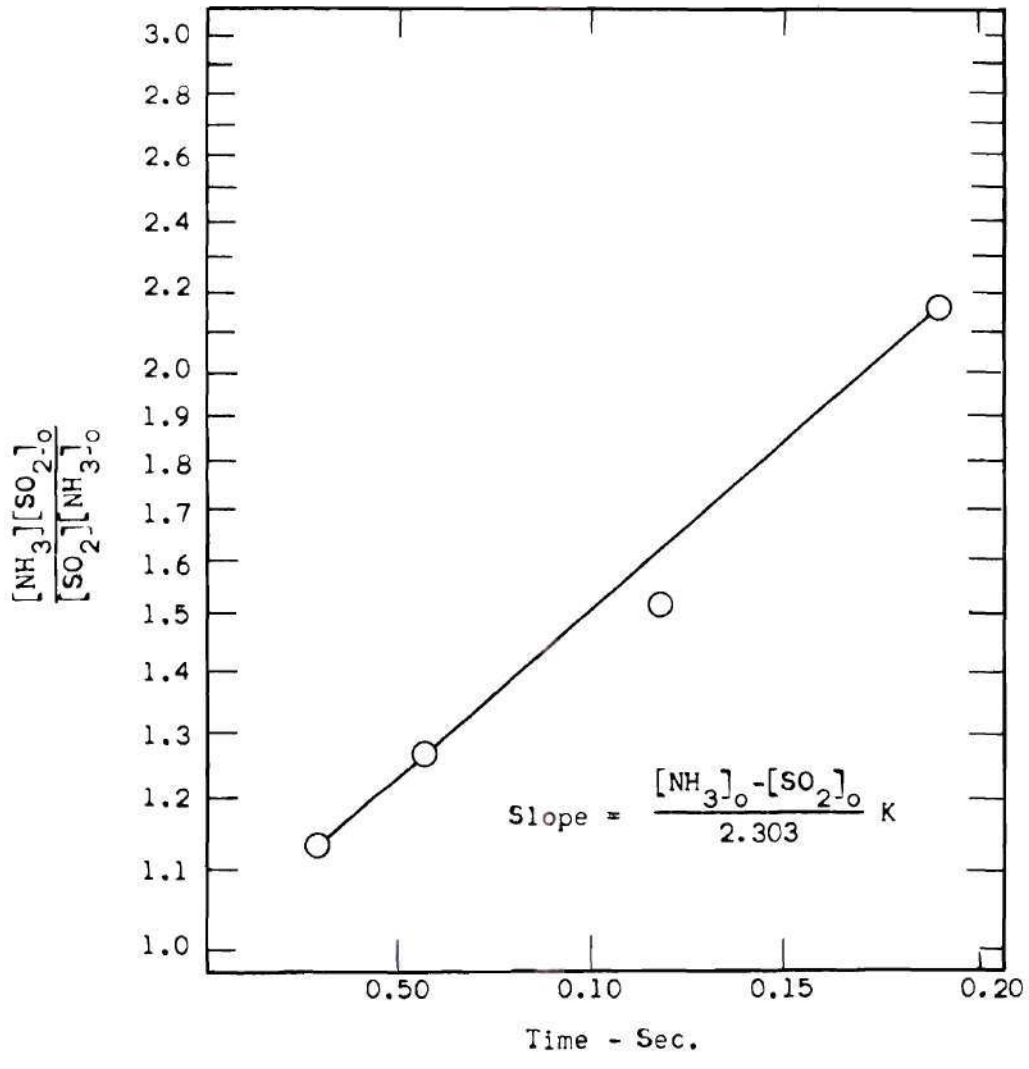

Figure 23. Integral Analysis of NH_3-SO_2 Reaction.

sulfate from the four reactant gases:

$$NH_3 + SO_2 \underset{k_2}{\overset{k_1}{\rightleftharpoons}} NH_3 \cdot SO_2 \qquad \text{(IX-9)}$$

$$NH_3 + NH_3 \cdot SO_2 \underset{k_4}{\overset{k_3}{\rightleftharpoons}} (NH_3)_2 \cdot SO_2 \qquad \text{(IX-10)}$$

$$(NH_3) \cdot SO_2 + O_2 \underset{k_6}{\overset{k_5}{\rightleftharpoons}} (NH_3)_2 \cdot SO_3 + O \qquad \text{(IX-11)}$$

$$(NH_3) \cdot SO_2 + O \underset{k_8}{\overset{k_7}{\rightleftharpoons}} (NH_3)_2 \cdot SO_3 \qquad \text{(IX-12)}$$

$$(NH_3)_2 \cdot SO_3 + H_2O \xrightarrow{k_9} (NH_4)_2SO_4 \qquad \text{(IX-13)}$$

Series A to D wherein the $(NH_3)_0$ is held at 27 mM-m^{-3} and $(SO_2)_0$ is varied, were designed to produce data for testing this model by the slope - intercept method identical to that used in Part 1 for the Mn^{++} catalyzed reaction. The rate expressions derived from this model, the details of which are given in Appendix G, were as follows:

$$\frac{dX}{dt} = k_1([NH_3]_o - \varphi X - 2[(NH_4)_2SO_4])([SO_2]_o - X - [(NH_4)_2SO_4]) \qquad \text{(IX-14)}$$

$$- k_2'X - k_9''X([H_2O]_o - X - [(NH_4)_2SO_4])$$

$$\frac{d[(NH_4)_2SO_4]}{dt} = k_9''X([H_2O] - X - [(NH_4)_2SO_4]) \qquad \text{(IX-15)}$$

where:

X = sum of concentrations of intermediates in Equations (IX-9) to (IX-13)

t = time, seconds

k_1 = .6940 $meter^3$ - (m mole - second)$^{-1}$

k_2' = .0218 sec^{-1}

k_9'' = .0464 $meter^3$ - (m mole - second)$^{-1}$

φ = moles SO_2 per mole of X. Assuming equal concentration of intermediates gives value of 1.66

This model was the result of attempting to formulate a scheme whereby rate expression should be essentially first order with respect to both SO_2 and NH_3 with an excess of H_2O vapor and be zero order with respect to oxygen. The intermediate $(NH_3)_2 \cdot SO_3$ in Equation (IX-12) could be written $NH_4SO_3NH_2$, ammonium sulfamate. Since this substance was identified in the x-ray diffraction analysis of Series D, some credence was given for the model. The logical route to ammonium sulfate by way of ammonium sulfite was not considered because of the numerous reports in the literature of the difficulty in avoiding sulfite formation when sulfate is desired and of the slow reaction of oxygen with sulfite to produce sulfate and also because of the oxygen conc. dependency in the resulting rate expression. In this work, no sulfite was ever identified in the various samples analyzed and apparently ammonium sulfate was produced with considerable ease. Equations (IX-14) and (IX-15) were solved simultaneously for Series A to H conditions by using 4^{th} order Runga Kutta numerical integration in a computer program. The fit of the calculated $(NH_4)_2 SO_4$ concentration to the experimental data was almost as good in all Series as that calculated from the model set forth by

Equation (IX-8). An example of the comparison is shown in Figure 26 Series C.

Series G to J reactions, with $[H_2O]_0$ limited to a range close to the stoichiometric requirement for ammonium sulfate production, resulted in two significant occurrences. Although water vapor was present in high enough initial concentration to produce ammonium sulfate, there was no indication of ammonium sulfate in the analysis of the product. On the basis of the estimated molecular weight of 93, the rate of formation of product does not match the rate predicted by Equation (IX-8) nearly as well as the Series A to F reactions wherein H_2O was in large excess. Series G to J composite product maintains the N : S ratio of 2 : 1. Total moles of product agree fairly well with the maximum based on limiting reactant.

Series K wherein oxygen concentration was limited to 31 $mM\text{-}m^{-3}$ or 1.5 times stoichiometric also resulted in no ammonium sulfate but with no amorphous material and more $(NH_3)_2 \cdot SO_2$. The Series K initial rate of product formation calculated by Equation (IX-8) follows the experimental rate (Figure 34) but the final number of moles of solid product experimentally far exceeds the maximum bases on the limiting concentration of the SO_2, 20.6 $mM\text{-}m^{-3}$.

All of the above results raise several questions. It is obvious from the analysis of the various samples that ammonium sulfate is not the only product of the reaction. When the concentrations of water or oxygen are reduced from a large excess to one and a half the stoichiometric equivalent, there is no ammonium sulfate formed. The question

Table 10. Series G-K Reactants and Products

	mMol - meter^{-3}				
Reactants	G	H	I	J	K
$[NH_3]_o$	40.4	20.9	40.4	60.1	47.3
$[SO_2]_o$	20.9	20.9	20.9	20.9	20.6
$[H_2O]_o$	31	16	16	16	668
$[O_2]_o$	← 8530 (Air) →				31

	Mole %	
Products	G-J	K
$(NH_3)_2 \cdot SO_2$	68	85
$NH_3 \cdot SO_2$	20	0
$NH_3 \cdot SO_3$	7	5
NH_4N_3	5	0
$NH_3H_7SO_4$	0	10
	100	100
Avg. Mol. Wt.	93	103

naturally arises as to what is the composition of the solid that initially precipitates out of the gas stream. It could be the result of the reaction,

$$NH_3(g) + SO_2(g) \longrightarrow NH_3 \cdot SO_2 \qquad \text{(IX-16)}$$

with the competing reactions:

$$NH_3 \cdot SO_2 + NH_3(g) \longrightarrow (NH_3)_2 \cdot SO_2(S) \qquad \text{(IX-17)}$$

$$nNH_3 \cdot SO_2 \longrightarrow (NH_3 \cdot SO_2)_n(S)$$

Further reaction with the H_2O vapor and O_2 could be a surface reaction of the gases with the solids.

$$(NH_3)_2 \cdot SO_2(S) + \tfrac{1}{2} O_2(g) \longrightarrow NH_4SO_3NH_2(S) \qquad \text{(IX-18)}$$

$$NH_4SO_3NH_2(S) + H_2O(g) \longrightarrow (NH_4)_2SO_4(S) \qquad \text{(IX-19)}$$

With the flow reactor used in this work, a reaction between an $NH_3 \cdot SO_2$ or $(NH_3)_2 \cdot SO_2$ solid and H_2O, O_2 gases would be facilitated by the solid being trapped in the reactor and provided with much exposure to the gases which flow by. The apparent independence of the number of moles of solid formed to the oxygen concentration would be explained by this scheme. The number of moles of solid formed appears to be dependent to some extent on the H_2O concentration which suggest the formation of $NH_3 \cdot SO_2$ and/or $(NH_3)_2 \cdot SO_2$ is catalyzed by H_2O vapors as has been suggested by previous researchers. If the reaction were one producing ammonium sulfate only with the rate dependent on $[H_2O]$ as in Equations (IX-14) and (IX-15), sulfate formation would be much lower than it actually is. This is shown on Figure 30 where moles of product calculated by Equations (IX-14) and (IX-15) is plotted.

There is the possibility that the first appearance of a solid reaction product is $(NH_3)_2 \cdot SO_2$ by the reaction

$$NH_3(g) + SO_2(g) \xrightarrow{k_1} NH_3 \cdot SO_2 \qquad \text{(IX-20)}$$

$$NH_3 \cdot SO_2 + NH_3(g) \xrightarrow{k_2} (NH_3)_2 \cdot SO_2 \ (c) \qquad \text{(IX-21)}$$

The kinetics of reactions of Equations (IX-20) and (IX-21) are thoroughly covered in the literature[58,59,60,61,62]. Rate expressions are written as follows:

$$\frac{d[SO_2]}{dt} = -k_1[SO_2][NH_3] \qquad \text{(IX-22)}$$

$$\frac{d[NH_3]}{dt} = -k_1[SO_2][NH_3] - k_2[NH_3][NH_3 \cdot SO_2] \qquad \text{(IX-23)}$$

$$\frac{d[NH_3 \cdot SO_2]}{dt} = k_1[SO_2][NH_3] - k_2[NH_3][NH_3 \cdot SO_2] \qquad \text{(IX-24)}$$

$$\frac{d[(NH_3)_2 \cdot SO_2]}{dt} = k_2[NH_3][NH_3 \cdot SO_2] \qquad \text{(IX-25)}$$

By dividing Equation (IX-24) by Equation (IX-22), time is eliminated as a variable:

$$\frac{d[NH_3 \cdot SO_2]}{d[SO_2]} = -1 + \frac{k_2}{k_1}\frac{[NH_3 \cdot SO_2]}{[SO_2]} \qquad \text{(IX-26)}$$

which can be solved for $(NH_3 \cdot SO_2)$:

$$[NH_3 \cdot SO_2] = \frac{[SO_2]}{K-1}\left[1 - \left(\frac{[SO_2]}{[SO_2]}\right)^{K-1}\right] \text{where } K = \frac{k_2}{k_1} \qquad \text{(IX-27)}$$

Similarly:

$$[NH_3]_o - [NH_3] = \left(\frac{2K-1}{K-1}\right)([SO_2]_o - [SO_2]) - \frac{[SO_2]_o}{K-1}\left[1 - \left(\frac{[SO_2]}{[SO_2]_o}\right)^{K}\right] \qquad \text{(IX-28)}$$

$$[(NH_3)_2 \cdot SO_2] = ([SO_2]_o - [SO_2]) - [NH_3 \cdot SO_2] \qquad \text{(IX-29)}$$

$$= [SO_2]_o - \frac{[SO_2]}{K-1}\left[K - \left(\frac{[SO_2]}{[SO_2]_o}\right)^{K-1}\right]$$

These equations together with the stoichiometric equations

$$[SO_2] = [SO_2]_o - [NH_3 \cdot SO_2] - [(NH_3)_2 \cdot SO_2] \qquad \text{(IX-30)}$$

$$[NH_3] = [NH_3 \cdot SO_2] - 2[(NH_3)_2 \cdot SO_2] \qquad \text{(IX-31)}$$

have been represented graphically[54] in generalized nomenclature as a plot of $\frac{[NH_3 \cdot SO_2]}{[SO_2]_o}$ vs. $1 - \frac{[SO_2]}{[SO_2]_o}$ with parameters of k_2/k_1 and $\frac{(NH_3)_o - NH_3}{(SO_2)_o}$.

This graphical representation can be used to determine k_2/k_1 by determining concentrations of reactants and products at any degree of completion of the reaction and reading k_2/k_1 off the graph. This procedure is described in detail in references 59 and 61. Unfortunately, the experimental data acquired in this work is not of sufficient accuracy or completeness to arrive at any conclusions as to whether the reactions of Equations (IX-20) and (IX-21) are valid.

A simpler treatment of Equations (IX-22) to (IX-25) is to use the steady state hypothesis:

Assume $$\frac{d[NH_3 \cdot SO_2]}{dt} = 0 = k_1[SO_2][NH_3] - k_2[NH_3][NH_3 \cdot SO_2] \qquad \text{(IX-32)}$$

$$[NH_3 \cdot SO_2] = \frac{k_1}{k_2}[SO_2] \qquad \text{(IX-33)}$$

Assuming the concentration of the intermediate is negligibly small:

$$\frac{d[(NH_3)_2SO_2]}{dt} = k_1([NH_3]_o - 2[(NH_3)_2SO_4])([SO_2]_o - [(NH_3)_2SO_4]) \quad (IX-34)$$

Equation (IX-34) is then identical to Equation (IX-5) and both schemes give the same results if the steady state hypothesis is applied to Equations (IX-20) and (IX-21). Benson[60] points out, however, that for values of K less than 100 the amount of SO_2 consumed before 99% of the steady state concentrations are reached rises from a fraction of .038 to .922 for K = .1.

Therefore, depending on the value of K the steady state hypothesis may or may not introduce significant error.

Aerosol Centrifuge

During the course of the research the aerosol centrifuge developed by Preining[39] was considered as a tool for the kinetic study. A Series L type reaction (Trace H_2O) was conducted in a flow tube for a period of time long enough to insure the reaction had gone to equilibrium. The reaction is reversible and the probable product, $(NH_3)_2 \cdot SO_2$ sublimes into its component gases. The results from the aerosol centrifuge run indicated the aerodynamic diameters of solid reaction product of NH_3:SO_2::2.1 gases in air are in the range from 1.2 μm to 2 μm with a mean of 1.5 μm.

Table 11. Sulfur Dioxide - Ammonia Reaction Parameters

Series A

Initial Concentration of Reactants, milli Mole-meter^{-3}

SO_2	3.98
NH_3	27.0
H_2O	668
O_2	8530 (air)

Product - Ammonium sulfate

Residence Time, sec.	0.029	0.057	0.119	0.190
Exp. Product Conc, mM-m^{-3}	1.02	2.65	3.46	3.84
Calculated Prod. Conc. mM-m^{-3}	1.44	2.27	3.22	3.66

Series B

Initial Concentration of Reactants, milli Mole-meter^{-3}

SO_2	6.05
NH_3	27.0
H_2O	682
O_2	8530 (air)

Products - Ammonium sulfate

Residence Time, sec.	0.029	0.057	0.119	0.190	0.286
Exp. Product Conc, mM-m^{3}	2.08	4.03	5.4	6.29	6.45
Calculated Prod. Conc. mM-m^{-3}	2.13	3.34	4.72	5.4	5.79

Table 11. (Continued)

Series C

Initial Concentrations of Reactants, milli Mole-meter^{-3}

SO_2	9.95
NH_3	27.0
H_2O	682
O_2	8530 (air)

Product - Ammonium sulfate

Residence Time, sec.	0.029	0.057	0.119	0.190	0.286	0.388
Exp. Prod. Conc., mM-m^{-3}	3.40	4.98	6.41	8.12	9.76	10.32
Calculated Prod. Conc. mM-m^{-3}	3.36	5.13	7.15	8.25	8.98	9.38
Residence time, sec		0.06	0.12	0.18	0.28	0.38
Calc. Prod. Conc., Eq's (13)+(14)		3.64	6.53	7.94	8.97	9.42

Series D

Initial Concentrations of Reactants, milli Mole-meter^{-3}

SO_2	27.0
NH_3	27.0
H_2O	682
O_2	8530 (air)

Product - Ammonium sulfate

Secondary Product - ammonium sulfamate

Residence Time, sec.	0.029	0.057	0.119	0.190	0.286
Exp. Prod. Conc., mM-m^{-3}	8.49	9.38	12.95	13.95	13.90
Calc. Prod. Conc., mM-m^{-3}	7.43	10.22	12.48	13.2	13.44

Table 11. (Continued)

Series E

Initial Concentration of Reactants, milli Mole-meter^{-3}

SO_2	0.14
NH_3	35.65
H_2O	682
O_2	8530 (air)

Product - Ammonium sulfate

Residence Time, sec.	0.057	0.119	0.190	0.286
Exp. Product Conc., mM-m^3	6.20	7.10	9.32	10.58
Calculated Product Conc., mM-m^3	6.30	8.38	9.33	9.82

Series F

Initial Concentration of Reactants, milli Mole-meter^{-3}

SO_2	20.6
NH_3	47.3
H_2O	668
O_2	8530 (air)

Product - Ammonium sulfate

Residence Time, sec.	0.029	0.057	0.119	0.190	0.286	0.388
Exp. Product Conc., mM-m^{-3}	9.0	10.5	15.1	16.6	18.3	19.6
Calculated Prod. Conc., mM-m^{-3}	9.66	13.33	16.73	18.3	19.29	19.8

Table 11. (Continued)

Series G

Initial Concentrations of Reactants, milli Mole-meter^{-3}

SO_2	20.9
NH_3	40.4
H_2O	31.1
O_2	8530 (air)

Product - (Estimated) 68% $(NH_3)_2SO_2$, 20% NH_3SO_2, 7% NH_3SO_3, 5% NH_4N_3

Residence Time, Sec.	0.104	0.212	0.338	0.51
Exp. Prod. Conc., mM-m^{-3}	13.2	14.6	17.4	17.4
Calculated Prod. Conc., mM-m^{-3} Eq.(17)	14.68	17.28	18.36	19.03
Residence Time, sec.	0.1	0.21	0.34	0.50
Calc. Prod. Conc., mM-m^{-3} Eq. (13)+(14)	0.93	2.04	3.22	4.63

Series H

Initial Concentrations of Reactants, milli Mole-meter^{-3}

SO_2	20.9
NH_3	20.7
H_2O	16.2
O_2	8530 (air)

Product - (Estimated) 68% $(NH_3)_2SO_2$, 20% NH_3SO_2, 7% NH_3SO_3, 5% NH_4N_3

Residence Time, Sec.	0.100	0.212	0.338	0.510	0.691	0.957
Exp. Prod. Conc., mM-m^{-3}	3.6	5.3	6.9	8.78	10.0	9.8
Calc. Prod. Conc., mM-m^{-3}	8.68	10.0	10.28	10.34	10.35	10.35

Table 11. (Continued)

Series I

Initial Concentrations of Reactants, milli Mole-meter^{-3}

SO_2	20.9
NH_3	40.4
H_2O	16.2
O_2	8530 (air)

Product - (Estimated) 68% $(NH_3)_2SO_2$, 20% NH_3SO_2, 7% NH_3SO_3, 5% NH_4N_3

Residence Time, Sec.	0.100	0.212	0.338	0.510	0.69	0.957
Exp. Prod. Conc., mM-m^{-3}	6.65	11.6	13.5	17.0	18.1	18.3
Calc. Prod. Conc., mM-m^{-3}	14.68	17.28	18.36	19.03	19.39	19.68

Series J

Initial Concentrations of Reactants, milli Mole-meter^{-3}

SO_2	20.9
NH_3	60.1
H_2O	16.2
O_2	8530 (air)

Product - (Estimated) 68%$(NH_3)_2SO_2$, 20% NH_3SO_2, 7% NH_3SO_3, 5% NH_4N_3

Residence Time, Sec.	0.100	0.212	0.338	0.510	0.611
Exp. Prod. Conc., mM-m^{-3}	7.1	14.0	20.4	20.3	20.3
Calc. Prod. Conc., mM-m^{-3}	18.2	20.26	20.75	20.88	20.9

Table 11. (Continued)

Series K

Initial Concentrations of Reactants, milli Mole-meter^{-3}

SO_2	20.6
NH_3	47.3
H_2O	668
O_2	31

Product - (Estimated) 85% $(NH_3)_2SO_2$, 10% $N_3H_7SO_4$, 5% NH_3SO_3

Residence Time, Sec.	0.029	0.057	0.119	0.189	0.2855
Exp. Prod. Conc., mM-m^{-3}	11.0	14.25	19.15	22.1	27.1
Calc. Prod. Conc., mM-m^{-3}	9.66	13.32	16.73	18.3035	19.29

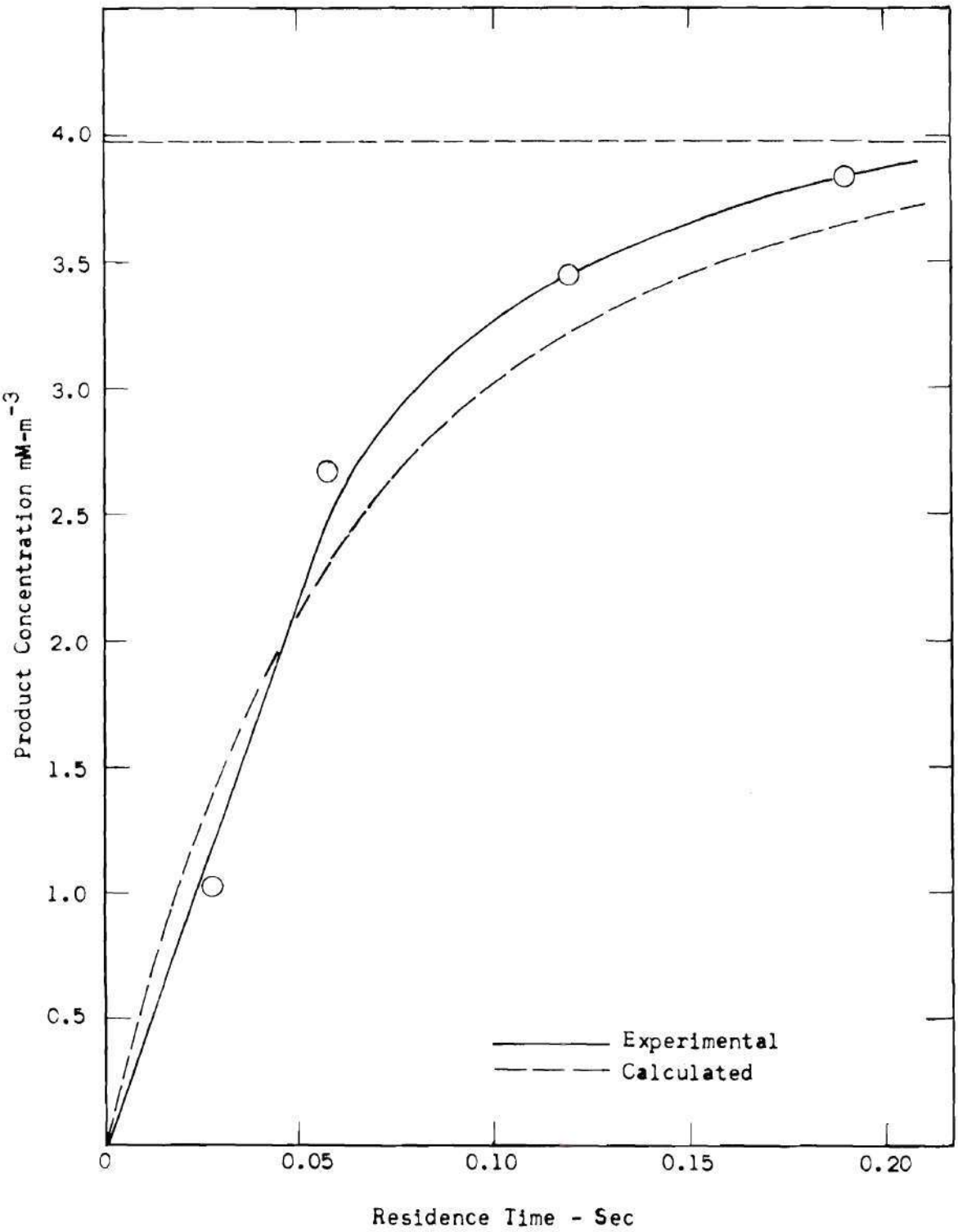

Figure 24. Series A Reactions - Prod. Conc. vs. Time.

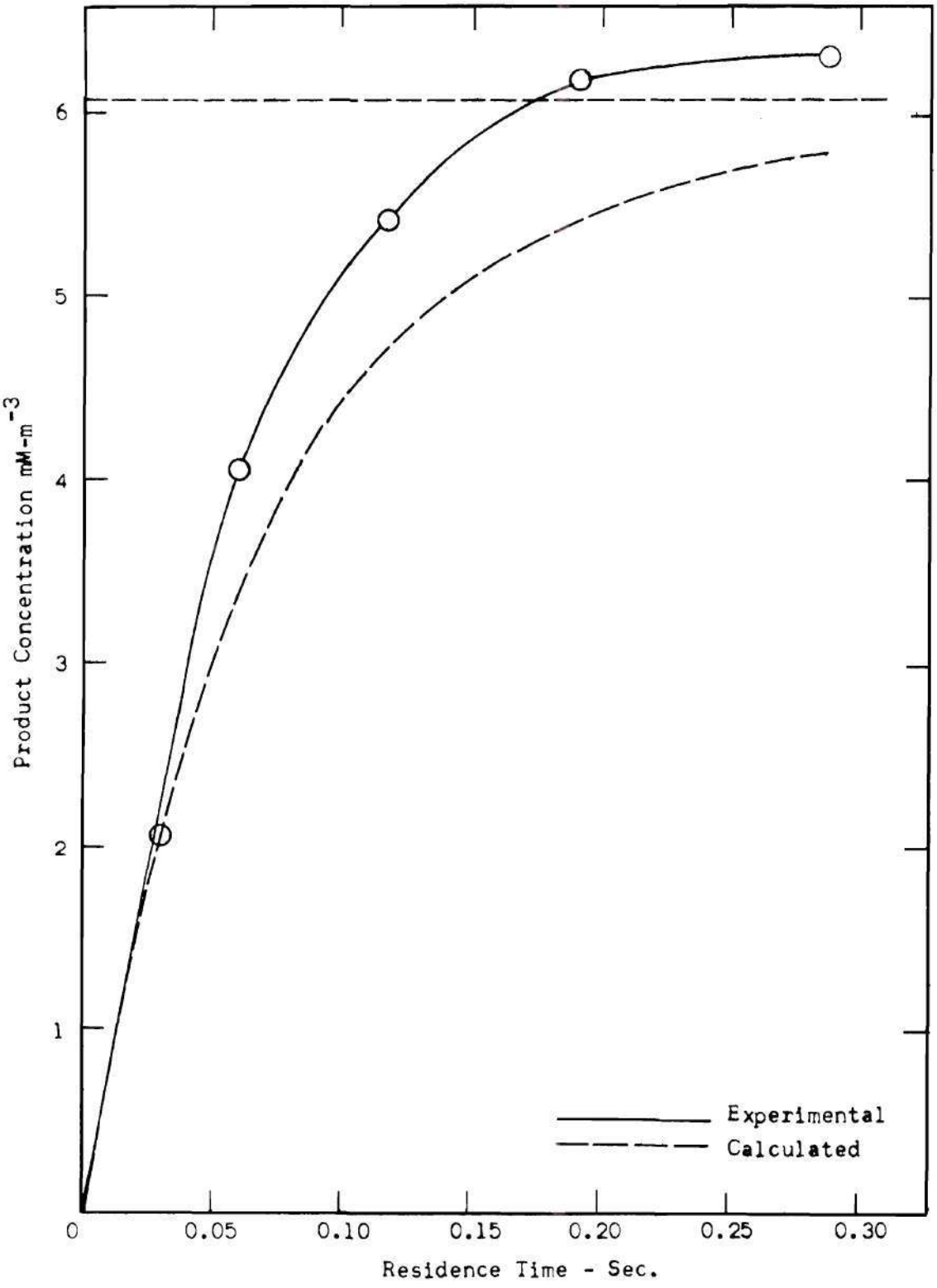

Figure 25. Series B Reactions - Prod. Conc. vs. Time.

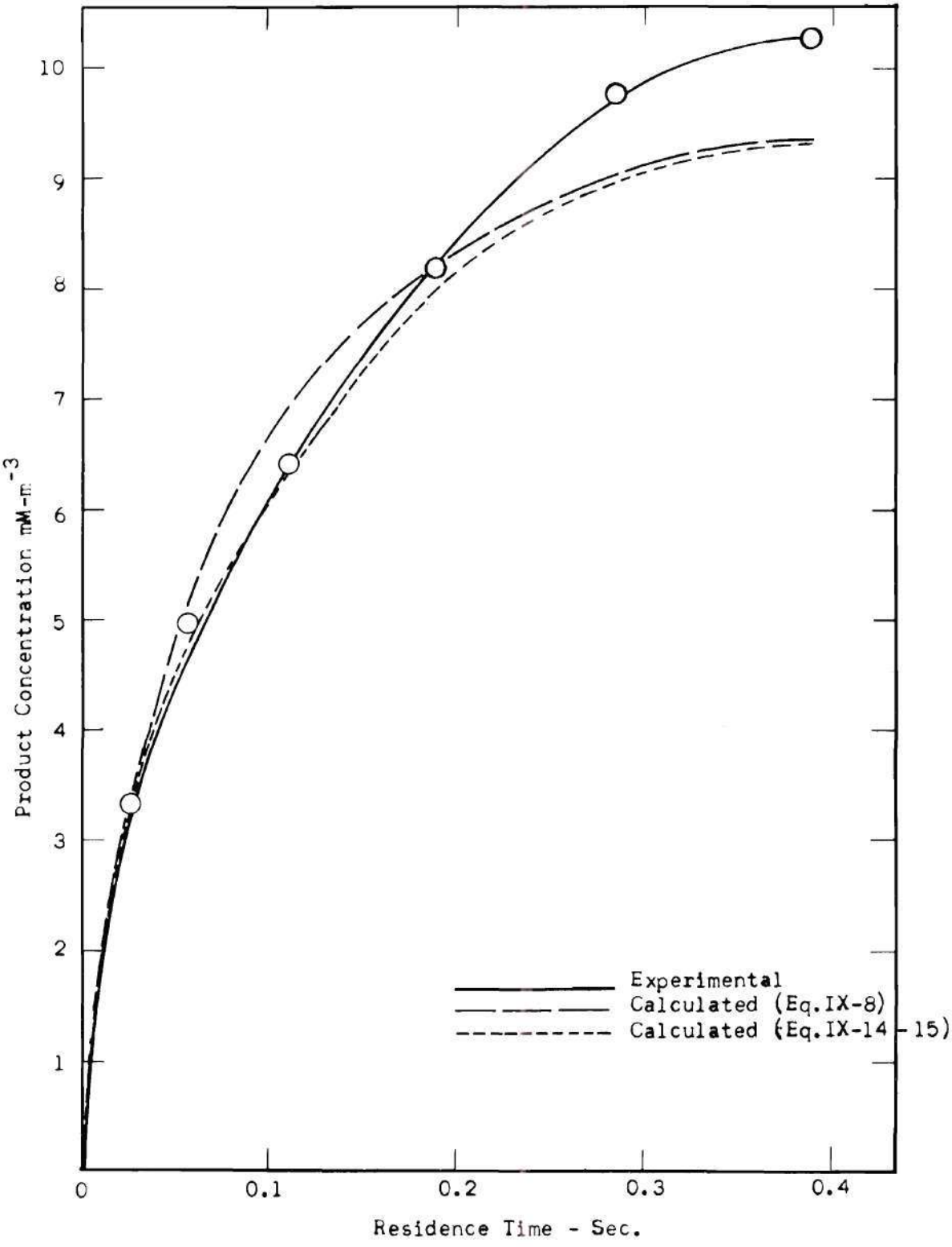

Figure 26. Series C Reactions - Prod. Conc. vs. Time.

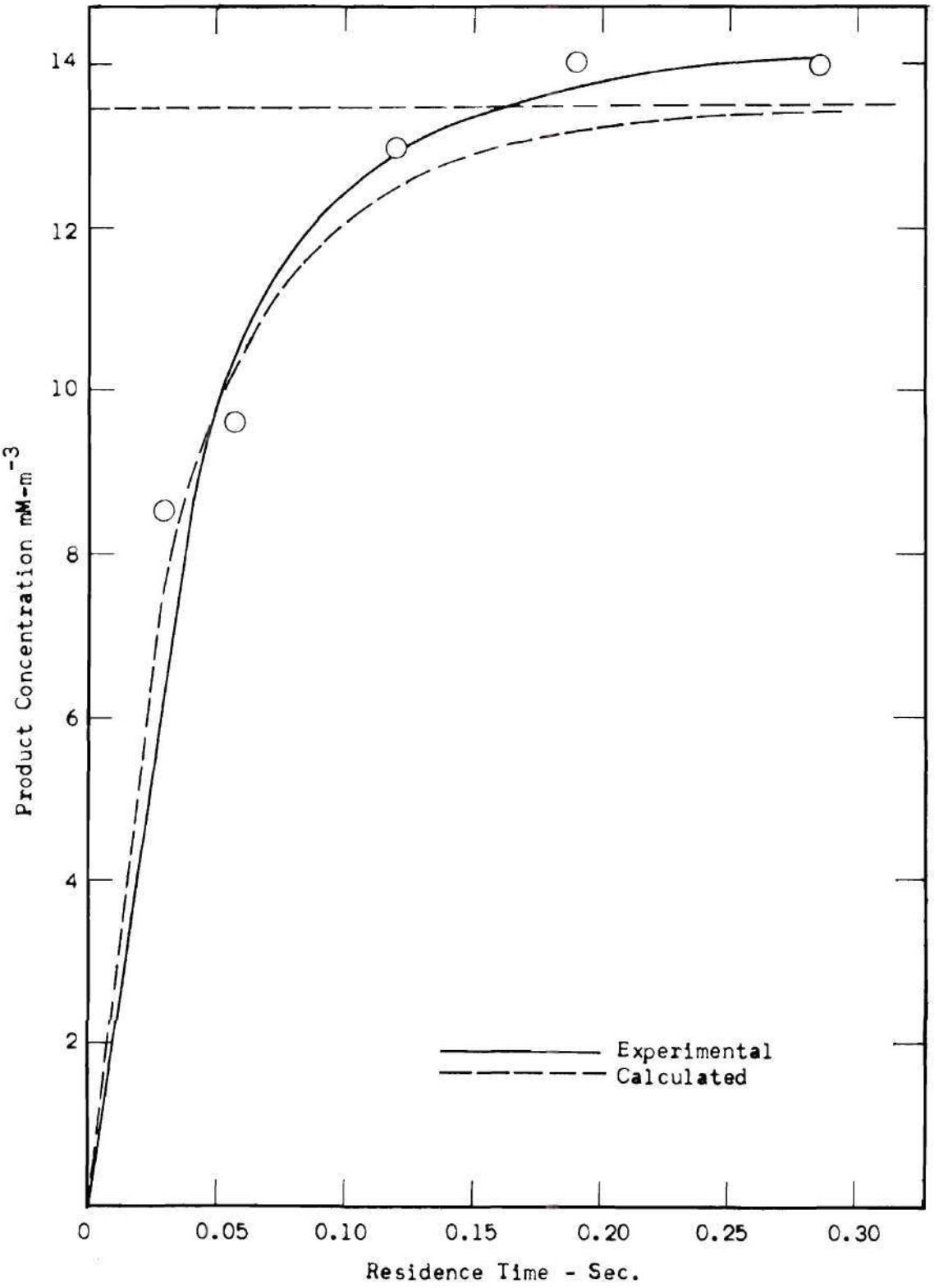

Figure 27. Series D Reactions - Prod. Conc. vs. Time.

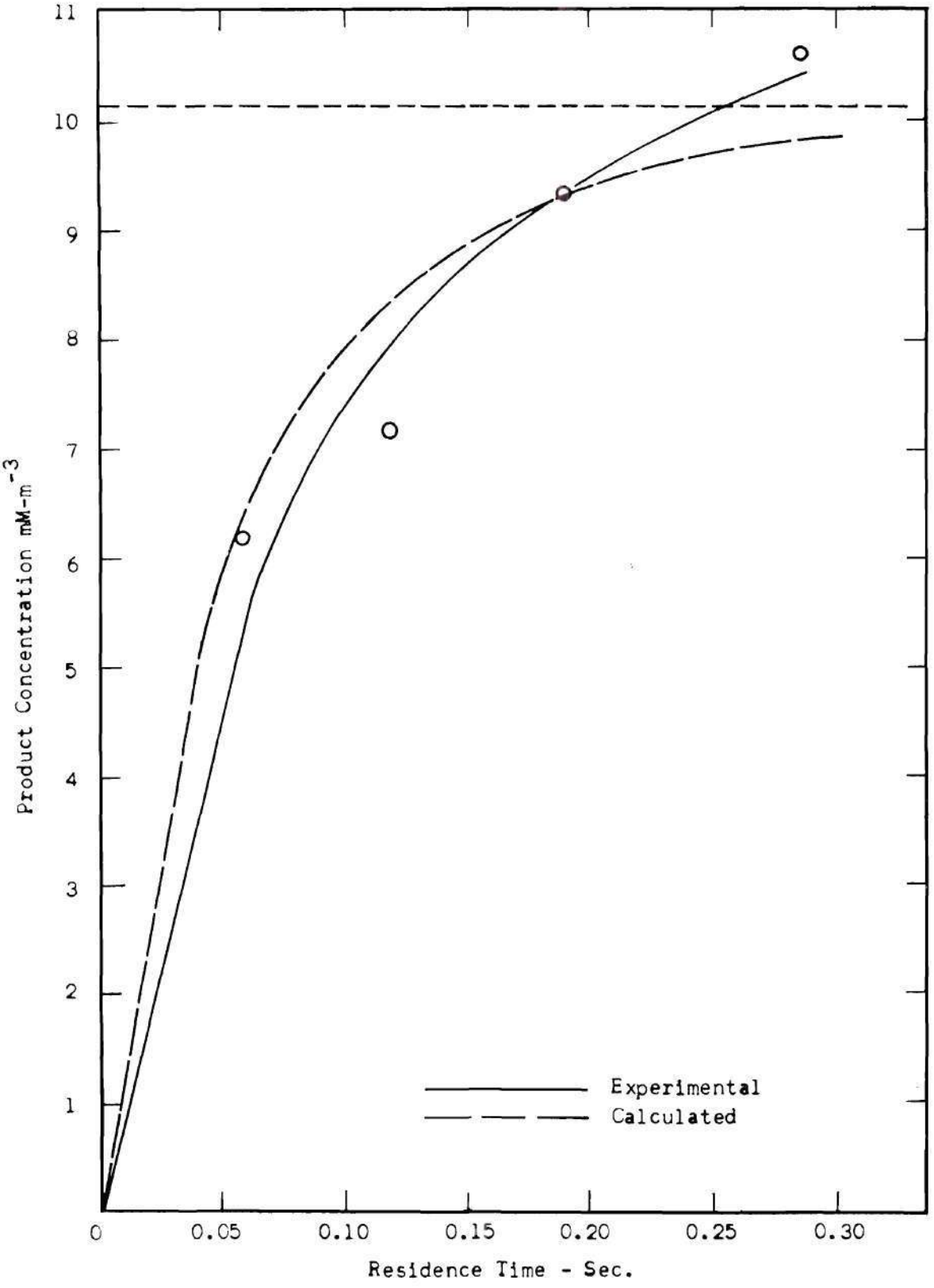

Figure 28. Series E Reactions - Prod. Conc. vs. Time.

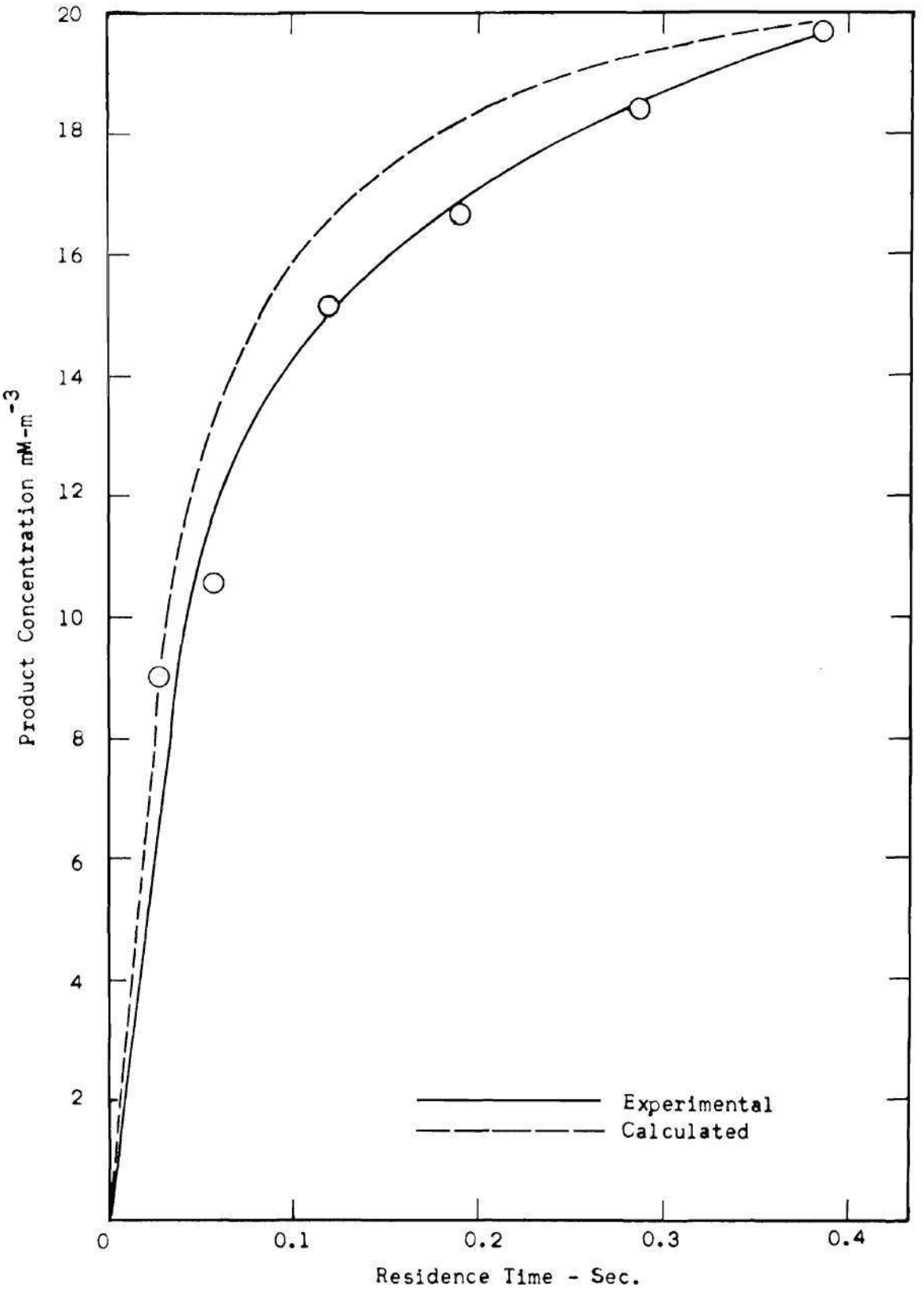

Figure 29. Series F Reactions - Prod. Conc. vs. Time.

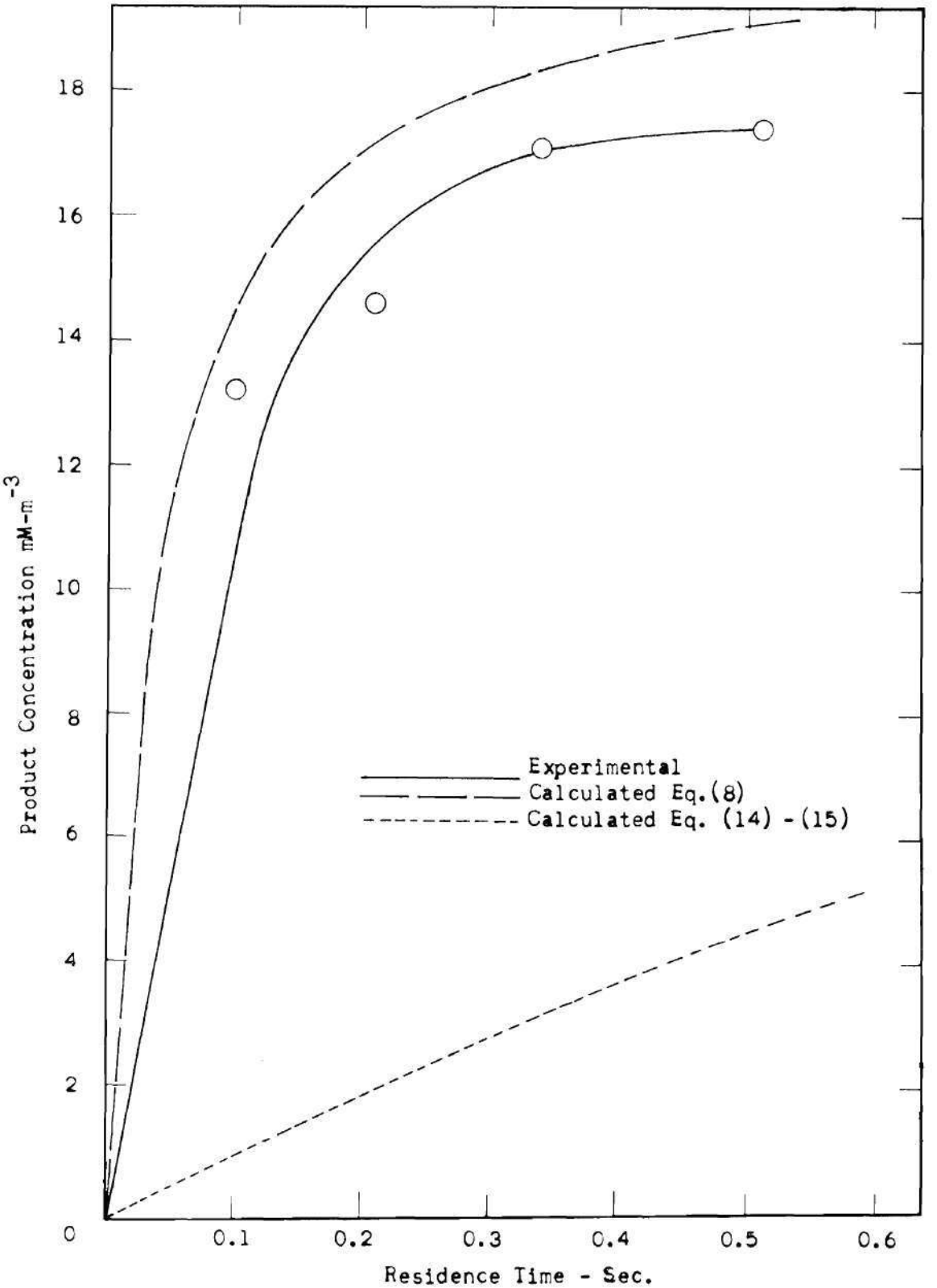

Figure 30. Series G Reactions - Prod. Conc. vs. Time.

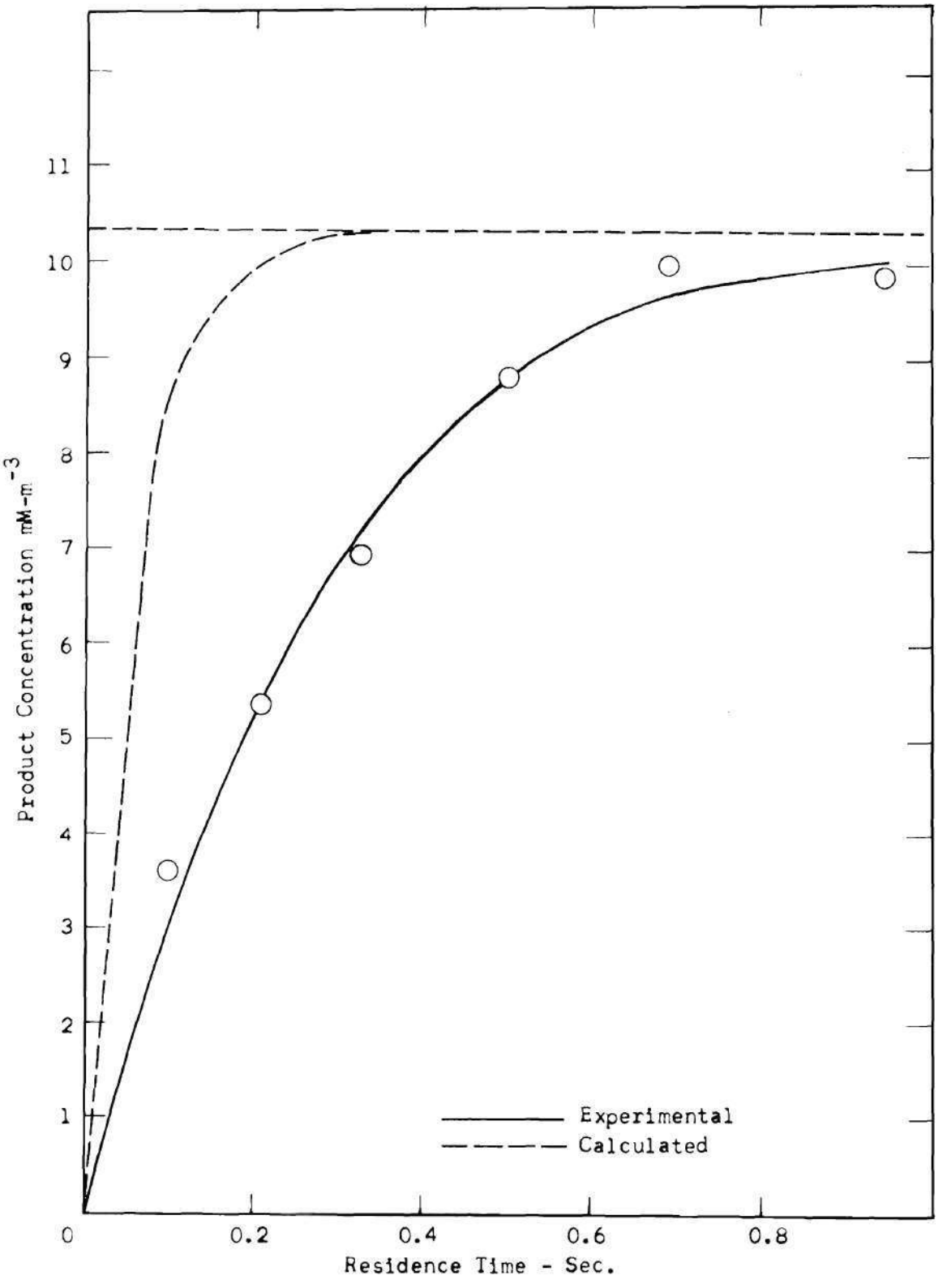

Figure 31. Series H Reactions - Prod. Conc. vs. Time.

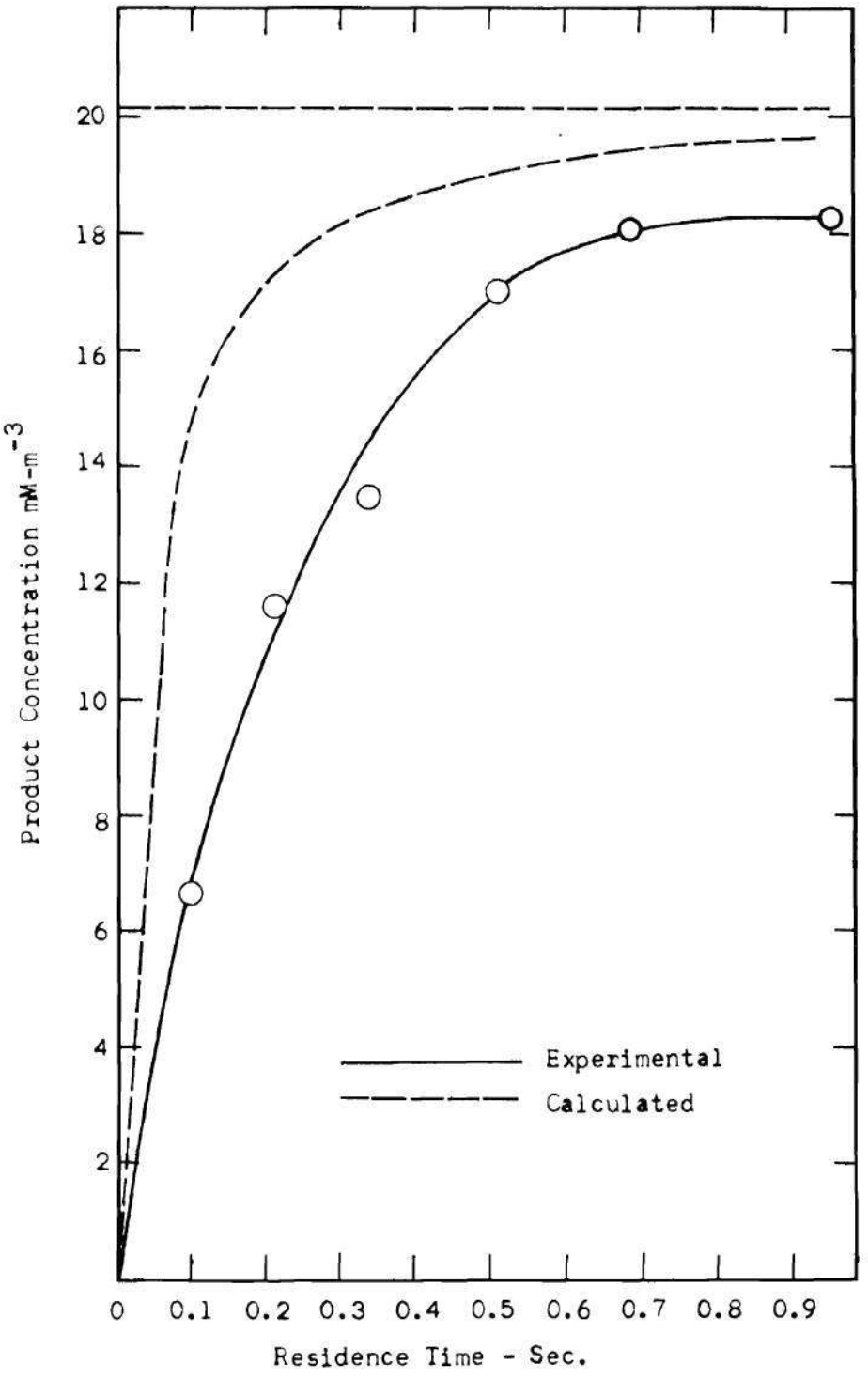

Figure 32. Series I Reactions - Product Conc. vs. Time.

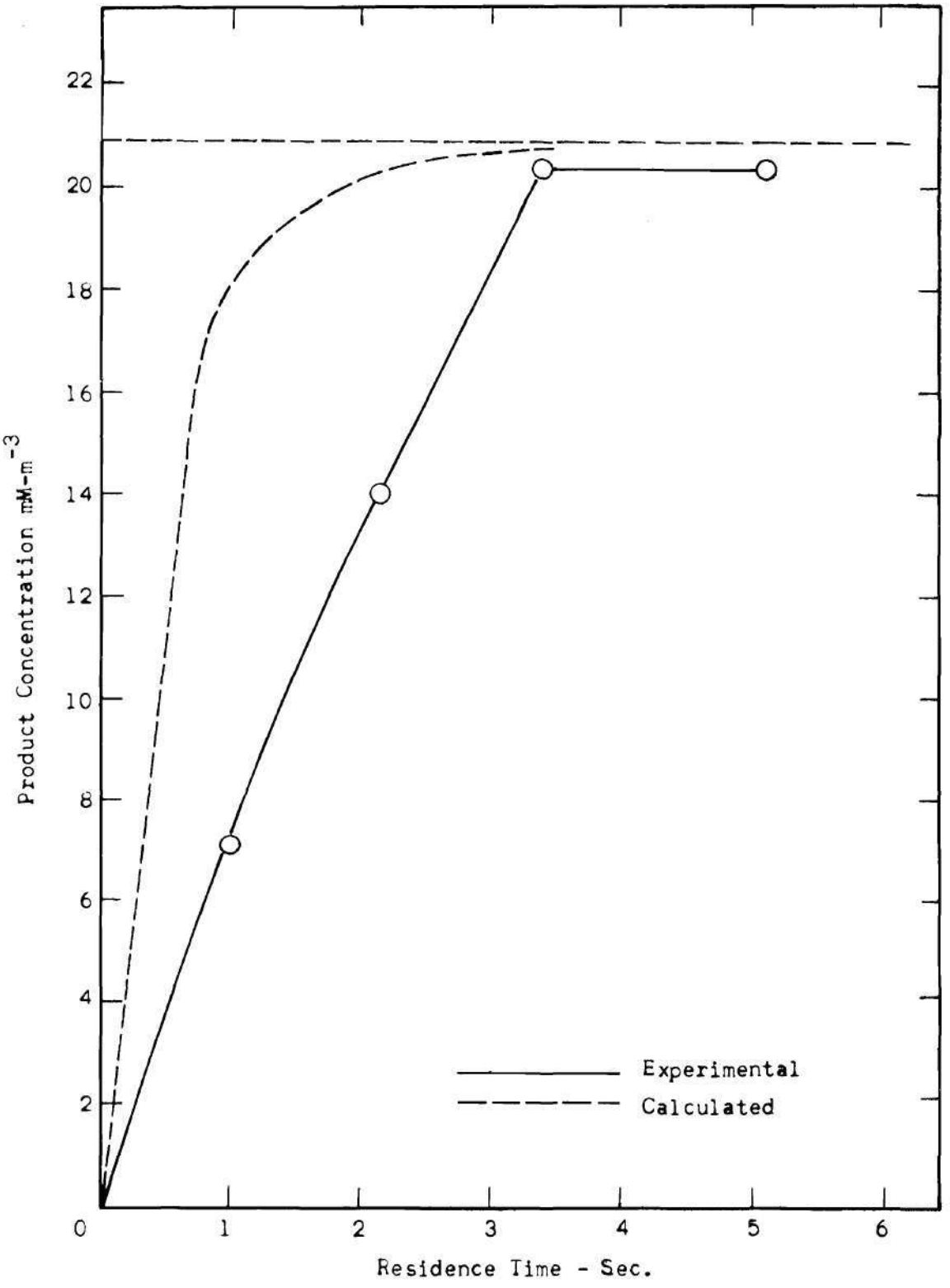

Figure 33. Series J Reactions - Prod. Conc. vs. Time.

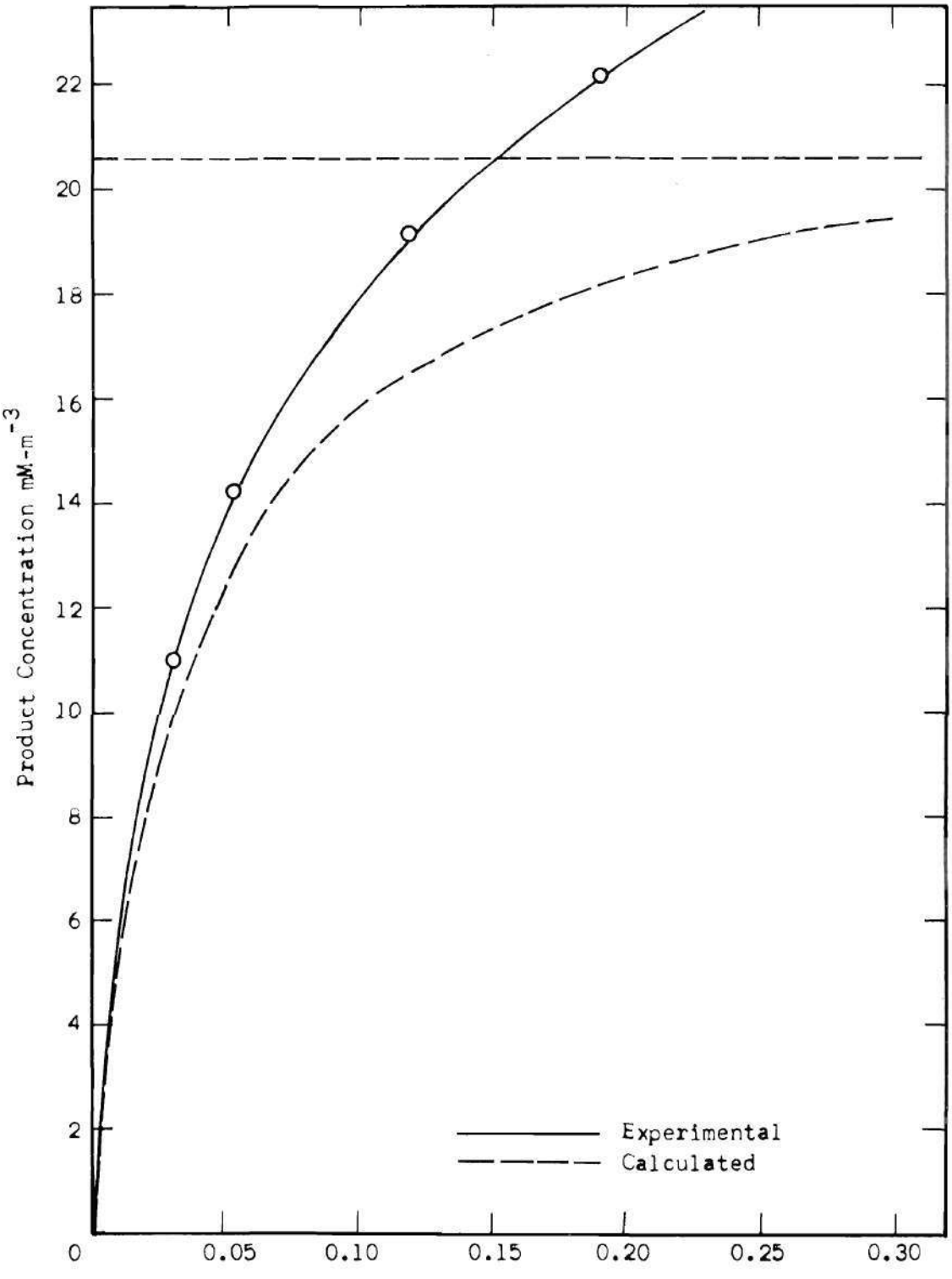

Figure 34. Series K Reactions - Prod. Conc. vs. Time.

CHAPTER X

CONCLUSIONS AND RECOMMENDATIONS

Conclusions

Ammonia gas and sulfur dioxide gas, in the molar ratio of $\geq 1 : 1$, in the concentration range of 4 to 60 millimoles per cubic meter, in air of at least 50% relative humidity, at 1 atmosphere and room temperature, react to produce almost all crystalline ammonium sulfate. At the lower ratio of NH_3 to SO_2 (1 : 1), 2 - 3% ammonium sulfamate will result in addition to the ammonium sulfate. The reaction goes to completion and the rate of formation of the solid reaction product, P, is fairly well represented by the rate equation:

$$\frac{dP}{dt} = K[NH_3][SO_2] \qquad (X\text{-}1)$$

with

$$[NH_3] = [NH_3]_o - 2P \qquad (X\text{-}2)$$

$$[SO_2] = [SO_2]_o - P \qquad (X\text{-}3)$$

$$K = .61 \ \frac{\text{meter}^3}{\text{millimole-sec.}}$$

Equation (1) is integrated to solve for P:

$$P = \frac{\text{Exp}\{Kt[NH_3]_o - 2[SO_2]_o)\} - 1}{\text{Exp}\{Kt[NH_3]_o - 2[SO_2]_o\}/[SO_2]_o - 2/[NH_3]_o} \qquad (X\text{-}4)$$

If the H_2O vapor is present only at a concentration of the same magnitude of the SO_2 and NH_3, the solid reaction product is not ammonium

sulfate. It does not fit any of the common diffraction patterns, contains an amorphous fraction, and is assumed to be essentially a mixture of $(NH_3)_2 \cdot SO_2$ referred to as ammonium amido sulfite and $NH_3 \cdot SO_2$ referred to as amido sulfurous acid. Secondary products of NH_3SO_3 and NH_4N_3 will be formed in small amounts. Equation (X-1) is in error by as much as 150% (high) in predicting intermediate products moles at time t. Equation (X-1), however, is fairly accurate in predicting final product moles and time of completion of reaction.

For trace amounts of H_2O vapor, all other conditions held the same as above, the same primary products are formed with additional secondary products of $(NH_4)_2 S_2O_7$ and $N_3H_7SO_4$. The rate of solid formation is much lower indicating the reaction is catalyzed by H_2O vapor.

With a large excess of water vapor but the oxygen concentration present only in the concentration range of the NH_3 and SO_2, again no ammonium sulfate is formed. The product does not fit any of the common diffraction patterns, is crystalline, and assumed to be $(NH_3)_2 \cdot SO_2$. Secondary products formed in small amounts are $N_3H_7SO_4$ and NH_3SO_3.

There is evidence the initial precipitation of solid from gas phase is $NH_3 \cdot SO_2$ and/or $(NH_3)_2 \cdot SO_2$ which consequently reacts with H_2O and O_2 to an extent dependent on the concentration of the latter.

The heterogeneous reaction of the four gaseous reactants, H_2O, O_2, SO_2, NH_3 in N_2 carrier gas to form solid reaction products is complex. The amount of product, rate at which it is formed, and identity of the product is dependent on the concentration of the reactants and probably on the method by which they are contacted. Apparently, an infinite variety of products of various compositions are possible.

Recommendations

1. The product identity and reaction rate of SO_2 - NH_3 reaction in the presence of large excesses of H_2O and O_2 should be determined for an $(NH_3)_0 : (SO_2)_o$ of $< 1 : 1$.

2. The product identity and reaction rate of SO_2 - NH_3 reactions with large excess of H_2O and O_2 at other temperatures would be of interest.

3. For reactions with a limited concentration of H_2O and O_2 an x-ray diffraction pattern is needed for $NH_3 \cdot SO_2$ and $(NH_3)_2 \cdot SO_2$. X-ray diffraction patterns are needed for mixtures of the various compounds encountered in this work. Other methods of qualitative and quantitative analysis to complement x-ray diffraction would be of value.

4. The nature of the reaction is in need of clarification. It should be determined under various experimental conditions if the initial solid product which precipitates from the gas phase is the same as the final product or if it is an intermediate which undergoes a surface reaction with the reacting gases to produce the final product. Comparison of batch and flow reactor data should throw some light on this matter. Also of help in clarifying the situation would be reaction rates and product (if any) resulting from reactions such as $NH_3 \cdot SO_2(s) + O_2(g)$, $NH_3 \cdot SO_2(s) + H_2O(g)$, $NH_3 \cdot SO_2(s) + NH_3(g)$, $(NH_3)_2 \cdot SO_2(c) + O_2(g)$, $(NH_3)_2 \cdot SO_2(c) + H_2O(g)$, $NH_4SO_3NH_2(c) + H_2O(g)$.

5. A study of the SO_2 - NH_3 reaction in the presence of a large excess of H_2O vapor but with limited O_2 concentration at high temperature would be applicable to SO_2 removal from combustion gases.

APPENDIX A

TEST DATA - SO_2 REACTIONS WITH AQUEOUS SOLUTIONS OF MANGANESE

Slope Intercept Tests

t[≈] min AOP[≈] PPM J[≈] mM-cc^{-1}

Run No.	49			28			54		
Temp., °C	25			25			25		
Press., mmHg	743			740			743		
B_o, mM/cc	0.003			0.003			0.003		
AIP, PPM	4748			4296			3847		
V_o, cc/min	1018			1018			1018		
V cc	10			10			10		
R_o mM/cc	2.56×10^{-3}			2×10^{-3}			1.1×10^{-3}		
$(dJ/dt)_o$	1.16×10^{-2}			1.13×10^{-2}			1.11×10^{-2}		
	t	AOP	J	t	AOP	J	t	AOP	J
	0	1558	0	0	1148	0	0	663	0
	2.0	1736	.039	2.9	1306	.034	2.9	772	.043
	4.9	1935	.066	4.9	1489	.062	4.9	923	.067
	6.9	2106	.093	6.9	1630	.086	6.9	1073	.092
	8.9	2277	.113	8.9	1750	.110	8.9	1207	.117
	10.9	2408	.135	10.9	1866	.132	10.9	1346	.140
	12.9	2538	.156	12.9	1968	.153	12.9	1479	.162
	14.9	2666	.175	14.9	2066	.175	14.9	1599	.183
	16.9	2785	.194	16.9	2171	.196			
Run No.	67			48			70		
Temp., °C	25			25			25		
Press., mmHg	739			743			739		
B_o, mM/cc	0.003			0.001			0.001		
AIP, PPM	3460			4807			4217		
V_o, cc/min	1018			1018			1018		
V cc	10			10			10		
R_o mM/cc	6×10^{-4}			6.7×10^{-3}			5.7×10^{-3}		
$(dJ/dt)_o$	1.08×10^{-2}			4.18×10^{-3}			4.15×10^{-3}		
	t	AOP	J	t	AOP	J	t	AOP	J
	0	461	0	0	3857	0	0	3212	0
	2.9	489	.039	2.9	3887	.015	2.9	3312	.012
	4.9	573	.065	4.9	3980	.023	4.9	3417	.020
	6.9	671	.093	6.9	4057	.030	6.9	3528	.028
	8.9	757	.116	8.9	4150	.036	8.9	3576	.033
	10.9	864	.140	10.9	4226	.042	10.9	3628	.038
	12.9	954	.164	12.9	4257	.047	12.9	3653	.043
	14.9	1062	.186	14.9	4329	.051	14.9	3702	.047

Appendix A (Continued)

Run No.	53			66			56	
Temp. °C	25			25			25	
Press., mmHg	739			742			742	
B_o, mM/cc	0.001			0.001			0.001	
AIP. PPM	3845			3403			2920	
V_o, cc/min	1018			1018			1018	
V, cc	10			10			10	
R_o mM/cc	5×10^{-3}			4.2×10^{-3}			3.3×10^{-3}	
$(dJ/dt)_o$	4.18×10^{-3}			4.2×10^{-3}			4.15×10^{-3}	
	t	AOP	J	t	AOP	J	t	AOP	J
	0	2857	0	0	2355	0	0	1960	0
	2.9	2909	.015	2.9	2427	.015	2.9	2018	.013
	4.9	2972	.023	4.9	2501	.023	4.9	2072	.021
	6.9	3035	.031	6.9	2577	.031	6.9	2126	.028
	8.9	3123	.038	8.9	2660	.038	8.9	2121	.035
	10.9	3190	.044	10.9	2731	.045	10.9	2227	.042
	12.9	3224	.050	12.9	2798	.050	12.9	2274	.048
	14.9	3275	.055	14.9	2824	.055	14.9	2338	.053

Run No.	74			75			133	
Temp. °C	25			25			1	
Press., mmHg				737			727	
B_o mM/cc	0.001			0.001			0.003	
AIP, PPM	2238			1903			4781	
V_o, cc/min	1018			1018			1018	
V, cc	10			10			10	
R_o mM/cc	2.1×10^{-3}			1.7×10^{-3}			2.2×10^{-2}	
$(dJ/dt)_o$	4.11×10^{-3}			4.1×10^{-3}			1.5×10^{-3}	
	t	AOP	J	t	AOP	J	t	AOP	J
	0	1252	0	0	986	0	0	4449	0
	2.9	1299	.013	2.9	1011	.014	2.28	4467	.0016
	4.9	1376	.021	4.9	1029	.023	4.28	4497	.0043
	6.9	1442	.027	6.9	1073	.030	6.28	4528	.0066
	8.9	1514	.034	8.9	1131	.035	8.28	4559	.0087
	10.9	1561	.041	10.9	1186	.042	10.28	4590	.0104
	12.9	1605	.042	12.9	1239	.046			
	14.9	1647	.052	14.9	1287	.050			

Appendix A (Continued)

Run No.	31	130	132
Temp. °C	1	1	1
Press., mmHg	740	727	727
B_o, mM/cc	0.003	0.003	0.003
AIP, PPM	4329	4309	3376
V_o, cc/min	1018	1018	1018
V, cc	10	10	10
R_o, mM/cc	1.96×10^{-2}	1.9×10^{-2}	1.49×10^{-2}
$(dJ/dt)_o$	1.42×10^{-3}	1.7×10^{-3}	1.33×10^{-3}

t	AOP	J	t	AOP	J	t	AOP	J
0	3969	0	0	3921	0	0	3070	0
2.76	3990	.0022	2.22	3940	.0018	2.23	3085	.0014
4.76	4016	.0047	4.22	3972	.0049	4.23	3113	.0038
6.76	4043	.0070	6.22	4004	.0077	6.23	3141	.0060
8.76	4070	.0091	8.22	4037	.0103	8.23	3170	.0079
10.76	4090	.0109	10.22	4070	.0125	10.23	3191	.0095
12.76	4103	.0126				12.23	3204	.0111
14.78	4116	.0142						
16.78	4129	.0157						

Run No.	131	146	140
Temp. °C	1	1	38
Press., mmHg	727	730	728
B_o, mM/cc	0.003	0.003	0.003
AIP, PPM	2588	1315	5154
V_o, cc/min	1018	1018	1018
V cc	10	10	10
R_o mM/cc	1.11×10^{-2}	5.3×10^{-3}	1.67×10^{-3}
$(dJ/dt)_o$	1.3×10^{-3}	1.02×10^{-3}	1.47×10^{-2}

t	AOP	J	t	AOP	J	t	AOP	J
0	2287	0	0	1088	0	0	1486	0
2.37	2303	.0015	2.59	1091	.0012	2.3	1602	.034
4.37	2332	.0038	4.59	1095	.0032	4.3	1718	.066
6.37	2361	.0059	6.59	1100	.0052	6.3	1838	.097
8.37	2390	.0077	8.59	1104	.0071	8.3	1924	.127
10.37	2419	.0093	10.59	1109	.0090			
12.37	2448	.0106	12.59	1113	.0108			
14.37	2459	.0117	14.59	1118	.0126			
16.37	2481	.0127	16.59	1123	.0144			

Appendix A (Continued)

Run No.	137	141	38
Temp. °C	38	38	38
Press, mmHg	736	728	739
B_o, mM/cc	0.003	0.003	0.003
AIP, PPM	4878	4537	4297
V_o, cc/min	1018	1018	1018
V, cc	10	10	10
R_o, mM/cc	1.69×10^{-3}	8.34×10^{-4}	9.34×10^{-4}
$(dJ/dt)_o$	1.48×10^{-2}	1.47×10^{-2}	1.46×10^{-2}

t	AOP	J	t	AOP	J	t	AOP	J
0	1489	0	0	746	0	0	818	0
2.01	1555	.027	2.24	863	.035	2.7	905	.037
4.01	1629	.057	4.24	985	.067	4.7	964	.069
6.01	1704	.087	6.24	1087	.099	6.7	1012	.098
			8.24	1181	.130	8.7	1030	.126
						10.7	1062	.154
						12.7	1098	.180
						14.7	1135	.206

Run No.	142	139	138
Temp. °C	38	38	38
Press., mmHg	728	736	736
B_o, mM/cc	0.003	0.003	0.003
AIP, PPM	3873	3711	3242
V_o, cc/min	1018	1018	1018
V cc	10	10	10
R_o mM/cc	1.75×10^{-4}	4.18×10^{-5}	4.24×10^{-5}
$(dJ/dt)_o$	1.46×10^{-2}	1.44×10^{-2}	1.45×10^{-2}

t	AOP	J	t	AOP	J	t	AOP	J
0	155	0	0	37	0	0	37	0
2.33	240	.036	2.28	55	.035	2.31	69	.030
4.33	323	.068	4.28	73	.068	4.31	101	.059
6.33	401	.100	6.28	92	.102	6.31	126	.088
8.33	464	.132				8.31	137	.117
10.33	529	.162						

Appendix A (Continued)

Run No.	112	111	113
Temp. °C	65	65	65
Press., mmHg	740	740	740
B_o, mM/cc	0.003	0.003	0.003
AIP, PPM	4193	4067	3940
V_o, cc/min	1018	1018	1018
V, cc	10	10	10
R_o, mM/cc	5.3×10^{-5}	3.2×10^{-5}	2.5×10^{-4}
$(dJ/dt)_o$	1.96×10^{-2}	1.96×10^{-2}	1.97×10^{-2}

t	AOP	J	t	AOP	J	t	AOP	J
0	175	0	0	104	0	0	824	0
2.1	325	.031	1.3	150	.017	1.31	924	.014
20.1	325	.30	16.3	150	.251	21.12	924	.340

Run No.	22	147	127
Temp. °C	11	38	25
Press., mmHg	737	727	733
B_o, mM/cc	0.003	0.003	0.003
AIP, PPM	4184	4541	4277
V_o, cc/min	1018	1018	1018
V, cc	10	10	10
R_o, mM/cc	9.5×10^{-3}	1.19×10^{-3}	1.882×10^{-3}
$(dJ/dt)_o$	3.9×10^{-3}	1.55×10^{-2}	1.41×10^{-3}

t	AOP	J	t	AOP	J	t	AOP	J
0	3515	0	0	1062	0	0	1091	0
2.21	3547	.008	113	3090	1.13	114	3546	.68
4.21	3579	.011	233	3780	1.72	234	3737	1.03
6.21	3612	.024	353	3975	2.08	354	3860	1.31
8.21	3645	.030	473	4175	2.37	474	3942	1.48
10.21	3678	.036						
12.21	3700	.041						
14.21	3725	.046						

Appendix A (Continued)

Run No.	134
Temp. °C	1
Press., mmHg	730
B_o, mM/cc	0.003
AIP, PPM	4253
V_o, cc/min	1018
V, cc	10
R_o, mM/cc	1.95×10^{-2}
$(dJ/dt)_o$	1.65×10^{-3}

t	AOP	J
0	3910	0
103	4150	.06
203	4165	.12
303	4182	.18
403	4200	.25

APPENDIX B

EQUILIBRIUM H_2SO_4 CONCENTRATION CALCULATION

P = 1 atm.

T = 298°K

Gas Phase: SO_2 - 4000 PPM (vol.)
air - O_2, N_2, H_2O Vapor

Liquid Phase: H_2O

$$H_2SO_4 \rightleftharpoons H^+ + HSO_4^- \rightleftharpoons H^+ + SO_4^=$$

$MnSO_4$ and Mn complexes, .003 molar

Dissolved SO_2, O_2, etc.

Reaction:

$$SO_2(aq) + \tfrac{1}{2} O_2(aq) + H_2O(\ell) \xrightarrow{Mn^{++}\ \text{catalyst}} H_2SO_4(aq) \qquad \text{(B-1)}$$

at equilibrium, $\sum \nu_i \mu_i = 0$

$$\mu_{SO_2} = \mu^o_{SO_2} + RT \ln f_{SO_2} \qquad \text{(B-2)}$$

$$\mu_{O_2} = \mu^o_{O_2} + RT \ln f_{O_2} \qquad \text{(B-3)}$$

$$\mu_{H_2O} = \mu^o_{H_2O} + RT \ln f_{H_2O} \qquad \text{(B-4)}$$

μ_i^o = chemical potential of pure substance at 25°C and 1 atm

f_i = fugacity of i

Method of attack: assume a concentration of H_2SO_4, solve for conc. of SO_2. Trial and error until conc. of $SO_2 = 4 \times 10^{-3}$ atm. partial pressure.

At equilibrium, fugacity of substance in gas phase = fugacity of

substance in liquid phase; use gas phase fugacities; assume ideal gas; use partial pressure of substances in gas phase.

Assume for first trial molality of sulfuric acid = 17.5 $\frac{\text{g mols } H_2SO_4}{1000 \text{ gm } H_2O}$

$\gamma_{\pm}$ = 1.473 (Ref. 58)

= Mean activity coefficient of Sulfuric Acid in Aqueous Solution

$$\text{Mole fraction } H_2SO_4 = \frac{17.5 \text{ g mols } H_2SO_4}{17.5 \text{ g mols } H_2SO_4 + \frac{1000}{18} \text{ g mols } H_2O} = .24$$

From Duecker and West,[65] at mole fraction H_2SO_4 = .24, degree of dissociation of H_2SO_4 to H_3O^+ and HSO_4^- = 100%

Degree of dissociation of HSO_4^- = .14

If we ignore dissociation of HSO_4^-, or assume only dissociation is

$H_2SO_4 \rightleftharpoons H^+ + HSO_4^-$

$$\mu_{H_2SO_4} = \nu_{H^+}\mu^{\square}_{H^+} + \nu_{HSO_4^-}\mu^{\square}_{HSO_4^-} + RT \ln \gamma_{\pm}^{\nu} m_{H^+}^{\nu_{H^+}} m_{HSO_4^-}^{\nu_{HSO_4^-}} \qquad \text{(B-5)}$$

where $\nu_{H^+} = \nu_{HSO_4^-} = 1$ = number of ions obtained by dissociation of one molecule of electrolyte

$\nu = \nu_{H^+} + \nu_{HSO_4^-} = 2$

$\mu_{HSO_4^-}$ = chemical potential of HSO_4^- ion in a hypothetical ideal solution in which the molality of this ion is unity

= -177,340 cal. 51st edition, D-70 Handbook of Chem. and Physics[66]

μ_{H^+} = 0 by convention

$m_{H^+} = m_{HSO_4} = 17.5$

$$-RT \ln \frac{\gamma_{\pm}^{\nu} m_{H^+}^{\nu_{H^+}} m_{HSO_4^-}^{\nu_{HSO_4^-}}}{P_{SO_2} P_{O_2}^{1/2} P_{H_2O}} = \nu_{H^+} \mu_{H^+}^{\square} + \nu_{HSO_4^-} \mu_{HSO_4^-}^{\square} - \mu_{SO_2}^{o} - \frac{1}{2} \mu_{O_2}^{o} - \mu_{H_2O}^{o} \qquad \text{(B-6)}$$

$\mu_{SO_2}^{o} = -71.79$

$\mu_{O_2}^{o} = 0$

$\mu_{H_2O\ (g)}^{o} = -54.64$

P_{O_2} = .21 atm, normal O_2 content of air

P_{H_2O}, estimated from data in Perry, 4th Ed., pg. 3-63 on partial pressure of H_2O over H_2SO_4 solutions

$$\%H_2SO_4 = \frac{17.5 \text{ gm mols } H_2SO_4 \times 98 \frac{\text{gm}}{\text{gm mol}}}{1000 \text{ gm } H_2O + (17.5 \times 98) \text{ gm } H_2SO_4} = \frac{1713}{2713} = 62.5\% \qquad \text{(B-7)}$$

$P_{total} \cong P_{H_2O}$ = 3 mm Hg at 25°C and 62.5°C H_2SO_4

$\frac{3 \text{ mm}}{760 \text{ mm}}$ = .00395 atm

$$-(1.986)(298)(2.303)\log \frac{(1.473^2)(17.5)(17.5)}{P_{SO_2}(.21^{1/2})(.00395)} = -177,350 + 71,790 + 54,640 \qquad \text{(B-8)}$$

$$\log \frac{368,000}{P_{SO_2}} = \frac{50,920}{1368} = 37 \qquad \text{(B-9)}$$

$$\log 368,000 - \log P_{SO_2} = 37 \qquad \text{(B-10)}$$

$$\log \frac{1}{P_{SO_2}} = 37 - 5.56 = 31.44 \qquad \text{(B-11)}$$

$$\frac{1}{P_{SO_2}} = 10^{31.44} \qquad \text{(B-12)}$$

$$P_{SO_2} = 10^{-31.44} \qquad \text{(B-13)}$$

Conclusion: Equilibrium acid concentration is higher than 17.5 molal.

APPENDIX C

SPECIFICATIONS OF GASES AND REAGENTS

Sulfur Dioxide - Commercial grade, Matheson Gas Products

99.90% minimum purity

100 PPM H_2O vapor, max.

50 PPM non volatile, max.

10 PPM acid, max.

Ammonia - anhydrous grade, Air Products

99.99% minimum purity

33 PPM H_2O vapor, max.

9.5 PPM residue, max.

25 PPM non basic gas, max.

2 PPM oil, max.

Nitrogen - commercial grade, Air Products

99.997% minimum purity

-94°F dew point, max. or 5 PPM H_2O, max.

impurities primarily CO_2 and H_2O

Manganese Sulfate, Monohydrate

Fisher Scientific Co., Certified A.C.S.

Assay $MnSO_4 \cdot H_2O$	100.9%
Insoluble	0.002%
Cl	0.0005%
Heavy Metals	0.0005%
Ni	0.001%
Zn	0.002%

APPENDIX D

EXPERIMENTAL EQUIPMENT DETAILS

Referring to Figures 1 and 22, the equipment items are listed below:

Rotameters

R1	No. 610	Matheson Gas Products
R2	Tube Size R215B, tube 603	Matheson Gas Products
R3	Tube 602	Matheson Gas Products
R4	Tube 603	Matheson Gas Products
R5	No. 610	Matheson Gas Products
R6	Tube 600	Matheson Gas Products
R7	Tube No. 02.F 1/8.20.5/36	Fisher and Porter Co.
R8	Tube Size R215B tube 603	Matheson Gas Products
R9	Tube 73	Matheson Gas Products

Valves

N-1 Nupro Double Pattern Very Fine Metering Valve, Stainless Steel, SS-2SGD. Preceded by Series 2F Inline Filler

All other needle valves - Nupro Series 2M stainless steel metering valves

All other valves - glass stopcock type.

IR SO_2 Analyzer

Beckman Model 215A Infrared Analyzer

Dew Point Hygrometer

Cambridge System Model 880

Recorder

Hitachi Perkin-Elmer Model 165-0021

Filters

Millipore RAWP 04700, RA 1.2μ, 47 mm.

APPENDIX E

PROCEDURE FOR NH_3 - SO_2 TEST AND SAMPLE CALCULATION

Experimental Run Procedure

1. Calibrate IR SO_2 Analyzer. First check zero point with nitrogen. Then use two mixtures of SO_2-N_2 which have been analyzed for SO_2 by the supplier. The one mixture contains approximately 5000 PPM SO_2; the top of the range of the instrument, and other is approximately 2500 PPM SO_2 for mid range calibration. Flush calibration gases from IR with nitrogen.

2. Set SO_2 concentration. Dry air at a flow rate equal to total gas flow during the run and SO_2 only are used. First determine background IR reading with dry air only which contains a trace of H_2O vapor. Then SO_2 is introduced to the air stream and approximately 500 cc/min. of the total flow are diverted through IR and the SO_2 flow is adjusted by the needle valve until concentration indicated by IR is desired value. Since the IR interprets water vapor as SO_2, using dry air eliminates the need for a freeze out trap. The SO_2 flow is then diverted to the drain line and the system flushed of SO_2 by dry air flow.

3. Humid air flow rates are adjusted to "run" conditions. After a few minutes exposure the reactor is taken out of the system and the reactor, less bottom assembly, is weighed (tare weight), then replaced. Ammonia flow through drain line is adjusted to desired value as read on the ammonia rotameter.

4. After rechecking all flow rates, the SO_2 and NH_3 streams are simultaneously switched from the drain lines to the air lines leading to reactor and a run has begun.

5. After a predetermined time the reactor, assembly now containing the solid reaction product is weighed again.

Sample Calculation - Run No. 35S

Desired run conditions; nominal values

SO_2 - 250 PPM, 70.3 milli Moles/cubic meter

NH_3 - 500 PPM 20.6 mM/m^3

O_2 - Content of air, ~ 210,000 PPM, 8530mM/m^3

H_2O - Excess, 16,500 PPM, 670 mM/m^3

Total gas flow rate - 3300 cc/min.

Temp. - 296°K

Pressure - 750 torr

Reactor filter - 1.2 micro meters

Run time - 20 minutes

Reactor volume - 11 cc

Residence time - .2 seconds

Rotameter readings

R1 0

R2 1910 cc/min.

R3 not used, by passed

R4 967 cc/min.

R5 22.6 cc/min.

R6 100.7 cc/min.

R7 1376 cc/min.

R8 2086 cc/min.

SO_2 Concentration

Dry air and SO_2 reading on IR = 280 PPM

Dry air reading on IR = 30 PPM

SO_2 concentration = 250 PPM

$$250 \text{ PPM } SO_2 \times \frac{1 \text{ cc } SO_2, \text{ STP}}{10^6 \text{ PPM } SO_2\text{-cc gas, STP}} \times \frac{\text{m-Mol } SO_2}{22.4 \text{ cc } SO_2, \text{ STP}} \times \frac{273^\circ K}{296^\circ K}$$

$$\times \frac{750 \text{ torr}}{760 \text{ torr}} \times \frac{10^6 \text{ cc gas}}{m^3 \text{ gas}} = 10.14 \frac{\text{mM } SO_2}{m^3}$$

NH_3 Concentration

$$\frac{\dfrac{22.6 \text{ cc/min. } NH_3}{967 \text{ cc/min air} + 22.6 \text{ cc/min } NH_3} \times 100.7 \text{ cc/min } NH_3 + \text{air}}{2086 \text{ cc/min} + 1376 \text{ cc/min}}$$

$$\times \frac{\text{m-M } NH_3}{22.4 \text{ cc } NH_3, \text{ STP}} \times \frac{273^\circ K}{296^\circ K} \times \frac{750 \text{ torr}}{760 \text{ torr}} \times \frac{10^6 \text{ cc gas}}{m^3 \text{ gas}} = 27 \frac{\text{mM } NH_3}{m^3}$$

H_2O Concentration

Air through R2 is bypassed around dryer. This air has dewpoint of 20°F = .0505 psia vapor pressure.[55]

Air through humidifier saturated at 73°F = 4019 psia vapor pressure

$$1910 \text{ cc/min air}(20^\circ F \text{ dewpoint}) \times \frac{.0505 \text{ psia}}{14.5 \text{ psia}} = 5.65 \text{ cc } H_2O/\text{min.}$$

$$2441 \text{ cc/min. air}(73^\circ \text{ dewpoint}) \times \frac{.4019 \text{ psia}}{14.5 \text{ psia}} = \frac{67.50 \text{ cc } H_2O/\text{min}}{72.15 \text{ cc } H_2O/\text{min total}}$$

$$\frac{72.15 \text{ cc } H_2O/\text{min.}}{4351 \text{ cc/min. (air} + H_2O)} = .0/655 \frac{\text{cc } H_2O}{\text{cc gas}} = 16550 \text{ PPM } H_2O \text{ vapor}$$

$$.01655 \frac{\text{cc } H_2O}{\text{cc gas}} \times \frac{\text{m-M } H_2O}{22.4 \text{ cc } H_2O, \text{ STP}} \times \frac{273°K}{296°K} \times \frac{750 \text{ torr}}{760 \text{ torr}}$$

$$\times \frac{10^6 \text{ cc gas}}{m^3 \text{ gas}} = 677 \frac{\text{mM } H_2O}{m^3}$$

Total gas flow through reactor

Reactor flow is sum of flows through rotameters R7 + R8 = 1376 cc/min. + 2086 cc/m = 3462 cc/min. $\frac{3462 \text{ cc/min.}}{10^6 \text{ cc/m}^3} = .003462 \text{ m}^3/\text{min}$

Residence time

$$t = \frac{10.96 \text{ cc reactor volume}}{\frac{3462}{60} \text{ cc/sec gas velocity}} = .19 \text{ sec}$$

Reaction Product

Wt. of reactor and reaction product	60.26821 gm
Wt. of reactor, tare weights	60.19396 gm
Wt. of reaction product	.07425 gm
Second tare weight determination	60.19531 gm
Tare weight difference	.00135 gm, 1.82% of reaction byproduct.

Reaction product - ammonium sulfate, formula weight = 132 gm

Ammonium sulfate in terms of concentration:

$$\frac{.07425 \text{ gm } (NH_4)_2SO_4}{.132 \text{ gm } (NH_4)_2SO_4/\text{mM}(NH_4)_2SO_4 \times .003462 \text{ m}^3/\text{min.} \times 20 \text{ run}} =$$

$$9.76 \frac{\text{mM}(NH_4)_2SO_4}{m^3}$$

APPENDIX F

Table 12. SO_2-NH_3 Reaction Details

Series A - Runs 68S, 70S, 71S, 72S, 76S

Constant Values for Series

Initial Conc., mM-m^{-3}		IR Analyzer, PPM		Rotameter Indicated Flow Rates, cc-min.$^{-1}$	
SO_2	3.98	SO_2 + Air	122	R1	bypassed
NH_3	27.0	Air	24	R2	2020
H_2O	668	SO_2	98	R3	bypassed
O_2	8530 (air)			R4	967
Product-Ammonium sulfate		*Humid air, cc-min^{-1}	4328	R5	22.6
Temp. 296 ± 1°K		**Reactor Flow,	3462	R6	100.7
Pres. 750 ± 5 torr		Reactor Filter μM	1.2	R7	1376
				R8	2086

Variable Values for Series

Run No.	76S	71S	72S	70S
Reactor Vol., cc	1.67	3.29	6.88	10.96
Residence time, sec.	.029	0.057	0.119	.190
Weighings, gm				
React. and Prod.	52.33055	51.68145	56.19582	60.40361
Tare	52.31652	51.65723	56.16421	60.33316
Product	0.01403	0.02422	0.03164	0.07045
Tare check	52.31714	51.65826	56.16517	60.33398
Tare difference	0.00062	0.00103	0.00096	0.00082
% of Prod. Wt.	4.4	4.2	3.0	1.2
Run Time, min.	30	20	20	40
Exp. Prod. Conc., mM-m^{-3}	1.02	2.65	3.46	3.84
Calc. Prod. Conc., mM-m^{-3}	1.44	2.27	3.22	3.66

*Sum of flows through R4 + R8 + R7 - R6

**Sum of flows through R7 + R8

Table 12. (Continued)

Series B - Runs 75S, 66S, 63S, 64S, 65S

Constant Values for Series

Initial Conc., $mM\text{-}m^{-3}$		IR Analyzer, PPM		Rotameter Indicated Flow Rates, $cc\text{-}min.^{-1}$	
SO_2	8530 (air)	SO_2 + Air	170	R1	bypassed
NH_3	27.0	Air	21	R2	2020
H_2O	682	SO_2	149	R3	bypassed
O_2	8530 (air)			R4	967
Product-Ammonium sulfate				R5	22.6
Temp.	296 ± 1°K	Humid Air, $cc\text{-}min^{-1}$	4328	R6	100.7
Press.	750 ± 5 torr	Reactor Flow, $cc\text{-}min^{-1}$	3462	R7	1376
		Reactor Filter, μm	1.2	R8	2086

Variable Values for Series

Run No.	75S	66S	63S	64S	65S
Reactor Vol., cc	1.67	3.29	6.88	10.96	16.50
Residence, sec.	0.029	0.057	0.119	0.190	0.286
Weighings, gm.					
React. and Prod.	52.34496	51.69300	56.21118	60.39666	65.43676
Tare	52.31641	51.63769	56.13717	60.31064	65.34865
Product	0.02855	0.05531	0.07401	0.08602	0.8811
Tare Check	52.31780	51.63857	56.13919	60.31195	65.35092
Tare Difference	0.00139	0.00088	0.00202	0.00131	0.00227
% of Prod. wt.	4.9	1.6	2.7	1.5	2.6
Run Time, min	30	30	30	30	30
Exp. Prod. Conc., $mM\text{-}m^{-3}$	2.08	4.03	5.4	6.29	6.45
Calc. Prod. Conc., $mM\text{-}m^{-3}$	2.13	3.34	4.72	5.4	5.79

Table 12. (Continued)

Series C - Runs 74S, 57S, 56S, 55S, 54S

Constant Values for Series

Initial Conc., $mM\text{-}m^{-3}$		IR Analyzer, PPM		Rotameter Indicated Flow Rates, $cc\text{-}min.^{-1}$	
SO_2	9.95	SO_2 + Air	262	R1	bypassed
NH_3	27.0	Air	17	R2	2020
H_2O	682	SO_2	245	R3	bypassed
O_2	8530 (air)			R4	967
Product-Ammonium sulfate		Humid Air, $cc\text{-}min^{-1}$	4328	R5	22.6
Temp.	296 ± 1°K	Reactor Flow, $cc\text{-}min^{-1}$	3462	R6	100.7
Press.	750 ± 5 torr	Reactor Filter, μm	1.2	R7	1376
				R8	2086

Variable Values for Series Concentrations [=] $mM\text{-}m^{-3}$

Run No.	74S	57S	56S	55S	54S	52S
Reactor Vol., cc	1.67	3.29	6.88	10.96	16.50	22.4
Residence time, sec	0.029	0.057	0.119	0.190	0.286	0.388
Weighings, gm.						
React. and Prod.	52.35508	51.69121	56.19390	60.26821	65.31783	81.74084
Tare	52.31628	51.64560	56.13522	60.19396	65.22860	81.64623
Product	0.03880	0.04561	0.05868	0.07425	0.08925	0.09461
Tare Check	52.31793	51.64747	56.13724	60.19609	62.22973	81.64812
Tare Difference	0.00165	0.00187	0.00202	0.00213	0.00113	0.00199
% of Prod. wt.	4.2	4.1	3.4	2.9	1.3	2.1
Run time, min.	25	20	20	20	20	20
Exp. Prod. Conc.	3.4	4.98	6.41	8.12	9.76	10.32
Calc. Prod. Conc.	3.36	5.13	7.15	8.25	8.98	9.38
Residence time, sec		0.06	0.12	0.18	0.28	0.38
Calc.Prod.Conc. by Eq's (13) + (14)		3.64	6.53	7.94	8.97	9.42

Table 12. (Continued)

Series D - Runs 81S, 78S, 79S, 73S, 80S

Constant Values for Series

Initial Conc., $mM\text{-}m^{-3}$		IR Analyzer, PPM		Rotameter Indicated Flow Rates, $cc\text{-}min.^{-1}$	
SO_2	27.0	SO_2 + Air	689	R1	bypassed
NH_3	27.0	Air (Background)	24	R2	2020
H_2O	682	SO_2	665	R3	bypassed
O_2	8530 (air)			R4	967
Product-Ammonium sulfate				R5	22.6
Secondary product-Ammonium sulfamate				R6	100.7
Temp.	296 ± 1°K	Humid air, $cc\text{-}min^{-1}$	4328	R7	1376
Press.	750 ± 5 torr	Reactor Flow, $cc\text{-}min^{-1}$	3462	R8	2086
		Reactor Filter, μm	1.2		

Variable Values for Series

Run No.	81S	78S	79S	73S	80S
React. Vol., cc	1.67	3.29	6.88	10.96	16.50
Residence time, sec.	0.029	0.057	0.119	0.190	0.286
Weighings, gm					
Reactor and Prod.	52.34950	51.70527	56.21800	60.47300	65.44021
Tare	52.31070	51.66076	56.16537	60.34512	65.37660
Product	0.03880	0.04451	0.05263	0.12788	0.06361
Tare Check	52.31203	51.66167	56.16738	60.41220	65.37953
Tare Difference	0.00133	0.00091	0.00201	0.00292	0.00293
% of Prod. wt.	3.4	2.0	3.82	2.3	4.6
Run Time, min.	10	10	10	20	10
Exp. Prod. Conc., $mM\text{-}m^{-3}$	8.49	9.38	12.95	13.95	13.90
Calc. Prod. Conc., $mM\text{-}m^{-3}$	7.43	10.22	12.48	13.20	13.44

Table 12. (Continued)

Series E - Runs 62S, 59S, 60S, 61S

Constant Values for Series

Initial Conc., $mM\text{-}m^{-3}$		IR Analyzer, PPM		Rotameter Indicated Flow Rates, $cc\text{-}min.^{-1}$	
SO_2	10.14	SO_2 + Air	267	R1	bypassed
NH_3	35.65	Air	17	R2	1910
H_2O	682	SO_2	250	R3	bypassed
O_2	8530 (air)			R4	967
Product-Ammonium sulfate				R5	22.6
Temp.	296 ± 1°K	Humid air, $cc\text{-}min^{-1}$	4291	R6	133
Press.	750 ± 5 torr	Reactor Flow, $cc\text{-}min^{-1}$	3462	R7	1376
		Reactor Filter, μm	1.2	R8	2086

Variable Values for Series

Run No.	62S	59S	60S	61S
Reactor Vol., cc	3.29	6.88	10.96	16.50
Residence Time, sec.	0.057	0.119	0.190	0.286
Weighings, gm				
React. and Prod.	51.69347	56.20065	60.40030	65.44310
Tare	51.63679	56.13573	60.31500	65.34620
Product	0.05668	0.06492	0.08530	0.09690
Tare check	51.63767	56.13675	60.31723	65.34735
Tare Difference	0.00088	0.00102	0.00223	0.00115
% of Prod. wt.	1.5	1.6	2.6	1.2
Run time, min.	20	20	20	20
Exp. Prod. Conc., $mM\text{-}m^{-3}$	6.2	7.1	9.32	10.58
Calc. Prod. Conc., $mM\text{-}m^{-3}$	6.30	8.38	9.33	9.82

Table 12. (Continued)

Series F - Runs 87S, 67S, 84S, 85S

Constant Values for Series

Initial Conc., $mM\text{-}m^{-3}$		IR Analyzer, PPM		Rotameter Indicated Flow Rates, $cc\text{-}min.^{-1}$	
SO_2	20.6	SO_2 + Air	531	R1	bypassed
NH_3	47.3	Air	24	R2	2020
H_2O	668	SO_2	507	R3	bypassed
O_2	8530 (air)			R4	967
Product-Ammonium sulfate				R5	44
Temp.	296 ± 1°K	Humid air $cc\text{-}min^{-1}$	4336	R6	92.5
Press.	750 ± 5 torr	Reactor Flow, $cc\text{-}min^{-1}$	3462	R7	1376
		Reactor Filter, μm	1.2	R8	2086

Variable Values for Series Concentrations [=] $mM\text{-}m^{-3}$

Run No.	87S	67S	84S	85S	86S	88S
React. Vol., cc	1.67	3.29	6.88	10.96	16.50	22.40
Residence Time, sec	0.029	0.057	0.119	0.190	0.286	0.388
Weighings, gm.						
React. and Prod.	52.36410	51.70524	56.25604	60.44894	65.47800	81.92140
Tare	52.31455	51.64746	56.17323	60.34791	65.37742	81.81382
Product	0.04955	0.05778	0.08281	0.08334	0.10058	0.10758
Tare check	52.31695	51.64844	56.17531	60.34997	65.37933	81.81351
Tare Difference	.00240	.00098	.00208	.00206	.00191	.00031
% of Prod. wt	4.8	1.7	3.0	2.5	1.9	0.3
Run time, min	12	12	12	12	12	12
Exp. Prod. Conc.	9.0	10.5	15.1	16.6	18.3	19.6
Calc. Prod. Conc.	9.66	13.33	16.73	18.3	19.29	19.81

Table 12. (Continued)

Series G - Runs 97S, 43S, 96S, 41S

Constant Values for Series

Initial Conc., $mM\text{-}m^{-3}$		IR Analyzer		Rotameter Indicated Flow Rates, $cc\text{-}min.^{-1}$	
SO_2	20.9	SO_2 + Air	531	R1	Bypassed
NH_3	40.4	Air (background)	16	R2	Bypassed
H_2O	31	SO_2	515	R3	80
O_2	8530 (air)			R4	967
Product-(Estimated)	68%$(NH_3)_2 \cdot 2O_2$, 20%$NH_3 \cdot SO_2$,			R5	44
	7%NH_3SO_3, 5%NH_4N_3			R6	45
Temp. 296 ± 1°K		Humid Air, $cc\text{-}min^{-1}$	2896	R7	1012
Press. 750 ± 5 torr		Reactor Flow, $cc\text{-}min^{-1}$	1974	R8	962
		Reactor Filter, μm	1.2		

Variable Values for Series

Run No.	97S	43S	96S	41S
Reactor Vol., cc	3.44	6.97	10.7	16.8
Res. Time, sec.	0.104	0.212	0.338	0.510
Weights, gm				
Reactor and Prod.	51.67264	56.04332	62.55056	65.26168
Tare	51.60013	55.96332	62.45623	65.16579
Product	0.07251	0.07995	0.09433	0.09589
Tare check	51.60125	55.96453	62.45992	65.16444
Tare Difference	0.00112	0.00116	0.00369	0.00135
% of Prod. wt.	1.5	1.5	3.9	1.4
Run time, min	30	30	30	30
Exp. Prod. Conc., $mM\text{-}m^{-3}$	13.2	14.6	17.1	17.4
Calc. Prod. Conc., $mM\text{-}m^{-3}$	14.68	17.28	18.36	19.03
Residence Time, sec.	0.2	0.21	0.34	0.51
Calc. Prod. Conc., mM^{-3} Eq. (13) + (14)	0.93	2.04	3.22	4.63

Table 12. (Continued)

Series H - Runs 17S, 36S, 18S, 19S, 20S, 35S

Constant Value for Series

Initial Conc., $mM\text{-}m^{-3}$		IR Analyzer		Rotameter Indicated Flow Rates, $cc\text{-}min.^{-1}$	
SO_2	20.9	SO_2 + Air	531	R1	Bypassed
NH_3	20.7	Air (background)	16	R2	Bypassed
H_2O	16.2	SO_2	515	R3	41.6
O_2	8530 (air)			R4	967
Product-(Estimated)	68%$(NH_3)_2 \cdot SO_2$, 20%$NH_3 \cdot SO_2$, 7%NH_3SO_3, 5%NH_4N_3			R5	22.6
				R6	44
Temp. 296 ± 1°K		Humid Air, $cc\text{-}min^{-1}$	2896	R7	1012
Press. 750 ± 5 torr		Reactor Flow, $cc\text{-}min^{-1}$	1974	R8	962
		Reactor Filter, μm	1.2		

Variable Values for Series	Concentrations [=] $mM\text{-}m^{-3}$					
Run No.	17S	36S	18S	19S	20S	35S
Reactor Vol., cc	3.29	6.97	11.10	16.8	28.5	31.5
Res. Time., sec	0.100	0.212	0.338	0.510	0.691	0.957
Weights, gm						
React. and Prod.	50.65485	55.99100	62.05470	66.98011	73.76943	90.86600
Tare	50.63522	55.96186	62.01657	66.93181	73.71455	90.81310
Product	0.01963	0.02914	0.03813	0.04830	0.05488	0.05390
Tare Check	50.63620	55.96307	62.01836	66.93417	73.71669	90.81046
Tare Difference	0.00098	0.00121	0.00179	0.00236	0.00214	0.00264
% of Prod. wt.	5.0	4.1	4.7	4.9	3.9	4.9
Run Time, min.	30	30	30	30	30	30
Exp. Prod. Conc.	3.6	5.3	6.9	8.78	10.0	9.8
Calc. Prod. Conc.	8.68	10.0	10.28	10.34	10.35	10.35

Table 12. (Continued)

Series I - Runs 21S, 22S, 23S, 24S, 30S, 34S

Constant Values for Series

Initial Conc., $mM\text{-}m^{-3}$		IR Analyzer		Rotameter Indicated Flow Rates, $cc\text{-}min.^{-1}$	
SO_2	20.9	SO_2 + Air	531	R1	Bypassed
NH_3	40.4	Air (Background)	16	R2	Bypassed
H_2O	16.2	SO_2	515	R3	42
O_2	8530 (air)			R4	967
Product-(Estimated)	68%$(NH_3)_2 \cdot SO_2$, 20%$NH_3 \cdot SO_2$, 7%NH_3SO_3, 5%NH_4N_3			R5	44
				R6	45
Temp. 296°K		Humid Air, $cc\text{-}min^{-1}$	2896	R7	1012
Press. 750 Torr		Reactor Flow, $cc\text{-}min^{-1}$	1974	R8	962
		Reactor Filter, μm	1.2		

Variable Values for Series Concentrations [*] $mM\text{-}m^{-3}$

Run No.	21S	30S	22S	23S	24S	34S
Reactor Vol., cc	3.29	6.97	11.10	16.8	28.5	31.5
Res. Time, sec.	0.100	0.212	0.338	0.510	0.691	0.957
Weights, gm						
React. and Prod.	50.6894	56.02577	62.41300	67.59076	83.89500	90.91465
Tare	50.65290	55.96187	62.33847	67.49725	83.79500	90.81310
Product	0.03655	0.06390	0.07453	0.09351	0.1000	0.10155
Tare check	50.65462	55.95886	62.34131	67.49881	3.79198	90.81431
Tare difference	0.00172	0.00301	0.00284	0.00156	0.00302	0.00121
% of Prod. wt.	4.7	4.7	3.8	1.6	0.3	1.2
Run Time, Min	30	30	30	30	30	30
Exp. Prod. Conc.	6.65	11.6	13.5	17.0	18.1	18.3
Calc. Prod. Conc.	14.68	17.28	18.36	19.03	19.39	19.68

Table 12. (Continued)

Series J - Runs 26S, 28S, 27S, 29S, 33S

Constant Values for Series

Initial Conc., $mM\text{-}m^{-3}$				Rotameter Indicated Flow Rates, $cc\text{-}min.^{-1}$	
SO_2	20.9	SO_2 + AIR	531	R1	Bypassed
NH_3	60.1	Air (background)	16	R2	Bypassed
H_2O	16.2	SO_2	515	R3	41.6
O_2	8530 (air)			R4	967
Product-(Estimated)	68%$(NH_3)_2 \cdot SO_2$, 20%$NH_3 \cdot SO_2$, 7%NH_3SO_3, 5% NH_4N_3			R5	65
				R6	46
Temp. 296°K		Humid Air, cc-min-1	2896	R7	1012
Press. 750 Torr		Reactor Flow, $cc\text{-}min^{-1}$	1974	R8	962
		Reactor Filter, μm	1.2		

Variable Values for Series Concentrations [=] $mM\text{-}m^{-3}$

Run No.	26S	28S	27S	29S	33S
Reactor Vol., cc	3.29	6.97	11.1	16.8	28.5
Res. Time, sec.	0.100	0.212	0.338	0.510	0.691
Weights, gm					
React. and Prod.	51.63909	56.03970	62.56783	65.28450	82.20900
Tare	51.60000	55.96186	62.45606	65.17036	82.09761
Product	0.03900	0.07784	0.11177	0.11414	0.11139
Tare Check	51.60195	55.96428	62.45897	65.17314	82.09560
Tare difference	0.00195	0.00242	0.00291	0.00278	0.00201
% of Prod. wt.	5.0	3.1	2.6	2.5	1.8
Run Time, min.	30	30	30	30	30
Exp. Prod. Conc.,	7.1	14.0	20.4	20.3	20.3
Calc. Prod. Conc.	18.2	20.26	20.75	20.88	20.9

Table 12. (Continued)

Series K - Runs 91S, 92S, 93S, 94S, 95S

Constant Values for Series

Initial Conc., $mM\text{-}m^{-3}$		IR Analyzer, PPM		Rotameter Indicated Flow Rates, $cc\text{-}min.^{-1}$	
SO_2	20.6	SO_2 + Air	531	R1	16
NH_3	47.3	Air	24	R2	2020
H_2O	668	SO_2	507	R3	Bypassed
O_2	31			R4	967
Product-(Estimated)	85%$(NH_3)_2 \cdot SO_2$, 10%$N_3H_7SO_4$, 5%NH_3SO_3			R5	44
				R6	92.5
Temp.	296 ± 1°K	Humid Air, $cc\text{-}min^{-1}$	4336	R7	1376
Press.	750 ± 5 torr	Reactor Flow, $cc\text{-}min^{-1}$	3462	R8	2086
		Reactor Filter, μm	1.2		

Variable Values for Series

Run No.	94S	95S	93S	91S	92S
Reactor Vol., cc					
Residence Time, sec.	0.029	0.057	0.119	0.190	0.286
Weighing, gm					
React. and Prod.	52.39474	51.75880	56.35783	60.55656	65.62064
Tare	52.31663	51.65772	56.22185	60.39900	65.42861
Product	0.07811	0.10108	0.13598	0.15756	0.19198
Tare check	52.31991	51.66176	56.22291	60.39905	65.43642
Tare difference	0.00328	0.00404	0.00106	0.00005	0.00781
% of React. Prod. wt.	4.2	4.0	0.7	0.0	4.1
Run Time, min.	20	20	20	20	20
Exp. Prod. Conc. $mM\text{-}m^{-3}$	11.0	14.25	19.15	22.1	27.1
Calc. Prod. Conc., $mM\text{-}m^{-3}$	9.66	13.32	16.73	18.3035	19.29

APPENDIX G

A MODEL CONSIDERED FOR THE REACTIONS OF $SO_2 + NH_3$ TO FORM AMMONIUM SULFATE

$$NH_3 + SO_2 \underset{k_2}{\overset{k_1}{\rightleftharpoons}} NH_3{\cdot}SO_2 \tag{G-1}$$

$$NH_3{\cdot}SO_2 + NH_3 \underset{k_4}{\overset{k_3}{\rightleftharpoons}} (NH_3)_2{\cdot}SO_2 \tag{G-2}$$

$$(NH_3)_2{\cdot}SO_2 + O_2 \underset{k_6}{\overset{k_5}{\rightleftharpoons}} (NH_3)_2{\cdot}SO_3 + O \tag{G-3}$$

$$(NH_3)_2{\cdot}SO_2 + O \underset{k_8}{\overset{k_7}{\rightleftharpoons}} (NH_3)_2{\cdot}SO_3 \tag{G-4}$$

$$(NH_3)_2{\cdot}SO_3 + H_2O \xrightarrow{k_9} (NH_4)_2SO_4 \tag{G-5}$$

Rate expressions are developed as follows:

Let $$A = [NH_3{\cdot}SO_2] \tag{G-6}$$

$$B = [(NH_3)_2{\cdot}SO_2] \tag{G-7}$$

$$C = [(NH_3)_2{\cdot}SO_3] \tag{G-8}$$

$$\frac{dA}{dt} = k_1[NH_3][SO_2] - k_2A - k_3A[NH_3] + k_4B \tag{G-9}$$

$$\frac{dB}{dt} = k_3A[NH_3] - k_4B - k_4B - k_5B[O_2] + k_6C[O] - k_7B[O] + k_8C \tag{G-10}$$

$$\frac{dC}{dt} = k_5B[O_2] - k_6C[O] + k_7B[O] - k_8C - k_9C[H_2O] \tag{G-11}$$

Let X be the sum of the concentration of the intermediates, then:

$$\frac{dS}{dt} = \frac{dA}{dt} + \frac{dB}{dt} + \frac{dC}{dt} \qquad \text{(G-12)}$$

By combining Eq's (G-9)(G-10) and (G-11) as in Eq (12)

$$\frac{dX}{dt} = k_1[NH_3][SO_2] - k_2A - k_9C[H_2O] \qquad \text{(G-13)}$$

The assumption is made that the ratio of each intermediate concentrate to the sum of the concentrations of the intermediates is constant:

$$\frac{A}{X} = \text{constant}, \quad \frac{B}{X} = \text{constant}, \quad \frac{C}{X} = \text{constant} \qquad \text{(G-14)}$$

With this assumption,

$$k_2A = k_2\frac{A}{X}X = k_2'X \quad \text{where } k_2' = k_2\frac{A}{X} \qquad \text{(G-15)}$$

If the concentration of H_2O vapor is large enough to be assumed constant:

$$k_9C[H_2O] = k_9\frac{C}{X}X[H_2O] = k_9'X \quad \text{where } k_9' = k_9\frac{C}{X}[H_2O] \qquad \text{(G-16)}$$

Equation (G-13) can be written:

$$\frac{dX}{dt} = k_1[NH_3][SO_2] - k_2'X - k_9'X \qquad \text{(G-17)}$$

By stoichiometry

$$[NH_3] = N_o - \Phi x - 2P \qquad \text{(G-18)}$$

$$[SO_2] = S_o - X - P \qquad \text{(G-19)}$$

where N_o = initial concentration of ammonia = $[NH_3]_o$

S_o = initial concentration of sulfur dioxide = $[SO_2]_o$

φ = moles of NH_3 per mole of X

P = concentration of ammonium sulfate

Eq (G-17) then becomes

$$\frac{dX}{dt} = k_1(N_o - \varphi x - 2P)(S_o - X - P) - k_2'X - k_9'X \qquad (G\text{-}20)$$

$$\frac{dX}{dt} = k_1(N_oS_o - 2S_oP - N_oP + 2P^2) + k_1X(-S_o\varphi - N_o + 2P + P\varphi) - k_2X - k_9'X \qquad (G\text{-}21)$$

In Equation (21) the X^2 term is neglected.

The assumption is made that the rate of change of the concentration of the sum of the intermediates is zero,

$$\frac{dX}{dt} = 0 \qquad (G\text{-}22)$$

Equation (G-21) can be solved for X:

$$X = \frac{-k_1(N_oS_o - 2S_oP - N_oP + 2P^2)}{k_1(-S_o\varphi - N_o + 2P + P\varphi) - k_2' - k_9'} \qquad (G\text{-}23)$$

From Eq. (G-5)

$$\frac{dP}{dt} = k_9'X = \frac{-k_9'k_1(N_oS_o - 2S_oP - N_oP + 2P^2)}{k_1(-S_o\varphi - N_o + 2P + P\varphi) - k_2' - k_9'} \qquad (G\text{-}24)$$

at time zero when

$$\text{concentration of ammonium sulfate} = 0 \qquad (G\text{-}25)$$

$$\left(\frac{dP}{dt}\right)_o = \frac{-k_9'k_1N_oS_o}{k_1(-S_o\varphi - N_o) - k_2' - k_9'} \qquad (G\text{-}26)$$

If

$$\frac{k_2' + k_9'}{k_1} = K_m \qquad (G\text{-}27)$$

$$\left(\frac{dP}{dt}\right)_o = \frac{k_9' N_o S_o}{S_o \varphi + N_o + K_m} \qquad \text{(G-28)}$$

Inverting Eq. (G-28)

$$\frac{1}{\left(\frac{dP}{dt}\right)} = \frac{\varphi}{k_9' N_o} + \frac{N_o + K_m}{k_9' N_o} \cdot \frac{1}{S_o} \qquad \text{(G-29)}$$

A plot of $1/\left(\frac{dP}{dt}\right)_o$ vs $1/S_o$ should give a straight line with a slope of $N_o + K_m/k_9' N_o$ and an intercept of $\varphi/k_9' N_o$ (G-30)

A plot of this experimental data, Series A, B, C, D, in which N_o is held constant at 27 mM/m^3 and SO_2 is varied from 3.98 mM/m^3 to 27 mM/m^3 is shown on Figure 35. The data plotted is listed in Table 13.

Table 13. Slope Intercept Data for k_9' and K_m

$N_o = 27.0\ mM\text{-}m^{-3}$

$\varphi = 1.667$

Series	S_o $mM\text{-}m^{-3}$	S_o^{-1} $(mM\text{-}m^{-3})^{-1}$	$(dP/dt)_o$ $mM/m^3\text{-}sec$	$(dP/dt)_o^{-1}$ $(mM/m^3\text{-}sec)^{-1}$
A	3.98	0.251	50	.0200
B	6.05	0.158	72	.0139
C	9.95	0.096	111	.0090
D	27.00	0.037	240	.0042

The value of 1.667 for φ was obtained by assuming equal concentrations of the three intermediates. From Figure 35 the intercept is .002 and the slope is .0857. From Eq (G-30):

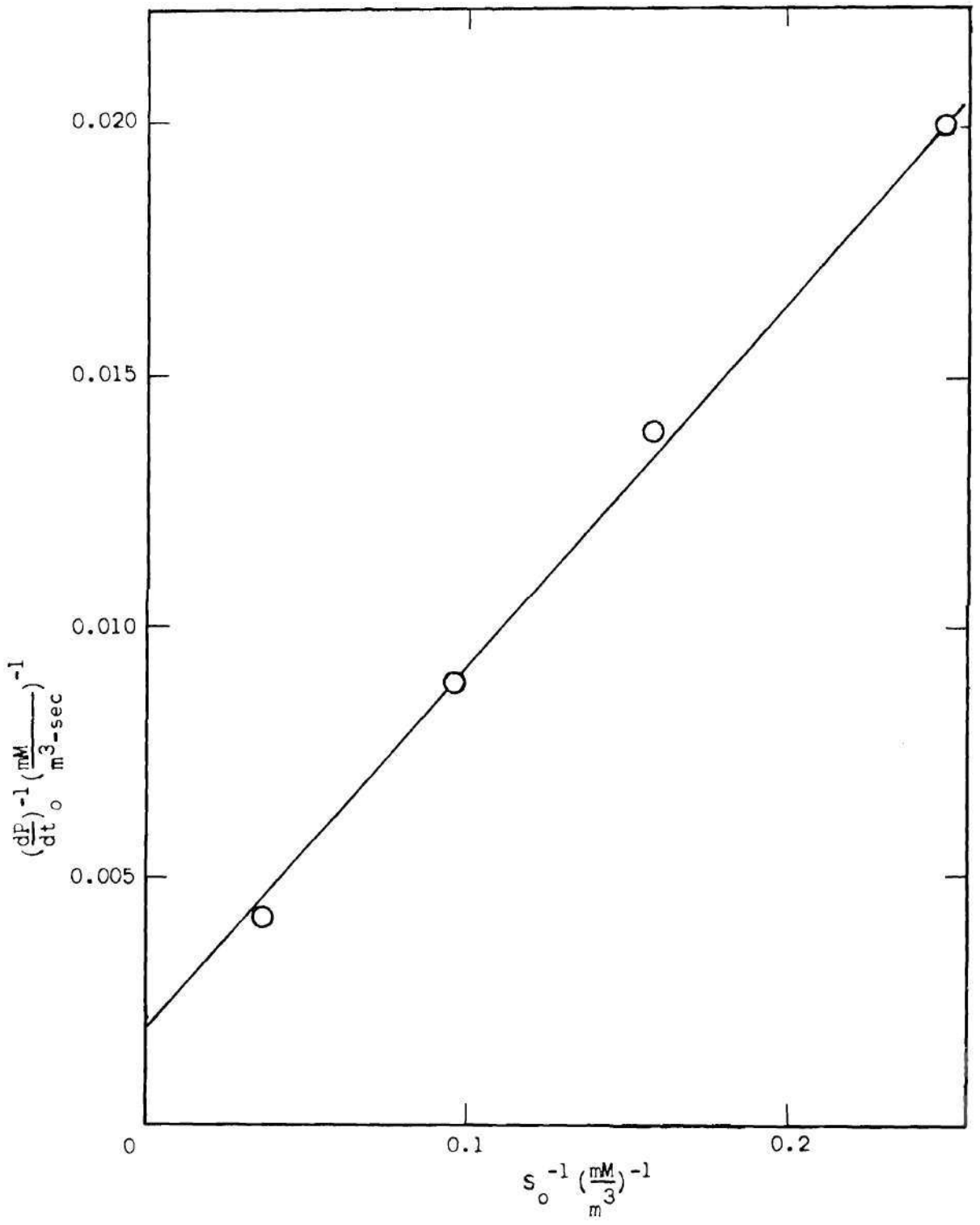

Figure 35. Slope Intercept Data for k_9' and K_m.

$$k_9' = \frac{\Phi}{\text{Intercept} \times N_o} = \frac{1.667}{(.002)(27)} = 31 \frac{\text{meter}^3}{\text{mM-sec}}$$

$$K_m = \text{slope} \times k_9' \times N_o - N_o \qquad \text{(G-31)}$$

$$K_m = (.0857)(31)(27) - 27 = 44.7 \qquad \text{(G-32)}$$

Equations (20) and (21) were solved by 4th order Runga Kutta numerical integration on the computer. The rate constant k_1 was determined by trial error to give the best fit of Series A to F experimental data. For any assumed value of k_1, k_2 was determined by Eq. (G-27).

Eq's (20) and (21) were generalized to include $[H_2O]$ as a variable by substituting k_9'' for k_9' by the relationship

$$k_9'' = \frac{k_9'}{[H_2O]} = \frac{31}{668} = .0464 \qquad \text{(G-33)}$$

$$\frac{dX}{dt} = k_1(N_o - \Phi X - 2P)(S_o - X - P) - k_2' X - k_9'' X(\ _o - X - P) \qquad \text{(G-34)}$$

$$\frac{dP}{dt} = k_9'' X (\omega_0 - X - P) \quad \text{where} \quad \omega_o = [H_2O]_o \qquad \text{(G-35)}$$

In solving these simultaneous differential equations by the method of Runga Kutta, a small value (10^{-6}) must be used for the initial concentration of X instead of zero for method to work.

APPENDIX H

ACCURACY OF RESULTS

SO_2 Reactions with Aqueous Solutions of Manganese

To determine the reproducibility of the tests, duplicate tests of initial reaction rate (of approximately 20 minutes duration) were made at temperatures of 1°C, 25°C, 38°C, and 65°C. Each of the duplicate tests at 1°C and 25°C produced recordings of off gas SO_2 concentrations that were indistinguishable when overlaid. At 38°C and 65°C results of duplicate tests varied by as much as ±4% from the average of the tests.

As stated in Chapter IV, the tests made for extended periods of time (400 minutes) are estimated to be accurate within ±10% of the true value. The major cause is volume fluctuations caused by the evaporation into or condensation from the gas stream. Sulfuric acid concentrations of the liquid at the end of the tests were determined by titration with NaOH and compared with the acid concentration calculated from the experimental SO_2 absorption. The value from titration agreed with the calculated to within 7% of the calculated.

Equipment accuracy is identical to that reported below.

SO_2 Reactions with NH_3 in the Gas Phase

As noted previously some of the tests produced a higher yield of solid product, calculated as millimoles of ammonium sulfate, than was

possible from the quantity of limiting reactant. The series with the highest error, Series B, yielded a product concentration of 6.45 mmoles/m^3 with a limiting reactant concentration of 6.05 mmoles/m^3 sulfur dioxide. This is an error of 6.63% based on the SO_2 concentration. Series F reactions yielded a product concentration 5% less than the limiting SO_2 concentration of 20.6 mM/m^3. Based on these results a general statement of accuracy would be that the concentration of solid product formed at any time is accurate to within 7%.

All rotameters, except R-5 (ammonia from cylinder) were calibrated with air and wet test meter. R-5 was calibrated with ammonia by absorbing the ammonia in concentrated sulfuric acid and weighing the acid before and after ammonia absorption. The R-5 calibration with ammonia resulted in higher values of flow than the manufacturers calibration, which is based on air by ~11%.

The Beckman Infra-red Analyzer has an advertised accuracy of ±1%.

The water was added to the air stream by bubbling through a column of water. Hygrometer measurements have confirmed this air to be saturated. The principal error would be in the temperature of the water. A ±1°C variation in temperature will produce an error of ±5% in H_2O concentration in the Series with the lower H_2O vapor concentration.

As previously reported, tests were reproducible to within 7.1% of the test with the lowest weight and tare weights before and after tests were within 5% of product weight.

BIBLIOGRAPHY

1. Junge, C., "Die Rolle der Aerosole und der gasformigen Beimengungen der Luft im Spurenstoffhaus half der Troposphäve," Tellus 5, 1 (1953).

2. Scott, W. D., and Hobbs, P. V., "The Formation of Sulfate in Water Droplets," Journal of the Atmospheric Sciences 24, 54 (1967).

3. Scott, W. D., and McCarthy, J. L., "The System Sulfur Dioxide-Ammonia-Water at 25°C," Industrial and Engineering Chemistry Fundamentals 6, No. 1, 40 (1967).

4. Matteson, M. J., Stöber, W., and Luther, H., "Kinetics of the Oxidation of Sulfur Dioxide by Aerosols of Manganese Sulfate," Industrial and Engineering Fundamentals 8, No. 4, 677 (1969).

5. Johnstone, H. F., "Progress in the Removal of Sulfur Compounds from Waste Gases," Combustion 5, No. 2, 19 (1933).

6. Johnstone, H. F., and Moll, A. J., "Formation of Sulfuric Acid in Fogs," Industrial and Engineering Chemistry 52, No. 10, 861 (1960).

7. Firket, J., "Fog Along the Meuse Valley," Transactions Faraday Society 32, 1192 (1936).

8. Schrenck, H. H., Heimann, H., Clayton, G. D., and Gefafer, W. M., "Air Pollution in Donora, Pa., Epidemiology of Unusual Smog Episode of Oct., 1948," U. S. Public Health Service Bulletin 306, 162 (1949).

9. Junge, C. E., and Ryan, T. G., "Study of the SO_2 Oxidation in Solution and Its Role in Atmospheric Chemistry," Quarterly Journal Royal Meteorological Society 84, 46 (1958).

10. Mossop, S. C., "Stratospheric Particles at 20 km," Nature 199, 325 (1963).

11. Gerhard, E. R., and Johnstone, H. F., "Photochemical Oxidation of Sulfur Dioxide in Air," Industrial Engineering Chemistry 47, No. 5, 972 (1955).

12. Scott, W. D., and Hobbs, P. V., "The Formation of Sulfate in Water Droplets," Journal of the Atmospheric Sciences 24, 54 (1967).

13. McKay, H. A. C., "The Atmospheric Oxidation of Sulfur Dioxide in Water Droplets in Presence of Ammonia," Atmospheric Environment 5, 7 (1971).

14. Hoather, R. C., and Goodeve, C. F., "The Oxidation of Sulfurous Acid. III. Catalysis by Manganous Sulfate," Transactions Faraday Society 30, 1149 (1934).

15. Bassett, H., and Parker, W. G., "The Oxidation of Sulfurous Acid," Journal American Chemical Society, 1540 (1951).

16. Wilkens, E. T., Smokeless Air 24, No. 88, 89 (1953). (Cited in Ref.17)

17. Johnstone, H. F., and Coughanowr, D. R., "Absorption of Sulfur Dioxide from Air," Industrial and Engineering Chemistry 50, No. 8, 1169 (1958).

18. Coughanowr, D. R. and Krause, F. E., "The Reaction of SO_2 and O_2 in Aqueous Solutions of $MnSO_4$," Industrial and Engineering Chemistry Fundamentals 4, No. 1, 61 (1965).

19. Cheng, R. T., Corn, M., and Frohliger, J. O., "Contribution to the Reaction Kinetics of Water Soluble Aerosols and SO_2 in Air at PPM Concentrations," Atmospheric Environment 5, 987 (1971).

20. Miller, J. M., and dePena, R. G., "Contribution of Scavenged Sulfur Dioxide to the Sulfate Content of Rain Water," Journal of Geophysical Research 77, No. 30, 5905 (1972).

21. Urone, P., Lutsep, H., Noyes, C. M., and Parcher, "Static Studies of Sulfur Dioxide in Air," Environmental Science and Technology 2, 611 (1968).

22. Renzetti, N. A., and Doyle, D. J., "Photochemical Aerosol Formation in Sulfur Dioxide-Hydrocarbon Systems," Intern. Journal Air Pollution 2, 327 (1960).

23. Schroeder, W. H. and Urone, P., "Thermal and Photochemical Reactions of Sulfur Dioxide in Air." Presented before the Division of Water, Air, and Waste Chemistry, 160th National ACS Meeting, Chicago (1970).

24. Wilson, W. E., Jr., and Levy, A., "A Study of Sulfur Dioxide in Photochemical Smog," Journal Air Pollution Control Association 20, 385 (1970).

25. Badar-ud-Din, and Aslam, M., "A Study of Ammonia-Sulfur Dioxide Reaction," Pakistan Journal of Scientific Research 5, No. 1, 6 (1953).

26. Kushnir, J. M., Malkin, H. I., Mohnen, V. A., Yencha, A. J., and McLaren, E. H., "Non-Photochemical Aerosol Formation from the Anhydrous Reaction between Ammonia and Sulfur Dioxide Gases," Publication No. 165 of Atmospheric Sciences Research Center, State University of New York at Albany.

27. Cann, E. D., "Dual Cycle Treatments of Sulfur Dioxide Containing Flue Gas and the Like," U. S. Patent 3,579,296 (1971).

28. West, J. H., and Jaques, A., "Improvements In or Relating to the Manufacture of Ammonium Compounds," British Patent 215,470, Class 1 (ii), Inorganic Compounds Sc., (1923).

29. Lamb, D., "An Implication of a Model of Ammonia-Sulfur Dioxide Reactions to the Atmosphere," Journal of the Atmospheric Sciences 28, 1082 (1971).

30. Scott, W. D., and Lamb, D., "Two Solid Compounds which Decompose into a Common Vapor. Anhydrous Reactions of Ammonia and Sulfur Dioxide," Journal of the American Chemical Society 92, 3943 (1970).

31. Scott, W. D., Lamb, D., and Duffy, D., "The Stratospheric Aerosol Layer and Anhydrous Reactions Between Ammonia and Sulfur Dioxide," Journal of the Atmospheric Sciences 26, 727 (1969).

32. Smith, W. S., and Gruber, C. W., "Atmospheric Emissions from Cool Combustion - An Inventory Guide," U. S. Department of Health, Education, and Welfare, Public Health Service Publication No. 999-AP-24 (1966).

33. Amdur, M. O., "Toxicologic Appraisal of Particulate Matter, Oxides of Sulfur, and Sulfuric Acid," Journal Air Pollution Control Association 19, 638 (1969).

34. Johnstone, H. F., and Leppla, P. W., "The Solubility of Sulfur Dioxide at Law Partial Pressures. The Ionization Constant and Heat of Ionization of Sulfurous Acid," Journal American Chemical Society 56, 2233 (1934).

35. Priestly, J., Experiments and Observations on Different Kinds of Air 2, Birmingham, England (1970). (Cited in ref. 26)

36. Ephraim, and Piotrowiski, Ber., 379 (1911). (Cited in ref. 26)

37. Schumann, Z. anorg chem. 23, 49 (1900). (Cited in ref. 26)

38. Ogawa, M., and Aoyama, S., Sci. Repts. Tokyo University, Series I 11, 121 (1913). (Cited in ref. 26)

39. Boscoe, G. F., "The Calibration of an Aerosol Centrifuge and a Study of Density Deviation in Condensation Aerosols," Master of Science Thesis, Georgia Institute of Technology, October (1972).

40. Dobereiner, Schiv. J. 17, 120 (1826). (Cited in ref. 25)

41. Forchhammer, Compt. Rend. 5, 395 (1837). (Cited in ref. 25)

42. Rose, Pogg Ann 61, 397 (1844). (Cited in ref. 25)

43. Divers, and Gawa, O., Journal Chemical Society 77, 327 (1900). (Cited in ref. 26)

44. Dobereiner, Schiv. J. 47, 119 (1826). (Cited in ref. 26)

45. Lewis, T. R., Amdur, M. O., Fritzhand, M. D., and Campbell, T.I., "Toxicology of Atmospheric Sulfur Dioxide Decay Products," Publication No. AP-111, U. S. Environmental Protection Agency (1972).

46. Friend, J. P., Prefrint, Atmospheric Environment.

47. Smith, E. W., and Finlayson, T. C., "Developments in the Treatment of Crude Gas, Gas Journal 172, 357 (1925).

48. Kiyoura, R., "Precipitation of Sulfur Dioxide from Hot Flue Gases," Staub, Reinholtung Luft 26, 524 (1966).

49. Vian-Ortuno, Iriarte-Fernandez, and Melcheso-Serrano," Process for the Production of Ammonium Sulfate," U. S. Patent 2,912,304, Nov. 10, 1959.

50. Chemical Abstracts 60, 5107b (1962).

51. Mascorello, J., Auclair, J., Hamelin, R., and Pelecier, C., "Sulfur Oxides Removal from Flue Gases. The Pilot Unit of the Saint-Owen EDI Station," Proceedings of the American Power Conference 31, 439 (1969).

52. Anderson, L. B., and Johnstone, H. F., "Gas Absorption and Oxidation in Dispersed Media," A.I.Ch.E. Journal 1, No. 2, 135 (1955).

53. Mellor, J. W., A Comprehensive Treatise on Inorganic and Theoretical Chemistry, Longmans, Green and Co. (1964).

54. Levenspiel, O., Chemical Reaction Engineering, Wiley (1967).

55. Keenan, J. H., and Keyes, F. G., Thermodynamic Properties of Steam, Wiley (1936).

56. Benson, S. W., The Foundations of Chemical Kinetics, McGraw-Hill (1960).

57. Harned, H. S., and Owen, B. B., The Physical Chemistry of Electrolytic Solutions, Reinhold (1943).

58. Benson, S. W., "The Induction Period in Chain Reactions," The Journal of Chemical Physics 20, No. 10, 1605 (1952).

59. Copson, R. L., and Payne, J. W., "Recovery of Sulfur Dioxide as Dilute Sulfuric Acid," Industrial and Engineering Chemistry 25, No. 8, 909 (1933).

60. Pearce, S. L., "The Treatment of Flue Gases from Modern Power Stations," Transactions Second World Power Conference, Berlin 4, 103 (1930).

61. Denbigh, K., The Principles of Chemical Equilibrium, Cambridge, 2nd Ed. (1968).

62. Duecker, W. W., and West, J. R., The Manufacture of Sulfuric Acid, American Chemical Society Monograph No. 144, Reinhold (1959).

63. Weast, R. C., Handbook of Chemistry and Physics, The Chemical Rubber Co., 51st Ed. (1970-71).

64. Perry, R. H., Chilton, C. H., and Kirkpatrick, S. D., Chemical Engineers Handbook, McGraw-Hill, 4th Ed. (1963).

VITA

Edwin M. Hartley, Jr. was born April 13, 1929 in Chicago, Illinois to the late Marion Platt and Edwin M. Hartley. He graduated from Moorestown High School, Moorestown, New Jersey in 1946. He served in the U. S. Army from 1946 to 1947 which included 1 year with the 88th Infantry Division in Europe. He attended the Georgia Institute of Technology in Atlanta, Georgia from 1948 to 1953 where he received the Bachelor of Chemical Engineering. Upon graduation he worked for the Proctor and Gamble Company as a Plant Engineer, in Atlanta, Ga. He was then transferred to Houston, Texas as Packaging Manager and in 1963 given a temporary assignment in Milan, Italy for P and G International. He returned to Atlanta, Ga. as Division Production Engineer. He left this position in 1965 to take the position of Chief Process Engineer - Acid Plants, with the Royster Co. in Bartow, Fla. In 1969 he enrolled as a graduate student in the School of Chemical Engineering. He received the Master of Science degree in Chemical Engineering in 1971 and taught in the School of Chemical Engineering during the 1971-72 school year. He is a member of Tau Beta Pi and the American Institute of Chemical Engineers.